UNIVERSIDAD AUTÓNOMA DE MADRID
FACULTAD DE CIENCIAS
DEPARTAMENTO DE BIOLOGÍA MOLECULAR

Characterization of new p38α MAPK functions in malignant cell transformation

Doctoral Thesis

Aneta Swat

Madrid, 2009

This thesis work was carried out at the Spanish National Cancer Research Centre (CNIO) in Madrid from 2004-2009; under the supervision of Dr. Angel Rodriguez Nebreda.

Index

Abbreviations

ActD	----	actinomycin D
ARE	----	AU-rich element
AREBP	----	ARE-binding protein
ASK1	----	apoptosis signal-regulating kinase 1
CAK	----	CDK activating kinase
Cbl	----	casitas B-lineage lymphoma
CDK	----	cyclin-dependent kinase
CHX	----	cycloheximide
CKI	----	cyclin-dependent kinase inhibitor
Conf	----	confluent
DMEM	----	Dulbecco Modified Eagle's Medium
DMSO	----	dimethyl sulfoxide
DTT	----	dithiothreitol
EDTA	----	ethylenediaminetetracetic acid
EGF	----	epidermal growth factor
EGFR	----	epidermal growth factor receptor
ER	----	estrogen receptor
ERK	----	extracellular signal-regulated kinase
FBS	----	fetal bovine serum
FC	----	fold change
FGFR	----	fibroblast growth factor receptor
GADD	----	growth arrest and DNA damage–induced
GAPDH	----	glyceraldehyde-3-phosphate dehydrogenase
GFP	----	green fluorescent protein
GST	----	glutathione S-transferase
HBD-ER	----	hormone-binding domain of the human estrogen receptor
IgG	----	immunoglobulin G
IP	----	immunoprecipitation
JNK	----	cJun-N-terminal kinase
KO	----	knock-out
MAPK	----	mitogen-activated protein kinase
MAPKAPK	----	MAPK-activated protein kinase
MEF	----	mouse embryo fibroblast
MEF2	----	myocyte enhancer factor 2
MEK	----	mitogen-activated or extracellular-signal regulated kinase kinase
MEKK	----	MAPK and ERK kinase kinase
MK	----	MAPKAPK

MKK	----	MAPK kinase
MKKK	----	MAPK kinase kinase
MKKKK	----	MAPK kinase kinase kinase
MLK	----	mixed-lineage kinase
MNK	----	MAPK-interacting kinase
mRNA	----	messenger RNA
MSK	----	mitogen- and stress-activated kinase
OD	----	optical density
OHT	----	4-hydroxytamoxifen
PAK	----	p21-activated kinase
PBS	----	phosphate buffer saline
PCR	----	polymerase chain reaction
PMSF	----	phenylmethylsulfonyl fluoride
PRAK	----	p38-regulated or activated protein kinase
pRb	----	retinoblastoma protein
qRT-PCR	----	quantitative reverse transcription-PCR
RIPA	----	radioimmunoprecipitation assay
ROS	----	reactive oxygen species
RTK	----	receptor tyrosine kinase
SAPK	----	stress-activated protein kinase
SD	----	standard deviation
SDS-PAGE	----	sodium dodecyl sulphate-polyacrylamide gel electrophoresis
SH2	----	Src-homology domain 2
shRNA	----	short hairpin RNA
Siah2	----	seven in absentia homolog 2
Spry2	----	Sprouty2
Ste	----	Sterile
STK	----	Ste20-like kinase
SubC	----	subconfluent
TAK	----	TGFβ-activated kinase
TAO	----	thousand and one-aminoacid kinase
TBP	----	TATA-bindig protein
TFR	----	transferin receptor
TKB	----	tyrosine kinase binding
TRAF	----	tumor necrosis factor receptor-associated factor
Trx	----	thioredoxin
TTP	----	tristetraprolin
Ub	----	ubiquitin
UV	----	ultraviolet

VEGFR	----	vascular endothelial growth factor receptor
WB	----	western blot
WT	----	wild-type

Abstract

p38α MAP kinase has been established in recent years as an emerging tumor suppressor, which seems to be accounted for by its negative effect on cell proliferation and its pro-apoptotic activity. Nevertheless, malignant cells are not only characterized by their limitless proliferation potential and the ability to overcome apoptosis, but also by their irresponsiveness to contact inhibition, a key mechanism regulating tissue homeostasis *in vivo*. Actually, one of the first pathological traits acquired by transformed cells consists in the *in vitro* ability to grow forming multi-layered foci, which is a marker of impaired contact inhibition.

Consequently, we have characterized the mechanisms coordinated by p38α to inhibit the loss of cell-to-cell contact inhibition. We have previously identified the protein kinase p38α as a novel regulator of contact inhibition, as p38α is activated upon cell-cell contacts and p38α-deficient cells are impaired in the confluence-induced proliferation arrest. We demonstrate now that $p27^{Kip1}$ plays a key role downstream of p38α to arrest proliferation at high cellular densities. Surprisingly, p38α does not directly regulate $p27^{Kip1}$ expression levels, but indirectly leads to confluent upregulation of $p27^{Kip1}$ and cell cycle arrest via the inhibition of mitogenic signals originating from the EGF receptor (EGFR). Hence, confluent activation of p38α uncouples cell proliferation from mitogenic stimulation by inducing EGFR degradation, which occurs mechanistically through the downregulation of the EGFR-stabilizing protein Sprouty2 (Spry2). In turn, Spry2 downregulation enhances the loading of the ubiquitin ligase cCbl onto EGFR, which primers the receptor for lysosomal degradation. Accordingly, confluent p38α-deficient cells fail to downregulate Spry2 and this allows them to sustain high levels of EGFR signaling that facilitate cell overgrowth and oncogenic transformation.

In parallel, we have also investigated the potential contribution of the transcriptional effect of p38α to its tumor suppressor activity, since p38α is well known to coordinate various cellular processes by transcriptional means, such as cell differentiation. This contrasts though with the majority of known tumor suppressor mechanisms coordinated by p38α occurring at the post-translational level. With the aim of unveiling new transcriptional mediators of the tumor suppressor effect of p38α, we have characterized, through a microarray-based approach, the differences in gene expression between H-Ras^{V12}-transformed wild-type (WT) and p38α-/- mouse embryo fibroblasts (MEFs). This analysis has revealed 202 genes regulated by p38α that had not been previously linked to p38α in the context of malignant cell transformation. 31 of these genes have been validated and confirmed by reverse transcription-PCR (RT-PCR) to be regulated by p38α, both in MEFs as well as in mouse tumor samples extracted from subcutaneous xenografts and syngeneic lung carcinogenesis models. 9 genes have been further selected for functional characterization. Interestingly, we obtained evidence that several

of them (i.e. *Gstm2, Cd9*) are functionally implicated in the regulation of H-Ras^{V12}-induced transformation by p38α. Moreover, about 10% of the p38α-regulated genes form a network positively stimulating EGF receptor (EGFR) signalling that is downregulated by p38α. This suggests that a main effect of p38α in malignant transformation may be the transcriptional inhibition of EGFR signaling.

Resumen

La proteína quinasa p38α ha sido establecida recientemente como un supresor de tumores, lo que parece deberse a su efecto negativo sobre la proliferación celular así como a su actividad pro-apoptótica. Sin embargo, las células cancerígenas no sólo se caracterizan por su limitada capacidad proliferativa y la habilidad de evadir la apoptosis, sino también por ser refractarias a la inhibición al contacto, un proceso clave para la regulación de la homeostasis tisular *in vivo*. De hecho, una de las primeras características patológicas adquiridas por las células transformadas (malignas) consiste en la habilidad de crecer *in vitro* formado focos (multiples capas de células apiladas verticalmente), un claro indicativo de la pérdida de inhibición al contacto.

En consecuencia, hemos caracterizado los mecanismos coordinados por p38α para inhibir la pérdida de inhibición al contacto. A este respecto, hemos identificado previamente la proteína quinasa p38α como un regulador nuevo de este proceso, ya que su actividad aumenta cuando las células entran en contacto. Ademas, las células que no expresan p38α (p38α-/-) son insensibles a la parada proliferativa inducida a altas densidades celulares (confluencia). Adicionalmente, ahora demostramos que $p27^{Kip1}$ desempeña un papel clave como mediador de p38α en la inducción de la parada proliferativa en confluencia. Sorprendentemente, p38α no regula de forma directa los niveles de expresión de $p27^{Kip1}$, sino que incide indirectamente sobre su expresión asi como sobre la parada proliferativa en confluencia, a través de la inhibición de la señalización mitogénica procedente del receptor de factor de crecimiento epidérmico (EGFR, *epidermal growth factor receptor*). Así, la activación confluente de p38α desacopla la proliferación celular de la estimulación mitogénica al inducir la degradación de EGFR, lo que ocurre, a un nivel mecanístico, a través de un descenso en los niveles de expresión de la proteína Sprouty 2 (Spry2), conocida por estabilizar a EGFR. A su vez, el descenso en Spry2 resulta en una mayor interacción de EGFR con la ubiquitina ligasa cCbl, responsable de dirigir al receptor hacia su degradación en el lisosoma. De acuerdo con esto, las células confluentes p38α-/- fallan en inducir un descenso en los niveles de Spry2, lo que les permite sostener unos mayores niveles de señalización de EGFR que facilita su crecimiento descontrolado y su transformación maligna.

En paralelo, hemos investigado la contribución potencial del efecto transcripcional de p38α a su función supresora de tumores, ya que se sabe que p38α puede regular varios procesos celulares a un nivel casi exclusivamente transcripcional, como es el caso de la diferenciación celular. Esto contrasta, sin embargo, con el hecho de que la mayoría de los mecanismos supresores tumorales adscritos a p38α ocurren a un nivel post-traduccional. Con el objetivo de identificar nuevos mediadores transcripcionales del efecto supresor tumoral de p38α, hemos caracterizado, por medio de un enfoque basado en la técnica de micromatriz de ADN (*microarray*), las diferencias de expresión

génica entre fibroblastos embrionarios de ratón (MEFs, *mouse embryo fibroblasts*) salvajes (WT, *wild-type*) y p38α-/- transformados por el oncogén H-Ras^{V12}. Dicho análisis ha revelado 202 genes regulados por p38α que no habían sido previamente asociados con p38α en el contexto de transformación celular maligna. 31 de ellos han sido validados mediante la técnica de transcripción reversa acoplada a la reacción en cadena de polimerasa (RT-PCR, *reverse transcription-polymerase chain reaction*) y se ha confirmado que su transcripción se encuentra regulada por p38α, tanto en MEFs como en muestras de tumores de ratón extraídas de xenotrasplantes subcutáneos y modelos singénicos de carcinogénesis pulmonar. 9 genes han sido adicionalmente seleccionados para ser caracterizados a un nivel funcional. Notablemente, tenemos evidencia de que varios de ellos (ej. *Gstm2*, *Cd9*) se encuentran implicados a un nivel funcional en la regulación por p38α de la transformación inducida por H-Ras^{V12}. Además, hemos encontrado que aproximadamente el 10% de los genes cuya transcripción se encuentra regulada negativamente por p38α pertenecen a un grupo interconectado de genes que estimulan la actividad de EGFR. Esto sugiere que un efecto importante de p38α en la regulación de la transformación celular podría consistir en la inhibición de la señalización de EGFR a nivel transcripcional.

Introduction

1. The Mitogen-Activated Protein Kinase (MAPK) family

Mitogen-activated protein kinases (MAPKs) consist of a highly-conserved family of proline-directed Ser/Thr protein kinases that play key signal transduction roles in eukaryotic cells. MAPKs are required for the coordination of the cell responses to virtually all types of extracellular stimuli (Cobb et al., 1994; Kyriakis and Avruch, 2001), which probably accounts for their high degree of conservation through eukaryotes. MAPK pathways are composed by different kinase modules in which a MAPK is activated upon phosphorylation by MAPK kinase (MAPKK/MAP2K), which in turn is activated when phosphorylated by a MAPKK kinase (MAP3K/MAPKKK) (Figure 1). At least eight different MAPK signaling cascades have been identified up to date in mammals (Bogoyevitch and Court, 2004), with each one showing some stimulus selectivity. They include the extracellular signal-regulated kinases (ERKs): ERK1 and ERK2; the Jun-N-terminal kinases (JNKs): JNK1, JNK2 and JNK3; the p38 MAP kinases (p38 MAPKs): p38α, p38β, p38γ, p38δ; the Big MAPK1 (BMK1)/ERK5 cascade; and the less studied, atypical MAPKs ERK3, ERK4, ERK7, and ERK8. Whereas the ERK1/2 pathway has been long known to be preferentially activated by mitogens (Cobb et al., 1994), both the JNK and p38 MAPK cascades are mostly responsive to stress and inflammatory cytokines (Kyriakis and Avruch, 2001) (Figure 1), which has more recently gained them both the more appropriate name of stress-activated protein kinases (SAPKs) (Kyriakis and Avruch, 2001). In contrast, little is known about the stimulus selectivity of the atypical ERK members ERK3 to ERK8 (Coulombe and Meloche, 2006), meanwhile the BMK1/ERK5 pathway is known to be activated by both mitogenic and stress stimuli (Coulombe and Meloche, 2006; Kyriakis and Avruch, 2001).

MAPKs require dual Thr and Tyr phosphorylation on their activation loops for full activation (Thr-Xaa-Tyr motif), which normally is catalyzed by the upstream MKKs (Figure 1). There are seven MKKs in mammals (Bogoyevitch and Court, 2004; Ichijo, 1999), including MEK1 and MEK2 in the ERK1/2 pathway, MEK5 in the BMK1/ERK5 cascade, MKK4 and MKK7 in the JNK pathway, and MKK3, MKK6 and MKK4 in the p38 MAPK pathway (Figure 1). In turn, MKKs are known to be activated by upstream MKKKs that also show some MKK specificity, although not as much as MKKs for MAPKs, as well as certain stimulus selectivity (Ichijo, 1999; Stalheim and Johnson, 2007). Once activated, MAPKs lead to the coordination of numerous cellular responses, which range from survival and proliferation to the regulation of gene expression (Figure 1). It is believed that the particular cell response engaged by a given stimulus is determined, in addition to the potential implication of other signalling pathways, by both the crosstalk

among different MAPK pathways as well as between the different isoforms within each MAPK subfamily.

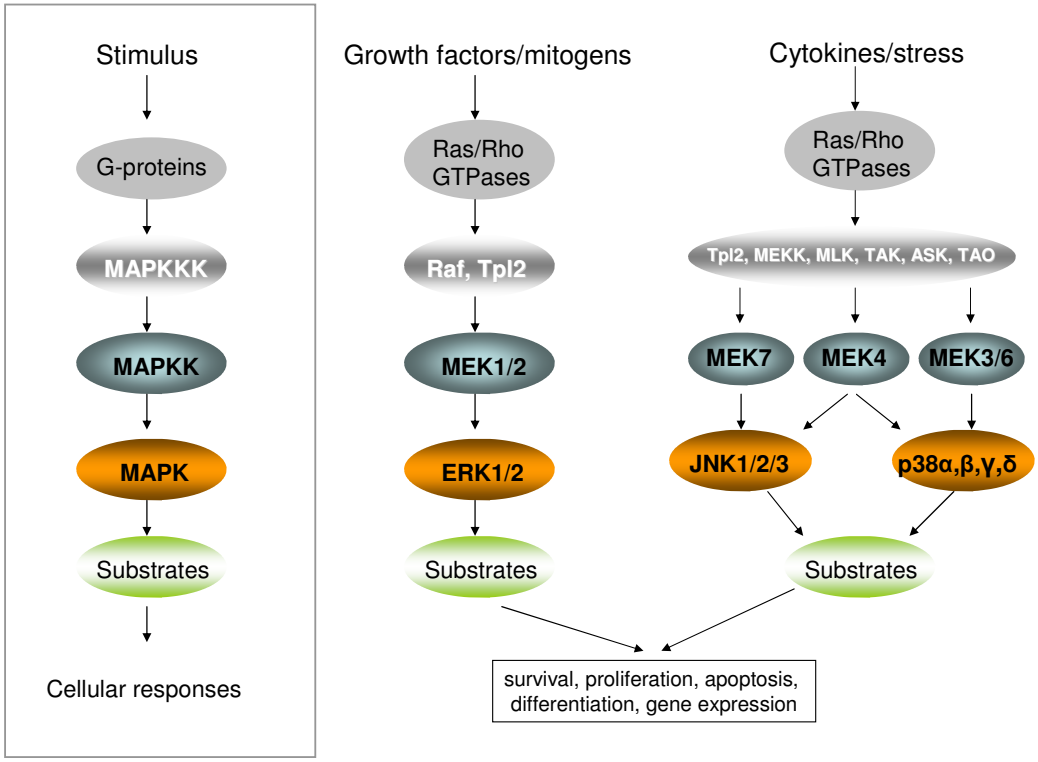

Figure 1. Simplified MAPK signalling scheme. The canonical MAPKs (ERKs, JNKs and p38 MAPKs) are activated in a three-tiered fashion by upstream MKKs, MKKKs and MKKK activators. The nature of the cellular response induced by MAPKs may vary, depending on stimulus and cell type.

Interestingly, whereas their individual stimulus selectivities usually serve to classify MAPKs in different subfamilies (in combination with the extent of homology within their kinase domains), the highly conserved mechanism of activation represents an unifying characteristic of the MAPK family. Noteworthy, MKKKs rarely act as stimuli sensors themselves and need to be coupled to cell receptors through upstream proteins in order to efficiently rely signaling cues (Figure 2). The proteins upstream of MKKKs are usually referred to as MKKKKs or MAP4Ks and include Sterile 20 (STE20) family kinases such as the MINKs (Nicke et al., 2005), the p21-activated kinases (PAKs) (Ichijo, 1999), and the STE20-like kinases (STKs) (Figure 2). Other proteins that are known to function upstream of MAP3Ks include small G-proteins of the Ras and Rho GTPase families, scaffold proteins such those belonging to the tumor necrosis factor (TNF) receptor-associated factors (TRAFs) (Ichijo, 1999) and the growth arrest and DNA damage–induced (GADD) proteins (Takekawa and Saito, 1998) (Figure 2).

In turn, MAPK activation leads to the phosphorylation of downstream targets. These include numerous transcription factors (Crump, 2007), although some MAPKs can also

activate other kinases (Figure 2) (Kotlyarov and Gaestel, 2007; Ono and Han, 2000) and many other proteins (Ono and Han, 2000).

Of note, neither MKKs nor MKKKs have been identified so far for the MAPKs ERK3, ERK4, ERK7, and ERK8 (Bogoyevitch and Court, 2004). This has led to the proposal that these MAPKs might not be activated in the canonical and well-conserved multi-tiered fashion described above and are consequently referred to as non-canonical MAPKs.

2. Signal transduction by p38 MAPK

Of special relevance for this work is the p38 MAPK group, which consists of four members: p38α, p38β, p38γ and p38δ showing 60% identity at the amino acid level. p38α and p38β, but not p38γ and p38δ, are ubiquitously expressed proteins (Nebreda and Porras, 2000), although p38α is normally expressed at higher levels than p38β and is usually regarded as the dominant isoform within this MAPK subfamily (Nebreda and Porras, 2000; Perdiguero et al., 2007). Accordingly, p38α deficiency is embryonic lethal in mice (Adams et al., 2000; Allen et al., 2000; Mudgett et al., 2000; Tamura et al., 2000) and adult p38α conditional knock-out (KO) mice show impaired lung differentiation (Ventura et al., 2007). In contrast, loss of p38β, p38γ or p38δ does not affect normal development in mice, indicating probably redundant functions with other p38 family members (Beardmore et al., 2005; Sabio et al., 2005).

2.1. Upstream activators and downstream effectors

p38 MAPKs are activated *in vivo* by environmental stresses and inflammatory cytokines and, to a lower extend, by serum and growth factors (reviewed in (Cuenda and Rousseau, 2007)). Among the twenty MKKKs identified so far (Stalheim and Johnson, 2007), six can activate the ERK pathway and fourteen lay upstream of JNKs, meanwhile only three of them have been shown to be relevant for the activation of p38 MAPKs *in vivo*, namely TAK1, MEKK5/Ask1, and MEKK4 ((Ichijo, 1999); Figure 2). Although some other MKKKs have been shown to activate p38 MAPKs *in vitro* (i.e. TAOs, MLK3, MEKK1), mouse models lacking these proteins do not show significant alterations in the activation of the p38 MAPK pathway (Stalheim and Johnson, 2007). On a related issue, mouse models deficient for p38 MKKs have confirmed that MKK3 and MKK6 are the dominant MKKs in the p38 pathway (Brancho et al., 2003), although MKK4 can also cooperate for p38 MAPK activation in some cases, such as after ultraviolet radiation (UV) (Nebreda and Porras, 2000). MKK3 and MKK6 are highly selective for p38 MAPK and do not activate JNKs or ERK1/2 (Cuenda and Rousseau, 2007). The canonical activation of p38 MAPK occurs via dual phosphorylation of its Thr-Gly-Tyr motif in the activation loop. MKK3 and MKK6 are in turn activated by phosphorylation by MAPKKKs

(MKKKs), the nature of which is cell type and stimulus specific since MKKKs have been shown to be preferentially activated by certain stimuli, hence coupling particular signaling cues with specific MAPK pathways. For instance, MEKK4 has been shown to couple the DNA-damage response with the activation of the p38 MAPK pathway through the GADD family member Gadd45a ((Takekawa and Saito, 1998); Figure 2). Similarly, TAK1 has been shown to be preferentially activated by pro-inflammatory cytokines (Stalheim and Johnson, 2007), whereas MEKK5/Ask1 is a key transducer of oxidative stress signals ((Matsukawa et al., 2004); Figure 2).

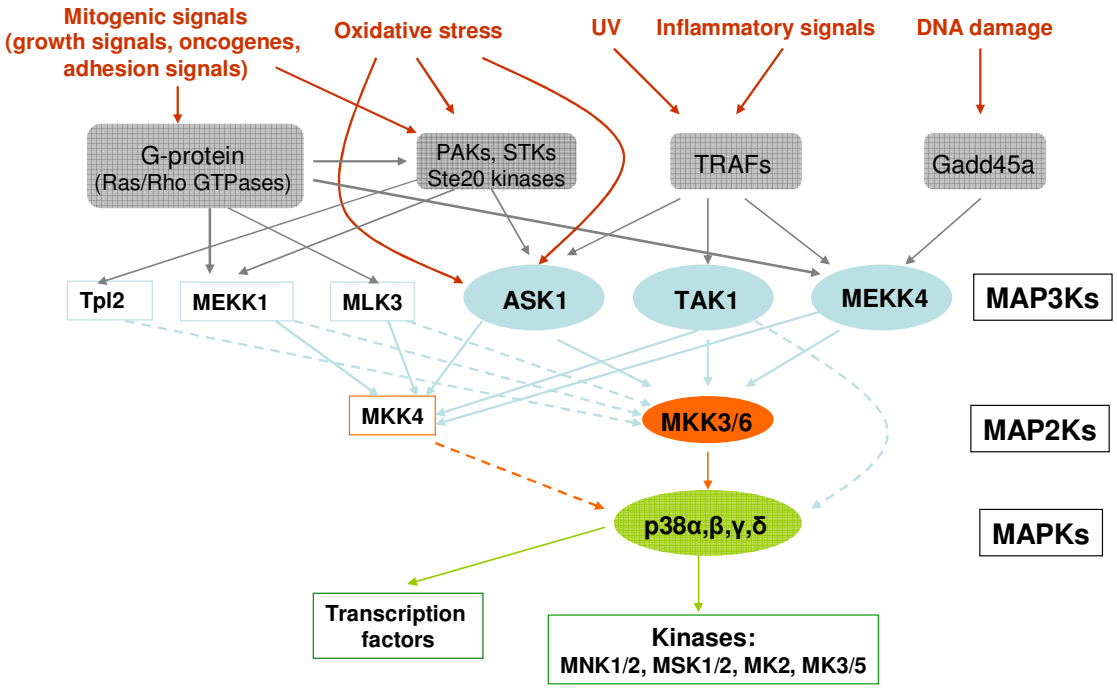

Figure 2. p38 MAPK pathway activators and effectors. Different types of stimuli originating from mitogenic signals, oxidative stress, ultraviolet radiation (UV), DNA damage or inflammatory signals result in the activation of MAPKKKs (i.e. ASK1, TAK1, MEKK4). MAPKKKs subsequently activate MAPKKs, which in turn activate MKK3/4/6 and downstream p38 MAPKs. Activated p38 MAPKs then phosphorylate several substrates, such as transcription factors and other kinases. Continuous lines indicate well established interactions *in vivo*; dashed lines indicates interactions derived from *in vitro* data with limited confirmation *in vivo*.

Physiological substrates of p38 have been mainly identified thanks to the availability of commercial pyridinil imidazole inhibitors, such as SB203580 and SB202190, which specifically target the p38α and p38β isoforms. To subsequently confirm the specificity of each p38 isoform toward its substrates, mice deficient in each p38 isoform have been generated. Overall, activation of the p38 MAPK pathway leads to the phosphorylation of Ser/Thr residues of its substrates which include wide range of transcription factors and kinases, such as the MAPK-activated protein kinases (MAPKAPs or MKs) MK2, MK3

and MK5; the mitogen- and stress-activated kinases (MSKs) MSK1 and MSK2 and the MAPK-interacting kinases (MNKs) MNK1 and MNK2 ((Kotlyarov and Gaestel, 2007); Figure 2).

2.2. Regulation of gene expression by p38 MAPK

Transcription is an important process in the regulation of gene expression, tissue and organ development and also in tumorigenesis (Levine and Tjian, 2003). Transcriptional initiation requires interaction between transcription factors and their regulatory sequences on the promoters of specific genes, which is often preceded by remodelling of local chromatin structures (Levine and Tjian, 2003; Orphanides and Reinberg, 2002).

One of the most important roles of p38 MAPK in the coordination of the cell responses is at the level of gene expression, mostly through the regulation of DNA transcription as well as mRNA translation. A number of cellular processes require p38-mediated transcriptional regulation. For instance, inflammation (Saklatvala, 2004), differentiation (Lluis et al., 2006), angiogenesis (Carter et al., 1999; Gauthier et al., 2005) and apoptosis (Bulavin et al., 1999; Cuadrado et al., 2007; Porras et al., 2004), were all shown to be regulated by p38 MAPK through gene expression-dependent mechanisms, the most prevalent of which consisting in the phosphorylation-dependent regulation of transcription factors, both activators and repressors (Perdiguero, 2008). Transcription factors activated by p38 MAPK include p53, which induces the expression of proteins involved in cell cycle arrest (i.e. $p21^{Cip1}$ or 14-3-3) and apoptosis (i.e. Apaf-1, Noxa) (Bensaad and Vousden, 2005), MEF2, which regulates the expression of muscle-specific genes required for muscle differentiation (Lluis et al., 2006), and NF-κB, which induces expression of various pro-inflamatory and pro-survival proteins (Karin, 2006). p38 MAPK can also phosphorylate and activate various transcriptional repressors, i.e. HBP1, which represses the expression of various genes, including cyclin D1 (Yee et al., 2004). Of note, transcription factors can be either phosphorylated directly by p38 MAPK or indirectly through downstream kinases (Figure 3).

p38 MAPKs can also play other fundamental roles in gene transcription in a transcription factor-independent manner (Crump, 2007). For instance, p38 has been shown to phosphorylate and activate the TATA-binding protein (TBP) that, when activated, binds to the TATA element on gene promoters and nucleates the assembly of transcription complexes, thus inducing gene expression. Accordingly, p38 MAPK has been shown to prime the expression of NF-*k*B and AP-1 target genes through this mechanism (Carter et al., 1999; Carter et al., 2001). Furthermore, a recently discovered mechanism of transcriptional regulation by p38 MAPK, which has been shown to be

conserved from yeast to humans (Alepuz et al., 2003; Perdiguero et al., 2007; Proft et al., 2006), consists in the recruitment of RNA polymerase II to target gene promoters. Interestingly, p38 is also currently emerging as a key regulator of gene transcription at another level, namely by inducing the remodelling of the chromatin structure around target genes (Crump, 2007). Finally, p38 MAPK has also been recently found to act as a transcriptional elongation factor in yeast (Pascual-Ahuir et al., 2006; Pokholok et al., 2006; Proft et al., 2006), although it remains to be determined whether this p38 role is conserved as well in higher eukaryotes.

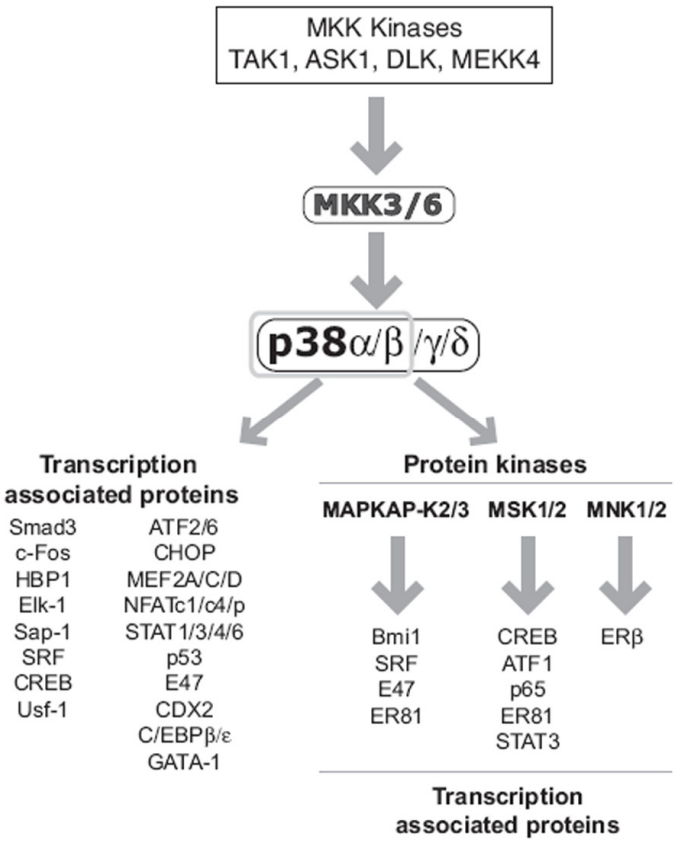

Figure 3. Regulation of gene expression by p38 MAPKs. p38 MAPKs can regulate gene expression by modulating the activity of multiple transcription factors, either by direct phosphorylation or through their downstream kinases MKs, MSKs and MNKs. p38α and p38β have been more intensively studied in this context. Adapted from (Perdiguero, 2008).

The interplay between p38 and downstream MSKs is important for the regulation of gene transcription (Figure 3). Conversely, MKs and MNKs have been reported as central coordinators of the regulation of mRNA translation by p38 MAPK (Kotlyarov and Gaestel, 2007). They have been proposed to act at different levels within the mRNA translation machinery. Namely, whereas MNKs mainly act at the level of translation initiation

(Kotlyarov and Gaestel, 2007), such as by phosphorylating and activating the translation eukaryotic initiator factor 4E (eIF4E) (Waskiewicz et al., 1999), MKs act in concert with p38 MAPK in the stabilization of mRNA transcripts (Kotlyarov and Gaestel, 2007). The latter is normally coordinated by modulating the binding to RNA as well as the expression levels of certain proteins, such as Tristetrapolin (TTP) and HuR, which in turn regulate mRNA stability in an AU-rich element (ARE)-dependent manner (Waskiewicz et al., 1999). Noteworthy, whereas the activation of p38 MAPK is normally associated with the stabilization of mRNA transcripts (Saklatvala, 2004), it has also been shown that certain mRNAs can be destabilized by p38 or its downstream kinases (Ambrosino et al., 2003). Of note, whereas the regulation of gene transcription is important for p38 to regulate cell differentiation (Lluis et al., 2006; Perdiguero, 2008), its involvement in translational regulation seems to be critical for the pro-inflammatory roles (Saklatvala, 2004).

3. Cellular functions of p38α MAPK in malignant transformation

In addition to the well established roles in survival and inflammation, p38α has also been associated during the last ten years with the process of cell transformation (Bulavin and Fornace, 2004; Dolado et al., 2007; Nebreda and Porras, 2000).

3.1. The process of malignant cell transformation

The adjective “transformed” normally refers to a cell that has lost some growth control mechanisms and likely acquired at least one of the following capabilities: independence of mitogenic signals to proliferate, evasion of programmed cell death (apoptosis), insensitivity to anti-growth signals, unlimited replicative potential, ability to invade and metastatize and also to induce angiogenesis (Hanahan and Weinberg, 2000). These pathological capabilities are acquired progressively by the future tumor cell during the process of malignant transformation, which refers to all cellular changes associated with the conversion of normal cells into tumorigenic ones. For instance, normal cells rely on exogenous mitogenic signals before they can transit from a quiescent state into an actively proliferating one, which is mainly controlled by the Ink4a/pRb pathway (Hanahan and Weinberg, 2000). These signals are transmitted into the cell by mitogenic transmembrane receptors that interact with intracellular signaling molecules. In contrast, transformed cells are able to proliferate in the absence of exogenous mitogenic stimulation, which makes them refractory to normal homeostatic regulation (Hanahan and Weinberg, 2000). This is possible because some oncogenes like Ras, Raf or Src are able to provide a sustained endogenous supply of mitogenic signals within the transformed cell, hence mimicking the situation of continuous

exogenous mitogenic stimulation (Hanahan and Weinberg, 2000). Furthermore, it is believed that the cell types composing the tumor environment (i.e. fibroblasts, inflammatory cells, endothelial cells) can also contribute to the independence of tumor cells from extracellular mitogens, for instance by continuously providing certain proliferative cytokines (Comoglio and Trusolino, 2005; Tlsty and Hein, 2001).

Once the cell has become transformed and has acquired most of the pathological capabilities mentioned above, it is then normally able to form macroscopic tumors *in vivo* and/or to invade and metastatize. These cells are termed tumorigenic or cancerous, respectively. The latter represent the ultimate achievement in cell transformation and underlay the true malignant nature of cancer (Chambers et al., 2002).

3.2. Overview of p38α roles in malignant transformation

p38α has been demonstrated in recent years, *in vitro* as well as *in vivo,* to be a potential tumor suppressor (Bulavin and Fornace, 2004; Dolado et al., 2007; Ventura et al., 2007). Inactivation of p38α enhances malignant transformation whereas its persistent activation inhibits tumorigenesis. Consequently, the p38 MAPK field has experienced an increasing interest in unveiling the functions of p38α in the context of oncogene-induced cellular transformation. For instance p38α has been shown to counteract oncogenic signals by inducing cell cycle arrest (Chen et al., 2000) and senescence (Haq et al., 2002; Wang et al., 2002).

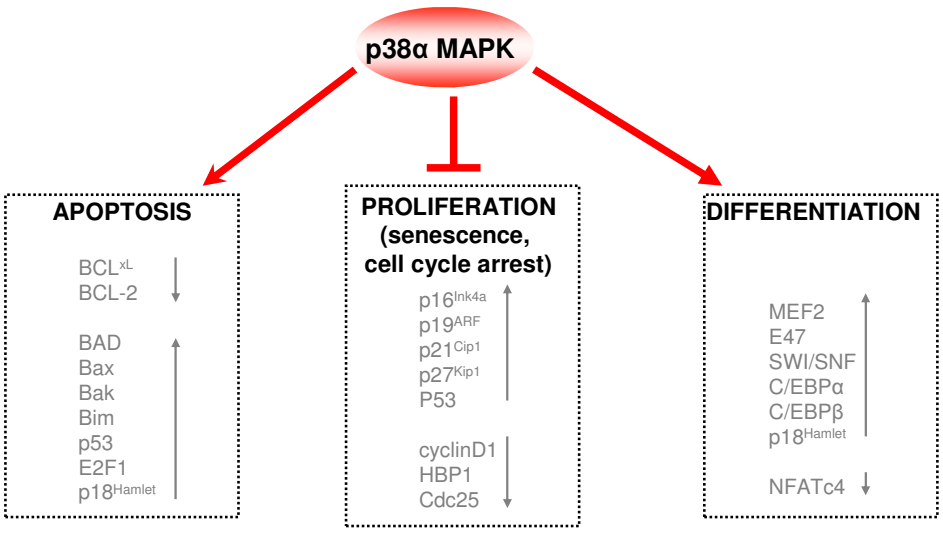

Figure 4. p38α MAPK pathway and tumor suppression. p38α coordinates various tumor suppressor functions through numerous downstream targets. These mostly affect the induction of apoptosis or differentiation and the inhibition of proliferation. Interestingly, whereas p38α modulates apoptosis and proliferation through both transcriptional (i.e. $p16^{Ink4a}$, cyclinD1) and post-transcriptional mechanisms (i.e. phosphorylation of Bcl-2 or Cdc25), the regulation of cell differentiation by p38α is mostly mediated by transcription factors. Arrows-up, positively regulated by p38α MAPK; arrows-down, negatively regulated by p38α MAPK.

In particular, the negative regulation of proliferation and the induction of differentiation by p38α were shown to mediate its inhibitory role on Ras-induced lung tumorigenesis *in vivo*

(Ventura et al., 2007). Furthermore, p38α has been found more recently to coordinate other tumor-suppressor mechanisms, such as the induction of apoptosis, which has consolidated the early association between p38α and tumor suppression (Figure 4). Of note, whereas much has been learnt on the functions of p38α in cancer, very little is known about the implication of other p38 family members in this process.

In support of the *in vivo* tumor suppressor activity of p38α, several proteins that inhibit p38α activity were found overexpressed in tumors and cancer cell lines. These include the phosphatases PPM1D/Wip1 and DUSP26/Mkp8 as well as the glutathione S-transferase members Gstm1 and Gstm2, which are inhibitors of apoptosis signal-regulating kinase 1 (ASK1), an upstream activator of p38 MAPK (Bulavin et al., 2002b; Dolado et al., 2007; Yu et al., 2007).

3.3. p38α functions in apoptosis

Apoptosis, a naturally occurring type of cell death, is an important process to prevent oncogenesis by removing genetically damaged cells (Lennon et al., 1991). Alterations in apoptotic/survival programs of the cell play an important role in cancer. Consequently, many proteins responsible for cell survival have been found upregulated in tumors, whereas numerous pro-apoptotic proteins have been found mutated or silenced in cancer (Johnstone et al., 2002).

Within the intracellular proteins regulating cell survival, p38 MAPKs play a major role, mostly by inducing apoptosis in response to numerous stimuli (Nebreda and Porras, 2000). For instance, p38α was previously shown to mediate apoptosis in cardiac cells (Wang et al., 1998) and neurons (Ghatan et al., 2000) upon stimulation with tumor necrosis factor-α (TNF-α) (Valladares et al., 2000) or transforming growth factor-β (TGF-β) (Edlund et al., 2003). p38α has been also shown to induce apoptosis in response to chemotherapeutic drugs (Olson and Hallahan, 2004), UV irradiation (Bulavin et al., 1999), serum withdrawal and substrate detachment (Fassetta et al., 2006; Porras et al., 2004), or in response to oxidative stress (Dolado et al., 2007). The mechanisms involved include phosphorylation-dependent inactivation of pro-survival proteins such as Bcl-2 and Bcl_{xL} (De Chiara et al., 2006; Farley et al., 2006; Grethe et al., 2004) as well as activation of mitochondrial pro-apoptotic proteins, namely BAD, Bim, Bax and Bak (Cai et al., 2006; Grethe et al., 2006; Kim et al., 2006). Additionally, *de novo* transcription of pro-apoptotic genes such as Fas, Bax, and Apaf-1 by the transcription factors p53, E2F1 or STAT3 mediate the regulation of both the extrinsic (via cell death receptors) and intrinsic (via mitochondria) apoptotic pathways by p38α MAPK (Bulavin et al., 1999; Hou et al., 2002; Porras et al., 2004; Sanchez-Prieto et al., 2000). Recently, a new p38α substrate has been identified, $p18^{Hamlet}$, which has been shown to contribute to the DNA damage-

induced apoptosis downstream of p38α by stimulating the expression of p53-regulated pro-apoptotic genes (Cuadrado et al., 2007). Moreover, a recent report has shown that p38α may sensitize cells to apoptosis by phosphorylating epidermal growth factor receptor (EGFR) and inducing its internalization (Zwang and Yarden, 2006), which shuts down EGFR pro-survival signaling.

3.4. Roles of p38α in cell proliferation

p38α was first recognized as a tumor suppressor based on the observation that it could inhibit the proliferation of oncogene-transformed cells *in vitro* (Chen et al., 2000). Consequently, the mechanisms by which p38α induces cell cycle arrest or cell cycle exit (i.e. senescence) in oncogene-transformed cells have been the subject of intense research. p38α has been shown to negatively regulate cell cycle progression, at both the G1 and G2 phases of the cell cycle, through transcriptional as well as post-translational mechanisms (Bulavin and Fornace, 2004). Of note, the anti-proliferative role of p38α has been recently shown to be of relevance *in vivo*, namely by determining the proliferative lifespan of hematopoietic stem cells (Ito et al., 2006).

3.4.1. p38α and senescence

Oncogene activation can lead sometimes to the process of premature senescence, which constitutes (together with apoptosis) an anti-cancer defense mechanism of primary cells. For instance, a well characterized model of premature senescence is that induced by oncogenic Ras genes in primary fibroblasts (Serrano et al., 1997).

Recent studies have shed light on the role of p38α in oncogene-induced senescence triggered by active Ras or its downstream effector Raf-1, which is a MAP3K. Namely, active Ras or Raf-1 have been shown to require p38α activity to induce premature senescence in human and mouse primary fibroblasts (Bulavin et al., 2002b; Bulavin et al., 2003; Wang et al., 2002). It seems that the MAP2Ks MKK3 and MKK6 are responsible, downstream of Ras/Raf, for constitutive activation of p38α and subsequent induction of senescence (Bulavin et al., 2002b; Wang et al., 2002). Of note, MKK3/6 activation by Ras/Raf may be wired via the ERK pathway through a mechanism involving the generation of oxygen radicals (Nicke et al., 2005). Conversely, Wip1, a phosphatase that inactivates p38α, abolished Ras-induced senescence in primary lung fibroblasts (Bulavin et al., 2002b). Altogether, these results indicate that p38α plays an important role in the induction of premature senescence by Ras. Interestingly, not only Ras but also other oncogenes, like the v-erb-b2 erythroblastic leukemia viral oncogene homolog 2 (ErbB2) were shown to induce premature senescence via p38α (Trost et al., 2005).

Regarding the signaling downstream of p38α that mediates Ras-induced senescence, increased expression of $p16^{Ink4a}$ was observed upon stimulation of p38α activity by Ras (Bulavin et al., 2004; Wang et al., 2002). Additionaly, p53 and p38-regulated or activated protein kinase-PRAK (also known as MAPKAP5 or MK5) were shown to be involved as well in the induction of premature senescence downstream of p38α (Sun et al., 2007). PRAK seems to be necessary for the Ras-induced transcriptional activity of p53. Following activation by the Ras-p38α cascade, PRAK directly phosphorylates p53 on Ser37 and this is necessary for p53 to activate transcription and mediate Ras-induced senescence.

3.4.2. Cell cycle regulation

Deregulation of the normal cell cycle machinery is considered a hallmark of cell transformation and cancer (Hanahan and Weinberg, 2000). Not surprisingly, tumor cells normally accumulate alterations in proteins restraining cell cycle progression, which provides them with a defective response to anti-mitogenic signaling and a limitless proliferative potential. Such proteins are normally nodal regulators of the cell cycle checkpoints. Two major cell cycle checkpoints have been characterized in mammals, that is the G1/S checkpoint, prior to DNA synthesis, and the G2/M checkpoint, prior to cell division (Zhou and Elledge, 2000). Consequently, the vast majority of cancer cells show an impaired control at the G1 and G2 phases of the cell cycle that allows them to continuously proliferate totally “unchecked” and further accumulate other genetic/genomic alterations (i.e. chromosomal instability) (Kawabe, 2004) .

At the molecular level, the mammalian cell cycle is regulated by a family of cyclin-dependent kinases (CDKs), the activity of which is controlled by its activators (cyclins) and inhibitors (Ink4, Cip and Kip families) (Malumbres and Barbacid, 2009) in each phase of the cell cycle (Figure 5). CDK4 and CDK6 are involved in early G1, whereas CDK2 is required to complete G1 and initiate S-phase (Malumbres and Barbacid, 2001). When cells re-enter the cell cycle from G0, D-type cyclins are upregulated and form complexes with CDK4 and CDK6 (Sherr and Roberts, 1995), which are subsequently activated by the CDK activating kinase (Cak) (Kato et al., 1994; Matsuoka et al., 1994). Later on, cyclin D-CDK complexes phosphorylate the Retinoblastoma protein (pRb), which induces the dissociation of E2F from the phosphorylated pRb into its free, transcriptional-competent form. The E2F transcription factor is then responsible for the transcription of a number of genes (Weinberg, 1995), among which is cyclin E, the activating partner of CDK2. Cyclin E-CDK2 complexes hyper-phosphorylate Rb, further activating E2F and creating a positive feedback loop.

In contrast to cyclins, the CKI (cyclin kinase inhibitor) proteins inhibit cell cycle progression by downregulating CDK activity. Members of the *Ink4/Arf* family of CKIs ($p15^{Ink4b}$, $p16^{Ink4a}$, $p18^{Ink4c}$ and $p19^{Arf}$) inhibit the activity of both CDK4 and CDK6, whereas members of the Kip/Cip family of CKIs ($p21^{Cip1}$, $p27^{Kip1}$ and $p57^{Kip2}$) may additionally inhibit the activity of CDK2 by binding both to cyclin E/CDK2 and cyclin A/CDK2 complexes (Sherr and Roberts, 1995). Kip/Cip proteins can also impinge on the activity of cyclin B/CDK1 complexes at G2/M (Figure 5).

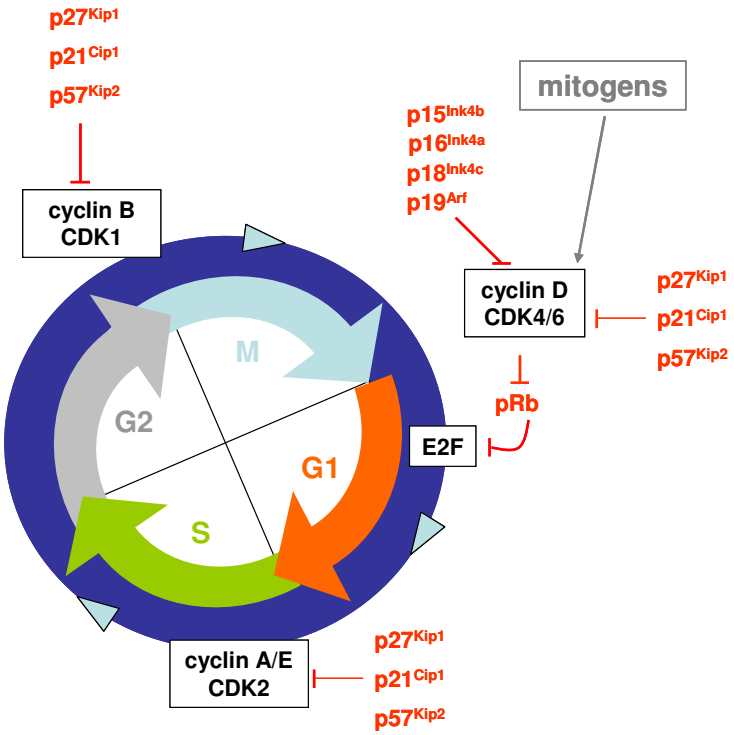

Figure 5. Simplified scheme of the mammalian cell cycle. The mammalian cell cycle consists of four phases, namely the control stages of G1 and G2, the DNA-replicating S phase and the M phase, where a tetraploid cell divides into two diploid daughter cells. Cell cycle progression is governed by a class of serine-threonine kinases, named cyclin-dependent kinases (CDKs), which are enzimatically activated by association with regulatory subunits called cyclins, phosphorylation by other kinases (i.e. Cak proteins) or inhibited by binding to negative regulators, such as the CDK inhibitors $p15^{Ink4b}$, $p16^{Ink4a}$, $p18^{Ink4c}$, $p19^{Arf}$, $p21^{Cip1}$, $p27^{Kip1}$ and $p57^{Kip2}$. As shown, mitogenic stimulation is the entry point to the cell cycle through G1.

3.4.2.a) Role of p38α

p38α has been shown to play an important role in the negative regulation of the G1/S and G2/M transitions through different mechanisms. For instance, p38α activity can contribute to the induction of the G1/S checkpoint in response to stimuli such as osmotic stress, reactive oxygen species (ROS) and oncogenic stress (Thornton and Rincon, 2009). p38α has been shown to induce cell cycle arrest at G1/S by transcriptionally inducing $p16^{Ink4a}$ (Bulavin et al., 2004; Wang et al., 2002) or by negatively regulating cyclin D1 expression ((Lavoie et al., 1996; Molnar et al., 1997); Figure 4). p38α may also

coordinate phosphorylation-mediated mechanisms that result in degradation of D-type cyclins (Casanovas et al., 2004; Casanovas et al., 2000) and Cdc25A (Goloudina et al., 2003) or in stabilization of $p21^{Cip1}$ and cell cycle arrest (Kim et al., 2002; Stepniak et al., 2006). p38α can also induce a G1/S checkpoint through the activation of p53, which also results in $p21^{Cip1}$ accumulation (Kim et al., 2002; Kishi et al., 2001). Moreover, p38α can sense the accumulation of ROS and induce the upregulation of $p16^{Ink4a}$ and $p19^{Arf}$, which in turn limits the lifespan of hematopoietic stem cells (Ito et al., 2006).

Apart form G1/S, p38α activity has been also associated with the regulation of the G2/M transition, both *in vitro* and *in vivo* (Diehl et al., 2000; Garner et al., 2002; Pedraza-Alva et al., 2006). p38α has been shown to be efficiently activated in late G2 after DNA-damaging agents like UV light, γ-irradiation and inhibitors of topoisomerase II or histone deacetylase (Bulavin et al., 2002a; Mikhailov et al., 2005). Mechanistically, MAPKAP kinase 2 (MK-2) has been identified as a key mediator of the p38-induced G2/M arrest (Manke et al., 2005). Thus, p38α phosphorylates and activates MK-2, which in turn phosphorylates Cdc25B and Cdc25C. This mediates Cdc25B/C binding to 14-3-3 proteins and their subsequent shuttling to the cytoplasm, which prevents Cdc25B/C from dephosphorylating (and activating) CDK1 and consequently induces a G2-phase delay (Bulavin et al., 2001; Lindqvist et al., 2004; Manke et al., 2005).

3.4.2.b) Role of $p27^{Kip1}$

$p27^{Kip1}$ was first identified as a CKI due to its ability to block the activity of cyclin E/CDK2 and cyclin A/CDK2 in G1-arrested cells by lovastatin, TGF-β or contact inhibition (Hengst et al., 1994; Koff et al., 1993; Polyak et al., 1994; Slingerland et al., 1994). $p27^{Kip1}$ protein levels are especially high in the quiescent state (G0), where CDK activity levels are almost undetectable. However, $p27^{Kip1}$ abundance is highly variable throughout the cell cycle, ranging from high levels in G0 and early G1 phase to low or almost undetectable protein levels when the cell cycle progress into the S and G2/M phases (Bloom and Pagano, 2003). There are many mechanisms aimed to regulate $p27^{Kip1}$ levels and function, including transcriptional regulation, post-translational modifications and nucleo-cytoplasmic shuttling (Figure 6); with the proteasome-mediated degradation of $p27^{Kip1}$ following phosphorylation being the most common one (Bloom and Pagano, 2003). Namely, $p27^{Kip1}$ was reported to be efficiently degraded in the nucleus during G1/S after phosphorylation on Thr187 by cyclin E-CDK2 complexes, which serves as a recognition site for the SKP2-SCF E3 ubiquitin ligase that primes the protein for proteasomal degradation (Tsvetkov et al., 1999). Other post-translational mechanisms involve phosphorylation on the stabilizing residue Ser10 (Ishida et al., 2000) as well as on various destabilizing residues. For instance, the tyrosine kinases

Src, Lyn and Bcr-Abl have been recently shown to induce $p27^{Kip1}$ proteasomal degradation via phosphorylation on the tyrosine residues Tyr74, Tyr88 and Tyr89 (Chu et al., 2007; Grimmler et al., 2007). Similarly Akt can phosphorylate $p27^{Kip1}$ on Thr157 and induce its nuclear export (Kim et al., 2009). Of note, cytoplasmic $p27^{Kip1}$ does not have an inhibitory function on the cell cycle because it cannot bind CDK/cyclin complexes. In contrast, cytoplasmic $p27^{Kip1}$ can promote cell migration and tumorigenesis by regulating actin cytoskeleton through the modulation of RhoA activity. Accordingly, $p27^{Kip1}$ has been recently reported to be oncogenic when it cannot inhibit CDKs (Besson et al., 2008).

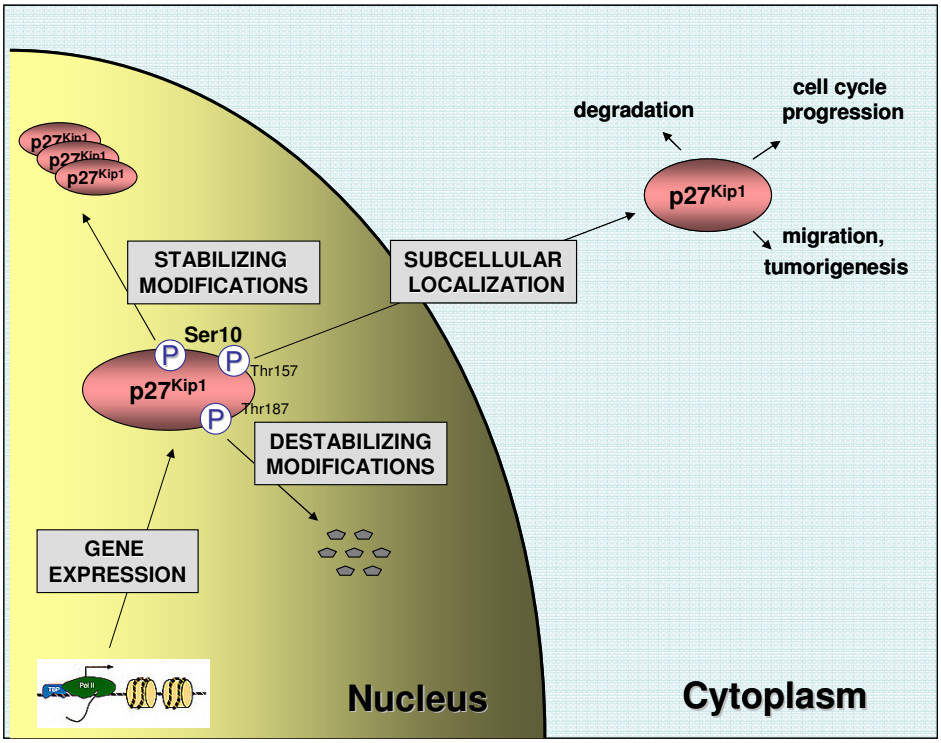

Figure 6. Schematic representation of the cellular mechanisms regulating $p27^{Kip1}$ abundance. $p27^{Kip1}$ is regulated at the level of transcription, post-translational modifications and subcellular localization.

4. Emerging roles of p38α in cell transformation: Control of anti-growth signals

During progression towards malignancy, transformed cells must not only self-produce mitogenic signals but also overcome certain external anti-proliferative stimuli, such as those inducing cell differentiation or imposed by high cellular density (Hanahan and Weinberg, 2000). These growth-inhibitory signals, usually relied by transmembrane surface receptors coupled to intracellular signaling pathways (Hanahan and Weinberg, 2000), are important to maintain proper tissue homeostasis. They normally block proliferation either by directing the cell cycle into quiescence or early G1 arrest, or by

inducing the cells into post-mitotic states usually associated with the acquisition of specific differentiation-associated traits (Hanahan and Weinberg, 2000).

4.1. Differentiation

Cellular differentiation is the process by which progenitor cells give rise to specialized cell types in a multicellular organism. Along this process, cells lose their proliferative abilities and exit the cell cycle. Accordingly, the vast majority of human tumors show differentiation defects (Potter, 1978) and differentiated cells within a tumor are usually weakly tumorigenic (Houghton et al., 2006). Consequently, tumor cells use various strategies to block terminal differentiation, such as overexpression of oncogenes like c-Myc (Foley and Eisenman, 1999), Notch in breast, pancreatic and lymphoid cancer (Sjolund et al., 2005) or Bcr-Abl in leukemia (Klein et al., 2006).

During the past few years, p38 MAPK has been established as an important regulator of myogenesis, the process by which myoblasts are converted to differentiated myotube (Cuenda and Cohen, 1999; Li et al., 2000; Wu et al., 2000). Sustained activation of p38 MAPK leads to upregulation of myogenic markers (Figure 4) and accelerates myotube formation. The mechanisms implicated involve the enhancement of the transcriptional activity of the myocyte enhancer factor-2 (MEF2) along with the phosphorylation of E47. These in turn, control the activation of muscle differentiation-specific genes (Lluis et al., 2005; Zetser et al., 1999; Zhao et al., 1999), the promotion of cell cycle exit prior to the onset of cell differentiation (Perdiguero et al., 2007), or the targeting of chromatin-remodelling enzymes to specific loci, thereby facilitating gene transcription (reviewed in (Crump, 2007; Perdiguero, 2008)). Apart from myogenesis, p38α has also been shown to be an important regulator of cellular differentiation in adipogenesis, neuronal plasticity, early stages of osteoclastogenesis from bone marrow precursors as well as in intestinal epithelial cell differentiation (Bost et al., 2005; Feng, 2005; Houde et al., 2001; Huang et al., 2006; Nebreda and Porras, 2000; Pickering et al., 2005). Importantly, forced activation of p38α in several human cancer cell lines (i.e. colon, muscle rhabdomyosarcoma or renal carcinoma) promotes differentiation and induces a less malignant phenotype (Daniel et al., 2004; Finn et al., 2004; Puri et al., 2000). In agreement with this, p38α deficiency in mouse lungs bearing K-Ras^{V12} facilitates tumorigenesis due to impaired stem/progenitor cell differentiation (Ventura et al., 2007). p38α has also been shown to induce the *in vitro* differentiation of embryonic stem cells into cardiomyocytes (Aouadi et al., 2006; Schmelter et al., 2006), as well as to mediate proliferation arrest in mesenchymal stem cells, which was concomitant with the onset of differentiation (Forte et al., 2006).

4.2. Contact inhibition

The proliferation of non-transformed cells is controlled by mitogenic and anti-mitogenic signals. It is believed that antiproliferative signals are imposed by cell-cell contacts, a cellular mechanism which is referred to as contact inhibition (Eagle and Levine, 1967). Actually, the term contact inhibition was coined half a century ago to refer to the process by which cells stop proliferating when they reach confluence (Abercrombie, 1979), ensuring constant tissue homeostasis in multicellular organisms (Carter, 1968). For example, contact inhibition ensures the proper size of each organ within an organism during the regeneration process after tissue injury. Upon reaching the proper organ size, cells stop dividing to ensure that the regenerating organ does not over-grow (Zeng and Hong, 2008). Normally, non-transformed cells arrest at G0/G1 as a confluent monolayer upon achievement of high cellular densities, whereas transformed cells are characterized by the emergence of multilayered foci (Figure 7). Accordingly, deregulation of contact inhibition leads to hyperplasia *in vivo* and facilitates tumor progression by providing the incipient malignant cell with unrestrained proliferative capabilities (Abercrombie, 1979). Not surprisingly, the majority of cancer cells are refractory to the confluence-induced proliferation arrest (Hanahan and Weinberg, 2000) and loss of contact inhibition is actually used as an *in vivo* prognostic factor in human cancer (Fuse et al., 2000).

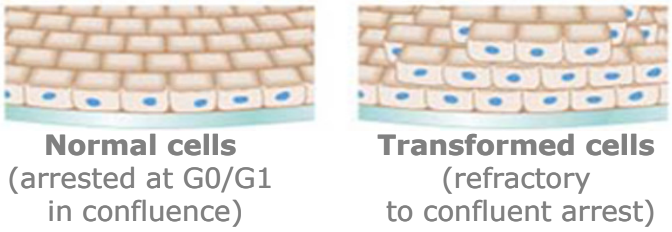

Figure 7. Contact-dependent inhibition of proliferation. Cells normally arrest proliferation when a single layer of cells is formed (left). In contrast, transformed cells continue proliferating after achieving saturation densities and progress through the cell cycle to grow in multilayers (right).

4.2.1. Signaling pathways regulating contact inhibition

In spite of the biological significance and potential diagnostic value of contact inhibition, the molecular mechanisms underlying this process have been elusive. Several hypotheses were proposed in the past to explain the onset of the contact-dependent growth arrest, such as the release of inhibitory compounds by the cells themselves (Koga et al., 1986; Lipkin et al., 1978), the influence of cell shape on growth (Folkman and Moscona, 1978) or the exhaustion of nutrients or growth factors in the culture medium (Holley and Kiernan, 1968). Nowadays, it is believed that membrane proteins act as sensors of cell-cell contacts (Curto and McClatchey, 2008; Heimark and Schwartz, 1985; Kinders et al., 1980), whereas at the other end, there is evidence indicating that

CDK inhibitors play a key role in the proliferation arrest. Namely, $p16^{Ink4a}$ (Wieser et al., 1999), $p27^{Kip1}$ (Polyak et al., 1994) or $p21^{Cip1}$ (Cho et al., 2008; Yanagisawa et al., 1999) have been shown to mediate the contact inhibition response in certain scenarios, although the signaling pathways leading to their upregulation as well as their individual contributions to the process are not well understood. Actually, $p27^{Kip1}$ was originally characterized as a protein inducing cell cycle arrest (by inhibiting CDK2/cyclin E complexes) in response to confluent growth in mammals (Polyak et al., 1994), in agreement with the fact that $p27^{Kip1}$-null mice display organ hyperplasia (Nakayama et al., 1996). Similarly, the *Ink4a*/*Arf* family member $p16^{Ink4a}$ has been also associated with the contact inhibition response through the inhibition of the CDK4-cyclin D1 complex, which is responsible for the inactivation of the gatekeeper for the G1/S transition, pRb (Wieser et al., 1999). As a consequence, pRb remains in its hypophosphorylated, active state and inhibits progression into S phase (Polyak et al., 1994; Wieser et al., 1999). Of note, p53 was shown to stimulate $p16^{Ink4a}$ expression to mediate cell-density growth arrest in G1 phase (Meerson et al., 2004). As for $p21^{Cip1}$, there is conflicting evidence on its role in contact inhibition as it can get either up- or downregulated in confluent cells depending on the cellular context (Perucca et al., 2009; Yanagisawa et al., 1999). Noteworthy, although $p27^{Kip1}$ and $p16^{Ink4a}$ have been consistently associated with the contact inhibition response, an open question concerns their degree of functional redundancy. Whatever this might be, the usual disruption of these two proteins in cancer may actually explain, at least in part, why virtually all cancer cells are non-responsive to contact inhibition.

Recent work has started to shed some light on the intracellular signals that regulate this process. For instance, the mammalian Hippo pathway, which was known to control organ size in *Droshophila*, has been proposed as an important regulator of contact inhibition in mammals (Zeng and Hong, 2008). In fact, the Hippo kinase (known as Mst1/2 in mammals) inhibits expression of proliferative and pro-survival proteins in confluence by inactivating the YAP transcription factor, which results in confluent cell cycle arrest (Zeng and Hong, 2008; Zhao et al., 2007). Conversely, interfering with the inhibition of YAP by Hippo/Mst facilitates cell transformation *in vitro* and results in organ hyperplasia *in vivo* (Zeng and Hong, 2008; Zhao et al., 2007).

But, how do cells transduce cell-cell contacts into activation of intracellular signaling pathways? The most obvious explanation is that membrane proteins in neighbouring cells interact as cells approach and this activates intracellular signaling pathways. However, although there are some membrane proteins described as mediators of contact inhibition, little is known about how they may get activated and subsequently engage intracellular signals in confluence (Gradl et al., 1995). It is assumed that upon

membrane contacts with neighbouring cells, non-transformed cells rely on membrane cadherins and/or proto-cadherins to trigger intracellular signals that ultimately lead to cell cycle arrest. For instance, N-cadherin in mammalian cells and the proto-cadherin Fat in *Drosophila Melanogaster* have been pointed out as possible membrane initiators of such signals, but solid evidence has to be provided yet. Downstream of these membrane proteins, β-catenin is also known to be important for contact inhibition by linking cadherins to the actin cytoskeleton (Dietrich et al., 2002; Gumbiner, 2000; Kemler, 1993). Thus, the loss of the cadherin/β-catenin complex leads to the disruption of contact inhibition and facilitates progress towards malignancy (Kato et al., 2005; Kudo et al., 2004; Salon et al., 2004; Vizirianakis et al., 2002). Accordingly, Gadd45a, a member of the growth arrest and DNA damage-inducible family of proteins was shown to be involved in regulation of contact inhibition by regulating β-catenin translocation to the cell membrane and cadherin binding. This was coupled to the depletion of β-catenin in the cytoplasm and nucleus, which in turn resulted in the downregulation of the β-catenin target gene cyclinD1 (Ji et al., 2007). Of note, Gadd45a was also shown to regulate contact inhibition downstream of $p27^{Kip1}$ (Zhang et al., 2003). Yet another membrane protein, NF2 (also known as Merlin) has been also previously connected to contact inhibition through the stabilization of adherent junctions (Curto et al., 2007) as well as by directly inhibiting EGFR pro-mitogenic signaling (Curto et al., 2007). Moreover, NF2 was also suggested to transmit signals from cell surface proteins to the Hippo core machinery, although the molecular mechanisms are scarce (Striedinger et al., 2008).

Noteworthy, it was previously shown that the stress-activated kinase p38α is involved in the regulation of contact inhibition as well. Indeed, confluent activation of p38α correlated in human and mouse fibroblasts with the upregulation of the cell cycle inhibitor $p27^{Kip1}$ (by unknown mechanisms) as well as with the induction of the subsequent proliferation arrest (Faust et al., 2005). Accordingly, genetic inactivation of p38α facilitated oncogene-induced malignant transformation of fibroblasts *in vitro* as well as tumorigenesis in nude mice (Dolado et al., 2007) and also resulted in organ hyperplasia *in vivo* (Ventura et al., 2007).

4.2.2. Deregulation of growth factor signaling in contact inhibition and cell transformation

It is important to understand the mechanisms underlying the density-dependent inhibition of growth in normal cells, as these may help to unveil how transformed cells overcome the density-dependent growth inhibition. On the one hand, it is well established that CKI proteins mediate the confluence-induced proliferation arrest. However, it was early acknowledged that contact inhibition is not only a matter of

inhibiting active proliferation in confluent cells, but also of desensitizing cell proliferation from further mitogenic stimuli (Curto and McClatchey, 2008; Levine et al., 1965). Hence, one possible mechanistic explanation for contact inhibition is that normal contact-inhibited cells are able to deplete the medium locally of growth factor activities, hence depriving its neighbours and inducing their proliferation arrest (Takahashi and Suzuki, 1996). Consistent with this idea, cultures of human skin epidermal carcinoma A431 cells displayed decreasing concentrations of soluble growth factors in the media as the cell density increased (Lichtner and Schirrmacher, 1990). However, a most likely possibility is that negative control mechanisms within confluent cells actually prevent the expression or activation of growth factor receptors independently of the availability of extracellular mitogenic factors (Takahashi and Suzuki, 1996). Not surprisingly, such cell surface receptors are found deregulated in cancer (Hanahan and Weinberg, 2000). For instance, growth factors receptors like EGFR (ErbB1/HER1) or HER2 (ErbB2/neu) have been found overexpressed in many cancers (Slamon et al., 1987; Yarden and Ullrich, 1988). Receptor overexpression may allow the cancer cell to become hyper-responsive to ambient levels of growth factors that normally would not trigger proliferation.

EGFR is a receptor tyrosine kinase (RTK) that belongs to the ErbB/HER family of ligand-activated RTKs. Other members of this family include ErbB2/Neu/HER2, ErbB3/HER3 and ErbB4/HER4 (Holbro et al., 2003). Over-activated RTKs can convert normal cells into malignant ones by providing them with sustained proliferative and anti-apoptotic signals as well as by promoting angiogenesis and metastasis (Arteaga, 2002). In particular, EGFR is a 170 kDa membrane protein, which consists of a single polypeptide chain of 1186 amino acids (Hunter, 1984; Ogiso et al., 2002) and is characterized by three main domains: an extracellular ligand binding domain, a transmembrane domain and an intracellular cytoplasmic domain that is responsible for the tyrosine kinase activity of the receptor (Holbro et al., 2003; Schlessinger, 2000). EGFR can bind several ligands such as epidermal growth factor (EGF), transforming growth factor (TGF), betacellulin (BTC), epiregulin (EPR), heparin-binding EGF like growth factor (HB-EGF) and amphiregulin (AR) (Hynes et al., 2001). Ligand binding induces receptor dimerization and autophosphorylation in various tyrosine sites in its cytoplasmic domain (rewieved in (Zandi et al., 2007)). These phosphorylated tyrosine residues in turn serve as binding sites for adapter and signaling molecules, resulting in the activation of several downstream signaling cascades. The most widely characterized ones are the Ras-Raf-MEK-ERK, PI3K-Akt and PLCγ-PKC pathways, which lead to cellular proliferation, survival and motility when activated, respectively (Chen et al., 1994; Datta et al., 1997; Pages et al., 1993) (Figure 8).

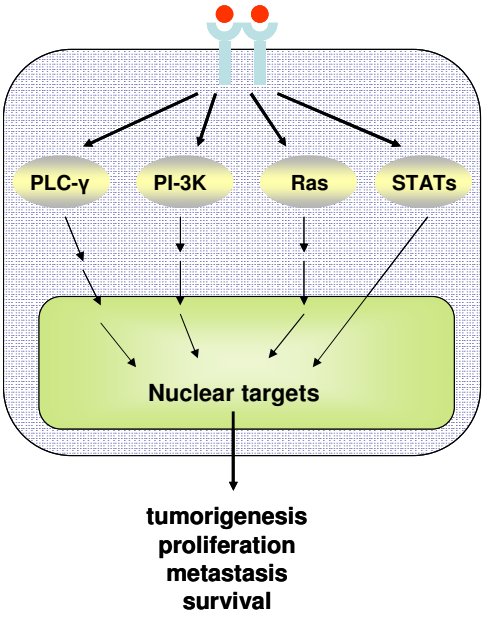

Figure 8. Simplified scheme of EGFR downstream signaling. Ligand binding to EGFR leads to receptor dimerization, autophosphorylation and activation of several downstream signaling pathways such as those of PLC-γ-CaMK/PKC, Ras-Raf-MEK-ERK, PI-3K-Akt-GSK and STATs. Activation of these signaling modules in turn leads to major cell responses such as survival and proliferation, among others.

4.2.2.a) Downregulation of EGFR by Cbl

For inactivation, EGFR needs to undergo dephosphorylation by tyrosine phosphatases or to be downregulated at the protein level. Indeed, receptor downregulation is the most widely described regulatory process to inactivate EGFR signaling. This involves EGFR internalization into endosomes followed by trafficking to and degradation in the lysosomes (Lipkowitz, 2003; Shtiegman and Yarden, 2003) (Figure 9). Of note, defective EGFR downregulation has been frequently linked to cell transformation due to sustained mitogenic signaling (Zandi et al., 2007). Mechanistically, the cytosolic domain of EGFR plays a crucial role in receptor downregulation, since it contains all the docking sites for the signaling molecules that participate in EGFR internalization and transport to the lysosomes. Consequently, a mutant EGFR form that lacks part of the intracellular domain responsible for receptor downregulation is oncogenic in mouse fibroblasts (Wells et al., 1990). This seems to be accounted for by the impaired interaction of the mutant receptor with its ubiquitin ligase cCbl, which promotes sustained EGFR mitogenic signaling (Wells et al., 1990).

cCbl is a RING finger type-E3 ubiquitin ligase that plays a prominent role in mediating ligand-dependent downregulation of RTKs (Thien and Langdon, 2001). The RING finger domain of cCbl is necessary for its E3 ubiquitin ligase activity (Joazeiro et al., 1999; Levkowitz et al., 1999) as it represents a binding site for an E2 ubiquitin-conjugating enzyme (Zheng et al., 2000), whereas its tyrosine kinase binding (TKB) domain is essential for substrate recognition (Levkowitz et al., 1999). Growth factor-induced activation of EGFR triggers its autophosphorylation followed by binding of cCbl to Tyr1045 on EGFR (Levkowitz et al., 1999). This induces the cCbl-mediated multiple mono-ubiquitination of EGFR (Mosesson et al., 2003) on the plasma membrane (Longva

et al., 2002). The receptor is then internalized via clathrin-coated pits by adaptor proteins such as Eps15 and subsequently progress through the endocytotic route (de Melker AA, 2004). First, in early endosomes, receptors are sorted either for recycling to the plasma membrane or destruction in the lysosome (Katzmann et al., 2002) (Figure 9).

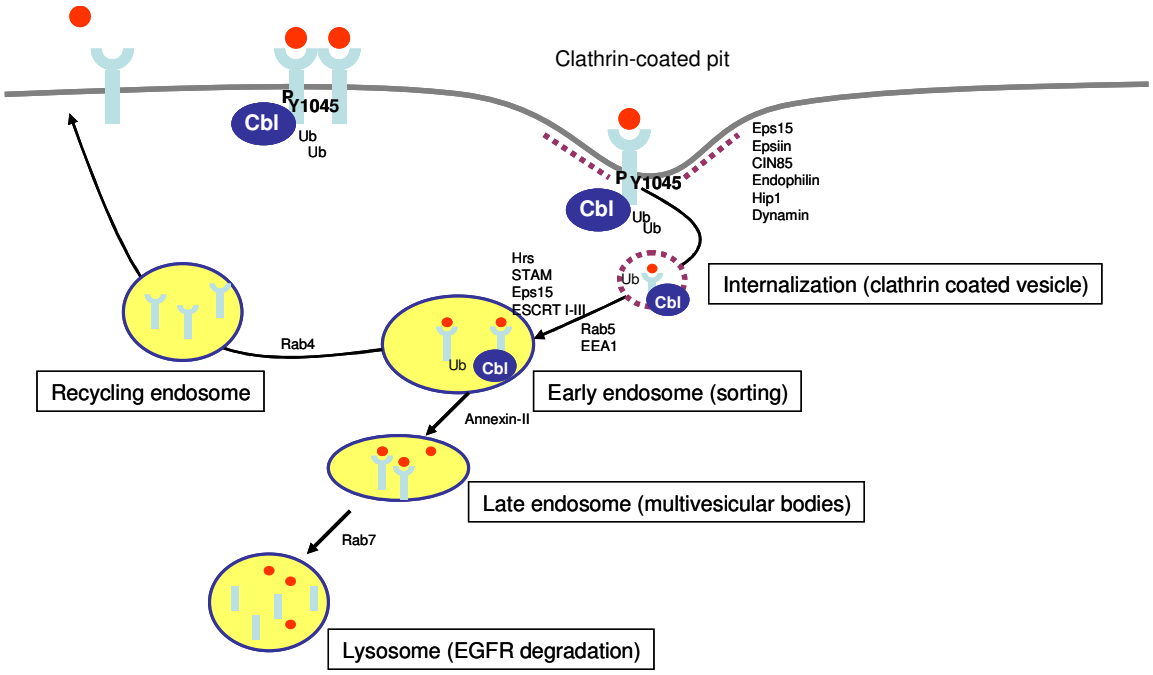

Figure 9. Mechanism of endocytic downregulation of EGFR. Ligand binding to EGFR triggers receptor autophosphorylation via receptor dimerization. cCbl associates with the active Y1045-phosphorylated EGFR in the plasma membrane and mediates its ubiquitination. This facilitates endocytosis of EGFR through clathrin-coated pits and subsequent trafficking to clathrin-coated vesicles (proteins such as Epsin, Eps15 or Hip1 are involved in cargo recruitment into clathrin-coated pits). The clathrin coated vesicle fuses then with an early endosome (where the sorting occurs), which is catalysed by the small GTPase Rab5 and its effector EEA1. Transport to early endosomes is mediated by Hrs, STAM and by ESCRT I-III. EGFR is probably dephosphorylated and deubiquitinated during the sorting step meanwhile it progresses to late endosomes and subsequent lysosomal degradation (Annexin-II participates in formation of late endosomes and Rab7 participates in transport of EGFR to lysosomes). EGFR can be also recycled back to the plasma membrane from early endosomes via the recycling endosomes if insufficiently ubiquitinated.

In the absence of cCbl recruitment, EGFR undergoes continuous recycling to the plasma membrane after mitogenic stimulation via early endosomes (Grovdal et al., 2004; Ravid et al., 2004). In contrast, cCbl binding to the receptor on Tyr1045 ensures proper trafficking of EGFR toward the lysosomes via late endosomes, followed by receptor degradation, which controls the intensity and duration of EGFR signaling. Consistent with this model, mutation of Tyr1045 leads to enhanced EGFR signaling that is more mitogenic than that of the WT protein (Levkowitz et al., 1999). Importantly, cCbl is crucial for EGFR sorting to lysosomes, wheras it seems that cCbl-mediated ubiquitination of

EGFR is not necessary for EGFR internalization from the plasma membrane (Duan et al., 2003; Grovdal et al., 2004; Ravid et al., 2004). Of note, cCbl can also bind to EGFR indirectly, through the adapter protein Grb2, which binds to the phosphorylated tyrosine residues 1086 and 1068 on EGFR (Zandi et al., 2007).

4.2.2.b) Regulation of Cbl function

cCbl function is negatively regulated by several proteins that are implicated in potentially carcinogenic signaling pathways (Polo et al., 2004). A well characterized negative regulator of cCbl-directed downregulation of EGFR is Sprouty2 (Spry2) (Swaminathan and Tsygankov, 2006). Spry2 belongs to the family of Sprouty proteins (Spry1, Spry2, Spry3 and Spry4) that were originally identified as antagonists of fibroblast growth factor (FGF) signaling during tracheal development in *Drosophila* (Hacohen et al., 1998). It has been shown that transient transfection of human Spry2 in cultured cells results in higher retention of EGFR on the cell surface despite growth factor stimulation (Wong et al., 2001). Indeed, the cCbl-mediated ubiquitination of EGFR is blocked by Spry2 and this in turn results in enhanced receptor recycling rather than lysosomal degradation, which causes persistent localization of EGFR at the plasma membrane and sustained mitogenic signaling (Wong et al., 2001).

Mechanistically, Spry2 binds to the RING-finger domain of cCbl in a constitutive manner and to the SH2-like domain of cCbl only following EGF stimulation, the latter being mediated by phosphorylation on Tyr55 of Spry2 by growth factor stimulation. Tyr55 on Spry2 functions as a docking site for the SH2 domain of cCbl and competes with cCbl binding to Tyr1045 in the activated EGFR (Hall et al., 2003; Rubin et al., 2005). Thus, Spry2 binding to cCbl relieves the negative regulation of EGFR by c-Cbl. Consequently, this inhibits EGFR endocytosis, resulting in the pathways downstream of EGFR, such as the Ras/MAPK pathway, being locked in an active state (Guy et al., 2003). Of note, Spry2 has a dual role in the regulation of RTK signaling since it may function as a negative regulator of fibroblast growth factor receptor (FGFR), vascular endothelial growth factor receptor (VEGFR) and Met (Guy et al., 2003; Rubin et al., 2005). In contrast, its function as an activator of RTK signaling is specific for EGFR and has been well established (Guy et al., 2003).

Aim of the work

The characterization of tumor suppressor proteins whose activity could be potentially stimulated for cancer therapy is an area of intense research. Accordingly, we have focused on the elucidation of two novel tumor suppressor mechanisms coordinated by p38α early in the process of malignant cell transformation:

1. Characterization of the mechanisms mediating the regulation of contact inhibition by p38α.

   A major aim of the work has consisted in unveiling the molecular circuitry coordinated by p38α to induce contact inhibition in confluence. The motivation underneath has come from the fact that contact inhibition is one of the first steps by-passed by transformed cells in their course towards malignancy. Furthermore, p38α MAPK was recently identified in our laboratory as a novel regulator of contact inhibition, since its activity increased upon achievement of high cellular densities and correlated with the confluence-induced proliferation arrest. However, the mechanisms responsible for this p38α function were largely unknown.

2. Identification of new transcriptional targets of p38α MAPK in the regulation of malignant transformation.

   The vast majority of tumor suppressor mechanisms coordinated by p38α have been reported to occur at the post-translational level, despite the recognized effect of p38α in the regulation of gene transcription and the profound changes in gene expression that normally accompany cancer progression. Thus, we have aimed to investigate the effect of p38α on the transcription of cellular proteins that may be linked to the process of malignant transformation.

Materials and Methods

1. Materials

1.1 Expression constructs

The human $p27^{Kip1}$ cDNA cloned into pBluescript-KS was obtained from the CNIO DNA collection (Gene Bank Accession number: NM_004064) and subcloned BamHI-EcoRI into pcDNA3.1, pGEX-KG and pBabe-puro. The S10A point mutation in $p27^{Kip1}$ was introduced by site-directed mutagenesis (QuickChange, Stratagene). The pBabe-puro-$p27^{Kip1}$-3M vector (Martin et al., 2005) was obtained from M. Barbacid (CNIO, Madrid, Spain). The constructs to express WT hSpry2 and the mutant hSpry2-Y55F in the pCEFL-KZ plasmid and the pLPCX retroviral vector were provided by J.M. Rojas (Madrid, Spain), (Martinez et al., 2007). The pcDNA3.1-based constructs encoding WT Siah2 or the ring finger mutant H99A/C102A (Siah2-RM) were a kind gift from Z. Ronai (Burnham Institute for Medical Research, La Jolla, CA, USA) (Khurana et al., 2006). The mutations T24A and S29A were introduced in Siah2 by site-directed mutagenesis and verified by DNA sequencing. The pRK5-HA-cCbl (Jozic et al., 2005) and the pcDNA3.1-HA-Ubiquitin constructs were kind gifts from J. Bravo (CNIO, Madrid) and I. Dikic (Goethe University Frankfurt, Germany), respectively. The pcDNA3.1-based constructs to express human EGFR WT and the mutant Y1045F (Zwang and Yarden, 2006) were kindly provided by Y. Yarden (The Weizman Institute of Science, Rehobot, Israel). To re-express p38α MAPK in p38α-deficient mouse fibroblasts in the rescue experiments, we used the retroviral construct MSCV-p38α (Ambrosino et al., 2003). pEFmplink-MKK6-DD and the bacterial expression constructs for GST-p38α and MBP-MKK6-DD were previously described (Alfonso et al., 2006; Ambrosino et al., 2003), as well as the pBabe-puro-H-Ras^{G12V} retroviral vector (Dolado et al., 2007). pEGFP was purchased from Clontech.

pBabe-puro-H-Ras^{V12} and pWZL-hygro-based constructs of Gstm2, Cd9, Mmp3, Egln3, Pmp22, Aig1, Ctsh, Nck2 and Rtn4 were used for the generation of retroviruses. Cloning details including origin of cDNAs, amplification primers and restriction sites are provided in Table 1. Myc-tagged versions of pWZL-hygro-Gstm2 and pWZL-hygro-Cd9 were prepared by site-directed mutagenesis on the non-tagged constructs and used to express Myc-Gstm2 or Myc-Cd9 in various cell lines. Myc-Gstm2 and Myc-Cd9 were also subcloned BamHI-EcoRI into pcDNA3.1 to generate the constructs pcDNA-Myc-Gstm2 and pcDNA-Myc-Cd9 used for transient transfection experiments in HEK293 cells.

Table 1. cDNA origin, cloning primers and restriction sites used for the 9 genes selected for functional validation

Gene name	Forward (5'-3')*	Reverse (5'-3')*	Restriction sites (5'–3')	cDNA collection
Aig1	cgGAATTCatggctcttgtcccctgtc	gtGTCGACtcaagctcacgccttccca	EcoRI-SalI	RIKEN
Mmp3	cgGGATCCatgaaaatgaagggtcttccg	cgGAATTCttaacaattaaaccagctattgc	BamHI-EcoRI	OBS
Cd9	cgGGATCCatgccggtcaaaggaggta	cgGAATTCctagaccatttctcggctcc	BamHI-EcoRI	RIKEN
Pmp22	cgGAATTCatgctcctactcttgttggg	gtGTCGACtcattcgcgtttccgcagg	EcoRI-SalI	MGC
Nck2	cgGGATCCatgacagaagaagtcattgtca	cgGAATTCtcactgtagggctcggacaa	BamHI-EcoRI	MGC
Rtn4	cgGAATTCatggtattgtcagcagagctg	ctGTCGACtcattctgctttgcacttcaat	EcoRI-SalI	MGC
Gstm2	cgGGATCCatgcctatgacactaggttac	cgGAATTCctactttgggttccaaaaggc	BamHI-EcoRI	RIKEN
Egln3	cgGGATCCatgcctctgggacacatcat	cgGAATTCtcagtctttagcaagagcaga	BamHI-EcoRI	MGC
Ctsh	cgGGATCCatgtgggctgcgctgcc	cgGAATTCttatacctgaggaatgggatag	BamHI-EcoRI	MGC

*, restriction sites are indicated in capital letters

1.2. Primary antibodies

Primary antibodies were generally diluted in 1% milk in PBS but phospho-specific antibodies were always diluted in 1% bovine serum albumin (BSA) in PBS. Their commercial references (in brackets) together with their dilutions and host species are provided in Table 2.

1.3. Secondary antibodies

Secondary antibodies used in Western Blotting were purchased from Molecular Probes and used at a concentration of 1mg/ml. These were:

- Alexa Fluor 680, goat anti-mouse IgG
- Alexa Fluor 680, goat anti-rabbit IgG
- Alexa Fluor 680, goat anti-rat IgG
- Alexa Fluor 680, donkey anti-goat IgG

1.4. Cell lines

Immortalized WT and p38α-/- MEFs, were established from primary MEFs derived from E11.5 and E12.5 embryos (Ambrosino et al., 2003) and were immortalized following the 3T3 protocol (Todaro and Green, 1963). Primary WT and $p27^{Kip1}$-/- MEFs (Kiyokawa et al., 1996) were kindly provided by A. Vidal (Univ. Santiago de Compostela, Spain) and subsequently immortalized by the 3T3 protocol. Human IMR90 lung fibroblasts, 293/Ampho cells and MDA-MB-231 breast cancer cells were obtained from the American Type Culture Collection (ATCC). Human kidney 293T cells were provided by M. Serrano (CNIO, Madrid) and used for transient infections. Human HEK293 cells and mouse NIH3T3 fibroblasts were also used for transient transfections.

Table 2. Primary antibodies used for Western Blotting and immunoprecipitations

Antibody	Dilution	Species
Santa Cruz Biotechnology		
$p27^{Kip1}$ (C19)	1:200	Rabbit
p38α (C20)	1:500	Rabbit
EGFR (1005)	1:200	Rabbit
$p21^{Cip1}$ (C19-G)	1:500	Goat
$p16^{Ink4a}$ (M-156)	1:200	Rabbit
phospho-Thr187-$p27^{Kip1}$ (SC-16324)	1:200	Rabbit
phospho-Y1173-EGFR (SC-12351)	1:100	Goat
cCbl (C-15)	1:200	Rabbit
Ubiquitin (P4D1)	1:100	Mouse
Siah2 (N-14)	1:200	Goat
Skp2 p45 (H-435)	1:200	Rabbit
Cell Signaling		
phospho-p38 MAPK (9211)	1:200	Rabbit
phospho-ERK (9101)	1:200	Rabbit
phospho-Akt (9271)	1:200	Rabbit
phospho-MAPKAP-K2 (3041)	1:200	Rabbit
phospho-Src (2101)	1:200	Rabbit
phospho-Y1045-EGFR (2237)	1:200	Rabbit
phospho-Y1068-EGFR (2234)	1:200	Rabbit
Sigma		
GFP	1:1000	Mouse
Tubulin (DM1A)	1:1000	Mouse
Sprouty2 (S1444)	1:500	Rabbit
BD Transduction Laboratories		
phospho-Ser/Thr (612543)	1:200	Mouse
Ras (clone18)	1:200	Mouse
Upstate Biotechnology		
phospho-Tyrosine (clone 4G10)	1:1000	Mouse
EGFR (06-129)	1:200	Sheep
Nck2 (07-100)	1:500	Rabbit
Novus Biologicals		
Egln3 (NB 100-303)	1:500	Rabbit

2. Methods

2.1. Mammalian cell culture

2.1.1. Maintenance and subculturing of cells

Cells were maintained in Dulbecco Modified Eagle's Medium (DMEM) supplemented with 10% heat-inactivated fetal bovine serum (FBS), 1% L-glutamine and 1% penicillin/streptomycin (all from GIBCO-Invitrogen) at 37ºC and 5% CO_2. To detach the cells for subculturing, cells were washed with PBS and incubated with 0.05% trypsin solution (Gibco-Invitrogen) for 5 min (0.5 ml of trypsin for 10 cm dish). Cells were subsequently resuspended in fresh media and passed to a new culture dish.

2.1.2. Cell harvesting

Cells were normally harvested for biochemical analysis following 2 washes with ice-cold PBS on ice, scrapping, resuspension in 2 ml of PBS and centrifugation at 2000 rpm and 4ºC for 5 min in 2 ml Eppendorf tubes. The supernatant was discarded and the cell pellet processed by lysis or frozen at -80ºC until required.

2.1.3. Cell freezing and thawing

Cells at 90% confluence in 10-cm dishes were trypsinized and resuspended in 5 ml of ice-cold freezing medium (90% fetal calf serum (Gibco-Invitrogen), 10% dimethyl sulfoxide) and subsequently dispensed as 1 ml aliquots into 1.5 ml cryo-tubes (Nunc). Cell suspensions were first stored at -80ºC for 2-3 days and then transferred to liquid nitrogen for long-term storage.

For thawing, vials were gently warmed at 37ºC in a waterbath until melting of 90% of the frozen suspension. Cell suspensions (1 ml) were then transferred into 15 ml Falcon tubes (Becton Dickinson) containing 9 ml of pre-warmed complete medium and centrifuged in a 5810 Eppendorf centrifuge at 1200 rpm for 5 min. The supernatant was removed and the cell pellet resuspended in 10 ml of complete medium and seeded into a 10-cm culture dish.

2.1.4. Cell treatments

The protein biosynthesis inhibitor cycloheximide (30 µg/ml, Sigma-Aldrich) was used to evaluate protein stability, whereas the transcriptional inhibitor actinomycin D (2 µg/ml, Sigma-Aldrich) was employed to assess RNA stability. MG132 (25 µM, Calbiochem) was used for 6 h to inhibit the proteasome. Recombinant murine EGF (50 ng/ml, REALIATech GMBH) was used to stimulate EGFR activity. SB203580 (10 µM,

Calbiochem) was used for 12 h to inhibit p38α and p38β activity. The following chemical inhibitors were all used for 8 h: PP2 (10 μM, Calbiochem) to inhibit Src, AG1478-Tyrphostin (10 μM, Sigma-Aldrich) to inhibit EGFR, PD98059 (15 μM, Calbiochem) to inhibit MEK1 and MEK2, LY294002 (30 μM, Calbiochem) to inhibit PI3K and SB216763 (40 μM, Calbiochem) to inhibit GSK3β. 4-hydroxytamoxifen (4-OHT) was used at 1 μM to induce the expression of an estrogen receptor (ER)-H-Ras^{V12} inducible system (De Vita et al., 2005).

2.1.5. Transient transfection

For transient transfections, cells were plated in 10-cm dishes at a density of 6 x 10^5 cells/plate. Cells were transfected on the following day with the Fugene6 reagent (Roche) as recommended by the manufacturer. Briefly, the Fugene6 reagent was diluted in serum-free DMEM without antibiotics or L-glutamine and incubated for 5 min. Plasmid DNAs were then added to the mixture and incubated for 30 min at room temperature. DNA complexes were then added dropwise on the culture plate and normally incubated for 36-48 h before cell harvesting for biochemical analysis.

2.1.6. Retroviral infection

Retroviruses were produced in 293T cells to generate stable cell lines. Briefly, 293T cells were transiently transfected and culture supernatants subsequently collected 48 h (first supernatant) and 72 h (second supernatant) post-transfection, filtered (0.45 μm PVDF filter, Millipore) and supplemented with 4 μg/ml polybrene (Sigma). MEFs at ~5x10^5 cells per 10-cm dish were firstly infected with 6 ml of the first supernatant, which was supplemented 24 h later with 3 ml of the second supernatant. Infected cells were purified 48 h post-infection with either 1–2 μg/ml puromycin for 1 week or 150–200 μg/ml hygromycin for 2 weeks.

2.1.7. Transformation and tumorigenicity assays

Cell proliferation assays were performed with the MTT cell proliferation Kit I (Roche), which measures cell proliferation via mitochondrial activity with a colorimetric reaction. Normally, 1000 cells/well were seeded in triplicates in 96-well plates and cell numbers monitored during the course of 5 days. Experiments were repeated at least three times. Values represent optical density (OD) at 595 nm.

Regarding focus formation assays with immortalized MEFs, 9x10^5 WT or p38α-/- cells were seeded in 10-cm plates and when they achieved 95% of confluence they were infected with the virus-containing supernatants from HEK293 Amphopak cells (Invitrogen). Infected cultures were fed with fresh complete medium every 2-3 days

during 10-15 days, after which cells were fixed with 4% paraformaldehyde/PBS solution and foci stained with 0.1% crystal violet (Sigma) and subsequently counted.

To measure anchorage-independent growth in soft agar, 6-cm culture dishes were first covered in duplicates with 3 ml of DMEM supplemented with 0.5% agar, 1% penicillin/streptomycin, 1% L-glutamine and 10% FBS. An upper layer was then prepared containing $5x10^4$ cells in DMEM with 0.35% agar, 1% penicillin/streptomycin, 1% L-glutamine and 10% FBS. Cells were let to grow into colonies during 14 days and 3 ml of fresh, complete medium was added to the upper layer every 3 days. Colonies were stained with 0.1% crystal violet (Sigma) upon experiment termination and counted if bigger than 0.2 mm. Pictures of representative fields were taken at 40x magnification with a Leica MZ6 microscope coupled to a RS Photometrics camera.

2.1.8. Cell density assays

Cell density was normally determined during the course of 7 days by the MTT assay (Roche) after seeding 1500 cells/well in triplicates in 96-well plates. Values represent optical density (OD) at 595 nm. Alternatively, cells were counted with a hemacytometer under the microscope. Briefly, cells were seeded in triplicates in 60-mm plates and grown to saturation (1-2 days after 100% confluence), followed by washing with PBS, trypsinization, Trypan Blue (Sigma) staining and counting with a Neubauer chamber (Carl Roth GmbH). Values represent number of cells $x10^4$. Samples labeled as "subconfluent" or "confluent" refer to cell cultures harvested at around 80% confluence or 1-2 days after reaching 100% confluence, respectively.

2.1.9. Knockdown of Sprouty2 (Spry2) by shRNA

Mission® shRNA lentiviral particles against mouse Spry2 (Gene Bank Accession number NM_011897) or scrambled negative control (Sigma) were used to knockdown Spry2 expression in p38α-/- MEFs. Transduction was performed in triplicates in 96-well plates according to the manufacturer's instructions. 48 h after transduction, cells expressing control or Spry2 shRNAs were selected with puromycin (1.5 µg/ml) for 1 week and clones with good levels of Spry2 downregulation were further cultured in antibiotic-containing media.

2.1.10. mRNA stability analysis

Actinomycin D (2 µg/ml) was added to the medium for the indicated times and total RNA was isolated (RNeasy kit, Qiagen) and used for quantitative reverse transcription (RT)-PCR.

2.1.11. Protein stability analysis

Cycloheximide (30 µg/ml) was added to the culture medium for the indicated times and total protein levels were analyzed by immunoblotting.

2.2. Preparation of cellular lysates

For preparation of cell lysates, cells were washed twice with ice-cold PBS, scraped on ice and harvested by centrifugation at 2000 rpm and 4ºC for 10 min in a refrigerated tabletop centrifuge (Eppendorf). The resulting pellets were stored at -80ºC until required or immediately resuspended in 100-600 µl of immunoprecipitation (IP) buffer (50 mM Tris-HCl pH 7.5, 150 mM sodium chloride, 1% (v/v) NP-40, 5 mM ethylenediaminetetraacetic acid (EDTA) pH 8.0, 5 mM ethylene glycol tetraacetic acid (EGTA) pH 8.0, and protease/phosphatase inhibitors as follows: 20 mM sodium fluoride, 1 mM phenylmethanesulphonylfluoride (PMSF), 2.5 mM benzamidine, 1 µg/ml leupeptine, 1 µg/ml aprotinine, 2 µM microcystine, 0.1 mM sodium orthovanadate). The suspension was vortexed, incubated on ice for 10 min, and centrifuged at 4ºC for 10 min and 13000 rpm to remove insoluble material.

2.3. Determination of protein concentration

Protein lysates were quantified by the Bradford assay (Protein Assay Kit, Bio-Rad) using bovine serum albumin (BSA) (Pierce) as standard. Absorbance at 595 nm was measured on a BiotrakTM II plate reader (Amersham Bioscience) and 40-70 µg of total protein were normally used for immunoblotting.

2.4. Immunoblotting

Total cell lysates were resolved by sodium dodecyl sulfate (SDS)-polyacrylamide gel electrophoresis (PAGE) in 8-12% Laemmli polyacrylamide gels, depending on the molecular weight of the protein of interest. After electrophoresis, proteins were electro-transferred to nitrocellulose membranes (Protran, Schleicher & Schuell) using wet transfer (Trans-well Blot®, Bio-Rad) systems. The efficiency of transfer was evaluated by staining with 0.1% Ponceau red in 5% acetic acid for 2 min. Ponceau was then washed out with PBS and the membranes blocked with 5% non-fat dry milk in PBS for 1 h at room temperature. Membranes were subsequently incubated overnight at 4ºC with the antibodies of interest as indicated in Table 2. After washing out the unbound primary antibodies with PBS (3 times, 5 min each), membranes were incubated with Alexa Fluor 680-conjugated secondary antibodies (Molecular Probes) for 1 h at room temperature and visualized and quantified using the Odyssey Infrared Imaging System (Li-Cor, Biosciences).

2.5. Immunoprecipitation

For immunoprecipitations, different cell lysis buffers were used depending on the target protein. Triton X-100 buffer (50 mM Tris-HCl pH 7.5, 150 mM NaCl, 1% Triton X-100, 1 mM EDTA and protease/phosphatase inhibitors) was used for $p27^{Kip1}$, Siah2 and cCbl immunoprecipitations with antibodies from Santa Cruz Biotechnology (Table 2). Modified radioimmunoprecipitation assay (RIPA) buffer (50 mM Hepes pH 7.4, 150 mM NaCl, 1 mM EGTA, 1% Triton-X-100, 1% NP-40, 0.5% sodium deoxycholate, 0.1% SDS, 3 mM dithiothreitol (DTT) and protease/phosphatase inhibitors) was used for EGFR immunoprecipitation with either Cetuximab (Im clone Systems, Inc) or Upstate (06-129) antibodies for human or murine EGFR, respectively. Cell lysates (0.5-1 mg) were first pre-cleared with 20 µl of Protein-G PLUS-Agarose beads (Santa Cruz Biotechnology) for 1 h at 4ºC and then incubated with 2 µg of antibody for 14 h at 4ºC. Immunoprecipitates were subsequently recovered by incubation with Protein G PLUS-Agarose beads for 1 h at 4ºC, washed 3 times with lysis buffer and then either analyzed by SDS-PAGE followed by immunoblotting or used as substrates for *in vitro* p38α kinase assays.

2.6. Ubiquitination assays

For EGFR ubiquitination assays, HEK293 cells or MEFs were serum-starved (0.5% FBS) during 12-48 h before EGF stimulation (50 ng/ml, 15 min). EGFR immunoprecipitates (collected as described in the imunoprecipitation section) were resolved by SDS-PAGE and immunoblotted with antibodies against ubiquitin (P4D1) and EGFR (SC-03) from Santa Cruz Biotechnology.

2.7. Immunofluorescence and confocal microscopy

Coverslips were rinsed in PBS, fixed in 4% paraformaldehyde for 30 min at room temperature and washed again with PBS. Non-specific sites were blocked by incubation in PBS containing 1% BSA and 0.5% Triton X-100 for 1 h at room temperature. Cells were then washed 4 times in PBS and incubated with the following primary antibodies (1/100): EGFR (06-129, Upstate), $p27^{Kip1}$ (C-19, SCBT), clathrin (C-20, SCBT), caveolin-1 (clone 2297, BD Transduction Laboratories), CD63/LAMP-3 and transferrin receptor both provided by J.J. Bravo and M. Montoya (CNIO, Madrid). After four washes with PBS, cells were incubated with Alexa Fluor 488 and 594 (1:500) secondary antibodies (Molecular Probes) for 30 min, stained with 4',6-Diamidino-2-phenylindole (DAPI, 0.1 µg/ml) for 2 min to visualize cell nuclei, and mounted in Mowiol. Samples were examined using confocal microscopy (Leica Microsystems).

2.8. Flow cytometry

Cell cycle profiles were obtained by flow cytometry analysis. Briefly, cell cultures were trypsinized, transferred to 15 ml Falcon tubes, washed twice with 10 ml of chilled PBS and fixed in 1 ml of ice-cold 70% ethanol added dropwise while vortexing. Fixed cells were stored at 4ºC for up to 1 week or at -20ºC for 1 month. Before analysis, cell pellets were washed with chilled PBS once and treated with RNAse (1 mg/ml, Qiagen) and propidium iodide (25 µg/ml, Sigma) at 37 ºC for 20 min. Cell cycle distributions were determined using 488 nm excitation and collecting fluorescence above 620 nm.

2.9. Protein purification and in vitro kinase assays

Recombinant GST and GST-$p27^{Kip1}$ mutants were expressed in the *Escherichia coli* BL21 (DE3) strain and purified following standard protocols. Briefly, bacteria were harvested after induction with isopropyl-beta-D-thiogalactopyranoside (IPTG) for 4 h at 37ºC, washed with cold PBS and lysed in Bacteria Lysis Buffer (50 mM Tris-HCl pH 8, 0.5 M NaCl, 1 mM EDTA, 1 mM PMSF, 1 mM benzamidine, 1% Triton X-100, 1 mg/ml lysozyme, protease inhibitors) for 15 min at 4ºC. After sonication and centrifugation at 10000 x*g* for 15 min at 4ºC, the supernatants were collected and incubated with glutathione-sepharose 4B beads (GE Healthcare) for 1 h at 4ºC. Beads were then washed with Bacteria Lysis Buffer free of Triton X-100 or lysozyme. Finally, the GST proteins were eluted with 20 mM glutathione in 50 mM Tris-HCl pH 8, 50 mM NaCl, 1 mM DTT and dialyzed against 50 mM Tris-HCl pH 8, 50 mM NaCl, 0.1 mM EDTA, 0.5 mM DTT and 5% glycerol. Purified proteins were stored at -80ºC.

In vitro kinase assays with p38α were carried out for 30 min at 30ºC in Kinase Assay buffer (50 mM Tris-HCl pH 7.5, 10 mM $MgCl_2$, 2 mM DTT, 200 µM adenosine triphosphate (ATP), 2 µCi ^{32}P-γATP). Reactions were performed in a final volume of 12 µl containing 0.8-1 µg of substrate and 200 ng of active p38α. The reaction was stopped by the addition of sample loading buffer and boiled at 95ºC for 3 min. Recombinant GST-$p27^{Kip1}$ proteins were used as substrates in radioactive assays, whereas Siah2-WT and Siah2-T24A/S29A immunoprecipitates were only used in cold assays (^{32}P-γATP free). Phosphorylated $p27^{Kip1}$ or Siah2 were resolved by SDS-PAGE and visualized by autoradiography or by immunoblotting with a specific phospho-Ser/Thr antibody, respectively.

2.10. Microarray procedures and data analysis

mRNA was extracted from three biological replicates of exponentially proliferating WT and p38α-/- MEFs expressing H-Ras^{V12} with the RNeasy Kit (Qiagen) according to manufacturer's instructions. RNA quality was checked spectrophotometrically by its

260/280 nm absorbance ratio as well as by RT-PCR. RNAs were labeled with Cy5 and Cy3, pooled, hybridized and processed with the Amersham Codelink 20K mouse platform (GeneCore Laboratory, EMBL). Data was subsequently analyzed with the GeneSpring 6.2 software (Silicon Genetics) to identify genes that were deregulated (± 1.5-fold) between the two cell lines analyzed with a 99% confidence level (0.01 cut-off value). Discriminated genes were analyzed with parametric ANOVA 1-way test. Deregulated genes were then classified by the Gene Ontology-based applications FatiGO and Source Batch database, as well as by PubMed search.

2.11. mRNA isolation and RT-PCR analysis

Total RNA was extracted from MEFs, nude mice or lung tissues using the RNeasy Kit (Qiagen) according to manufacturer´s instructions. RNA concentration was determined by measuring the absorbance at 260 nm and the quality monitored by the ratio of absorbance at 260/280 nm and by 1% agarose gel electrophoresis. cDNA was prepared using M-MLV reverse transcription (Invitrogen) and used as the template for PCR amplification. PCR primers were designed for the selected genes by using Vector NTI 8 (InforMax) and used at a final concentration of 160 nM. RT-PCR conditions were as follows: reverse transcription at 37ºC for 90 min, denaturation at 95ºC for 2 min, followed by 30-35 cycles of denaturation at 95ºC for 45 s, annealing at 55ºC for 45 s and elongation at 72ºC for 60 s. A final step of elongation at 72ºC for 10 min was performed. The products of the RT-PCR reaction were analyzed by 1% agarose gel electrophoresis, stained with ethidium bromide and imaged in the Gel Doc 2000 system (Bio-Rad). Primers used for semiquantitative RT-PCR are listed in Appendix Table 1.

Quantitative RT-PCR (qRT-PCR) analysis was performed in a 7900HT Fast Real-Time PCR System (Applied Biosystems). Total RNA (1 µg) was reverse transcribed, diluted 1:10 and amplified in triplicates by PCR (40 cycles) with the primers listed in Table 3, by using the 2X SYBR GreenER qPCR SuperMix (Invitrogen) in a final volume of 20 µl. Relative quantities (Δcycle threshold values) were obtained by normalizing against *GAPDH*.

2.12. Statistical analysis

All results are expressed as mean ± standard deviation (SD) of at least three independent experiments. Statistical analysis was performed using the Student's *t* test with a statistically significant P-value (p)< 0.01.

Table 3. Primers used for qRT-PCR

Gene symbol	Genbank Acc. No.	Forward (5'-3')	Reverse (5'-3')
Cdkn1b (p27^{Kip1})	NM_009875	GAGGTGGAGAGGGGCAGC	TTCGGGGAACCGTCTGAAAC
Siah2	NM_009174	AGCAAGCAGCCGCCGCCG	GGTTCCTGATGCTGGGCGTT
Egfr	NM_207655	CTGCCAAGGCACAAGTAACA	ATTGGGACAGCTTGGATCAC
Aig1	NM_025446	GCTCCATCCTGTGCAACTAC	TTTAGTACTTCTCCAAGCAGG
Rab3b	NM_023537	TGGGTTTGACTTCTTTGAAGC	AATGGAGAGAAGCGGAGGAG
Loxl1	NM_010729	GCCTTGACCGTCGTTACTCG	GCTTCGCACGGGCAAGTAAG
Mmp3	NM_010809	TACTGAAGGTGGTACAGAGC	GCATAGGCATGAGCCAAGAC
Ralgds	NM_009058	AATGCCATCTCCTCCATCCTG	ATGTCACCACTTGGCTGGGC
Cd9	NM_007657	GATTCGACTCTCAGACCAAG	ATCCTTGCTCCGTAACTTTTG
Tnfrsf23	NM_024290	TTCAGCCACGTCTCCAGTC	TGAAAGAGTTGCCTCCATGG
Nck2	NM_010879	GGCACTGCACTGAGCAATG	GGACACAGCTCTCGGAGTG
Rtn4	NM_024226	GAAGACTGGAGTGGTGTTTG	GCTGTTCACATGACCAAGAG
Gstm2	NM_008183	ATGGGGGACGCTCCTGACT	AAGTCAGGGCTGTAGCAAAC
Egln3	NM_028133	TCAGACACTCTCTTTGCCAG	CGAGGGTGGCTAACTTTCG
Hck	NM_010407	TTCTTCAAGGGGATCAGCCG	GAGCCCATCCTTCCCCTTC
Klf5	NM_009769	CCAGTTCGACAAACCAGACG	GTTGTGAATCGCCAGTTTGG
Eps8	NM_007945	GACCGAGCTGTGAGCCTG	GCCTCTTCTGTTTCCCACC
Lamp2	NM_010685	ACACGATGGAAGCAGTTGTG	GAGTCAGGTTGTAAGTTAAAAC
Anxa8	NM_013473	CAGGAGGGCGTCAGCGTG	GGCATCGTGCAGCTCCTTG
Arfgap3	NM_025445	TCGTGGTTCCAGCTTCGATG	ATGCCTGCATAGCACCACTG
Prkca	NM_011101	TCGGACGACTCGGAATGAC	CCAGCACCATGAGGAAGTTG
Ctsl	NM_009984	CGCCTTCGGTGACATGACC	CTGATTGCCTTGAGCGTGAG
Hoxa5	NM_010453	GCTACGGCTACAATGGCATG	GCTGCTGATGTGGGTGCTG
Traf1	NM_009421	CTGAAATCATGTGCCCCTTTG	TTCCTGGCTCTCACAGCAAG
Plcg2	NM_172285	AGGACTTTGAGCGAGCCAAG	CGGAGGCTGATGCTGTTTC

Results

1. Regulation of contact inhibition by p38α MAPK

1.1. p38α regulates cell density in confluence

We have previously reported that p38α-deficient mouse embryo fibroblasts (MEFs) seem to be more susceptible to the loss of contact inhibition induced by oncogenic insults (Dolado et al., 2007), which led us to investigate the connection between p38α and the establishment of contact inhibition response. In support to the idea that p38α triggers contact inhibition, we observed that p38α deficient mouse embryonic fibroblasts (MEFs) achieved much higher saturation density in confluent conditions of growth than their WT counterparts (Figure 10A). Moreover, we could modify cell density in confluence by modulating p38α activity, either by inhibiting p38α in WT MEFs using the p38α/β chemical inhibitor SB203580 or by stably reconstituting p38α into p38α-/- MEFs (Figure 10B).

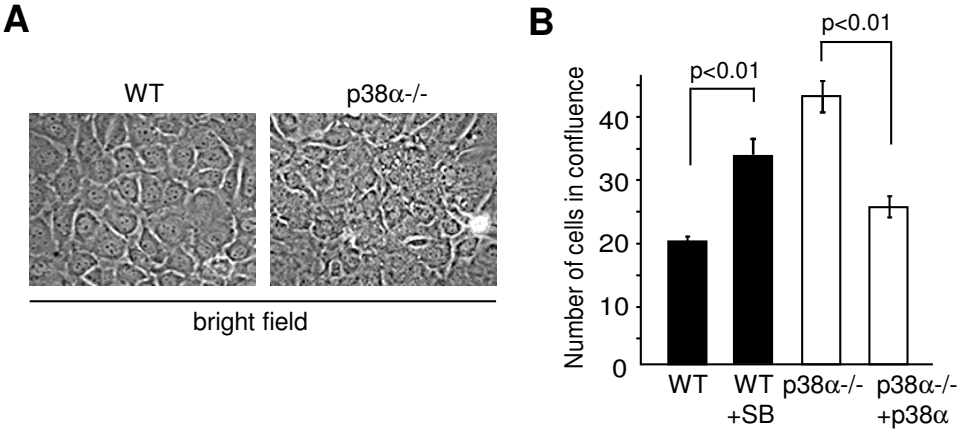

Figure 10. p38α-deficient MEFs are impaired in contact inhibition. (A) Morphology of confluent WT and p38α-/-MEFs. **(B)** WT, p38α-/- and p38α-/- with p38α added-back MEFs were grown to confluence and cells were counted. SB203580 (10 μM) was added to confluent WT cultures 12 h before counting. Number of cells in confluence, number of cells x10^4.

Consistently, we observed that confluent cells deficient in p38α displayed impaired G0/G1 cell cycle arrest along with a higher percentage of cells in S phase (Figure 11A), indicating that the higher saturation densities observed in p38α-deficient cells (Figure 10) are likely due to a defect in confluent proliferation arrest. We also observed an increased expression of cell proliferation markers such as cyclin D1 and phosphorylated Rb in confluent p38α-/- MEFs (Figure 12). Of note, WT and p38α-/- MEFs proliferated similarly in sparse conditions of growth and also have similar cell morphology and size (Alfonso et al., 2006; Dolado et al., 2007), which supports a specific function for p38α in triggering cell cycle arrest induced by high cellular density.

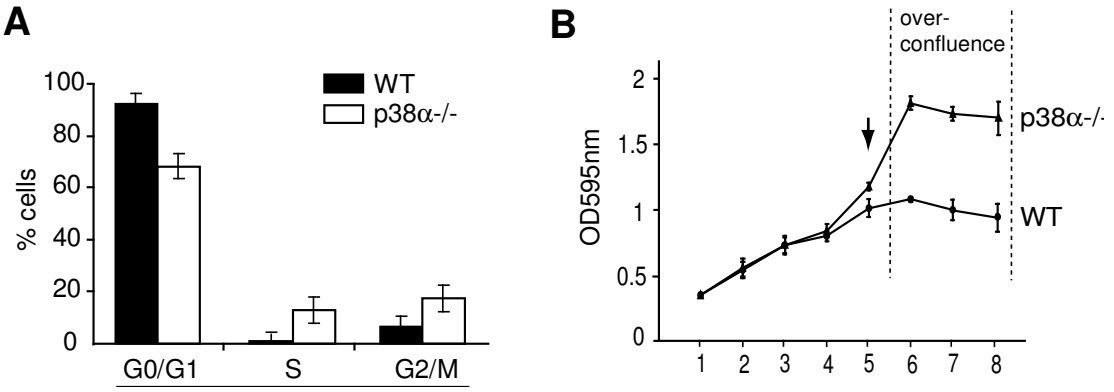

Figure 11. Proliferation of confluent MEFs is enhanced in the absence of p38α. (A) The percentages of confluent WT and p38α-/- cells in G0/G1, S and G2/M phases were quantified by flow cytometry. **(B)** MTT cell proliferation curves of WT and p38α-/- MEFs. The arrow indicates the onset of confluence.

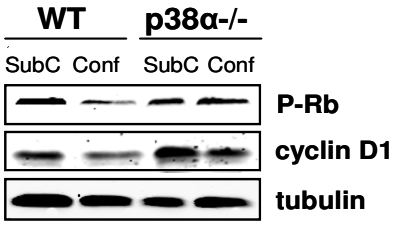

Figure 12. Upregulation of proliferation markers in confluent p38α-/- MEFs. WT and p38α-/- MEFs grown to sparse (SubC) or confluent (Conf) conditions were immunoblotted against proliferation markers.

Of note, we did not observe significant differences in cell volume between confluent p38α-/- and WT MEFs (Figure 13), indicating that the higher cellular density observed in confluent p38α-/- cultures is due to a more intense squeezing (as cells are unable to stop proliferating) rather than to intrinsic changes in cell volume. Interestingly, we observed that p38α activity strongly increased in MEFs early upon achievement of confluent conditions of growth and was sustained over time, which correlated with upregulation of the cell cycle inhibitor $p27^{Kip1}$ (Figure 14).

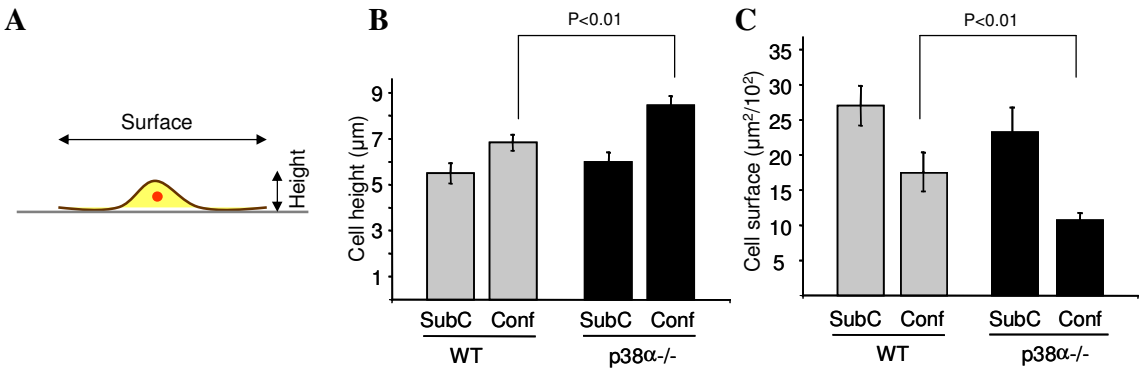

Figure 13. Cell volume is similar between confluent WT and p38α-/- MEFs. (A) Schematic representation of cell height and surface. Cell height **(B)** and surface **(C)** were determined by using confocal microscopy in confluent cell cultures (n=10). SubC, subconfluent; Conf, confluent.

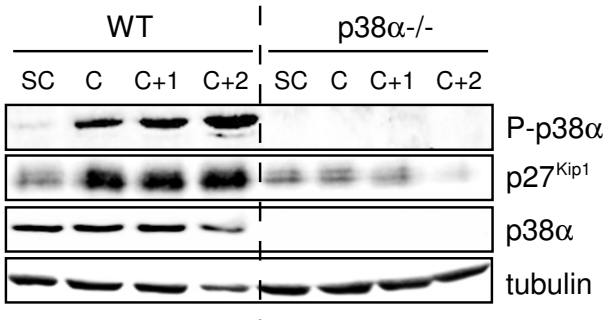

Figure 14. p38α activation correlates with p27^{Kip1} accumulation in confluence. WT and p38α-/- MEFs grown to sparse (SC) or confluent (C) conditions, as well as 1 day (C+1) or 2 days (C+2) post-confluence, were analyzed by immunoblotting.

1.2. p27^{Kip1} accumulation in confluent cell cultures depends on p38α MAP kinase activity

We have previously reported that confluent MEFs rely on p38α activity for the high density-induced cell cycle arrest, and this also correlated with the accumulation of the cell cycle inhibitor p27^{Kip1} ((Faust et al., 2005); see also Figure 14). To address whether the p38α-p27^{Kip1} connection was operational in cells other than MEFs, we analyzed p38α activation and p27^{Kip1} levels also in mouse NIH3T3 cells and human IMR-90 lung fibroblasts. In agreement with a broadly conserved role for p38α in the regulation of contact inhibition, we observed that NIH3T3 and IMR90 fibroblasts behaved as MEFs in that they all activated the p38 MAPK pathway and accumulated p27^{Kip1} when grown to high cellular densities (Figure 15). Conversely, treatment with the chemical inhibitor SB203580, which inhibited p38 MAPK signaling as confirmed by the impaired phosphorylation of the p38-downstream targets MAPKAPK-2 (MK-2) and Hsp27, impaired p27^{Kip1} accumulation in confluence (Figure 15).

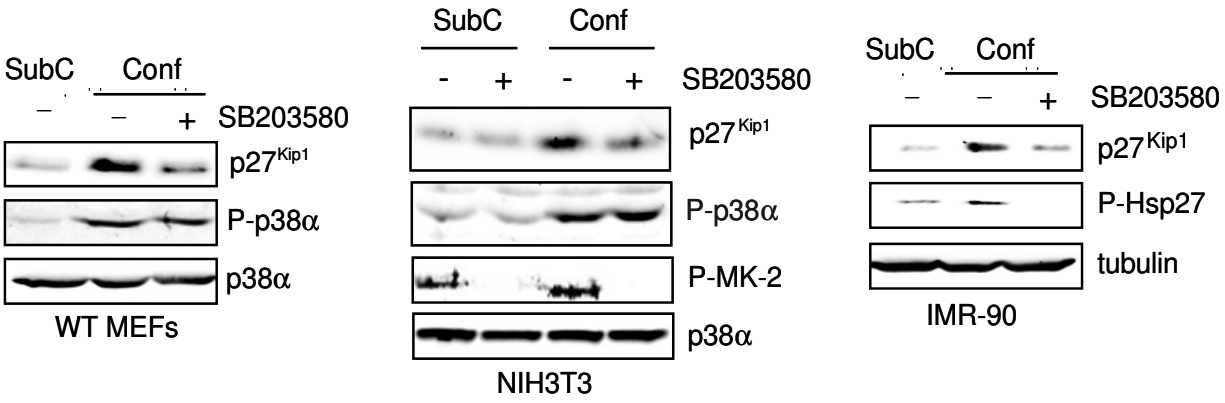

Figure 15. p27^{Kip1} accumulation in confluence requires p38α activity. Immunoblot analysis of subconfluent (SubC) and confluent (Conf) WT and p38α-/- MEFs **(left)**, NIH3T3 mouse fibroblasts **(middle)**, and IMR90 human fibroblasts **(right)**. Cells were treated with either DMSO (-) or SB203580 (10 μM) for 12 h, as indicated.

Interestingly, SB203580 had no effect on the levels of $p27^{Kip1}$ in confluent p38α-/- MEFs, whereas retroviral reconstitution of p38α into p38α-/- MEFs completely rescued $p27^{Kip1}$ accumulation to the levels of confluent WT cells (Figures 16A and B), supporting that p38α is the main p38 family member regulating $p27^{Kip1}$ (Faust et al., 2005) and p38β hardly contributes to the process. Altogether, these results indicate a causal link between p38α activation and the subsequent accumulation of $p27^{Kip1}$ in confluent cells.

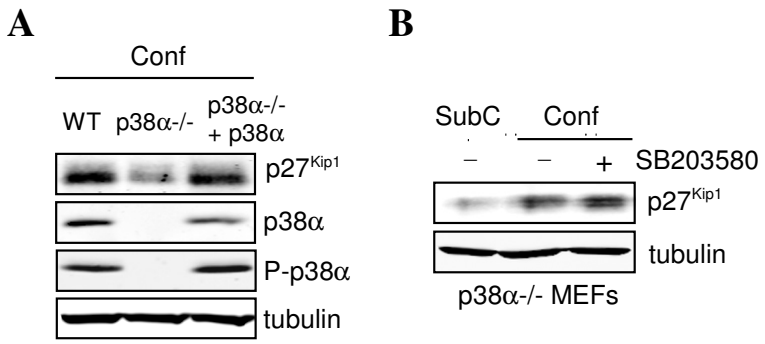

Figure 16. p38α is the main p38 MAPK isoform regulating cell contact inhibition and $p27^{Kip1}$ accumulation. (A-B) WT, p38α-/- and p38α-/- with p38α added-back MEFs were grown to subconfluence (SubC) or confluence (Conf), treated overnight with the specific p38α/β MAPK inhibitor SB203580 (10 μM) as indicated, and analyzed by immunoblotting.

We also analyzed the expression pattern of other cell cycle inhibitors that have been suggested to contribute to the contact inhibition response in some cases (Cho et al., 2008; Wieser et al., 1999). We failed to detect expression of $p16^{Ink4a}$, whereas $p21^{Cip1}$ was downregulated in confluent cells and inversely correlated with $p27^{Kip1}$ levels (Figure 17), in agreement with results from other groups (Yanagisawa et al., 1999). This suggests that $p27^{Kip1}$ is a major cell cycle regulator in contact inhibition. In line with this idea, p38α regulates $p27^{Kip1}$ levels in NIH3T3 cells (Figure 15, middle), which lack $p16^{Ink4a}$ due to the deletion in *Ink4/Arf* locus.

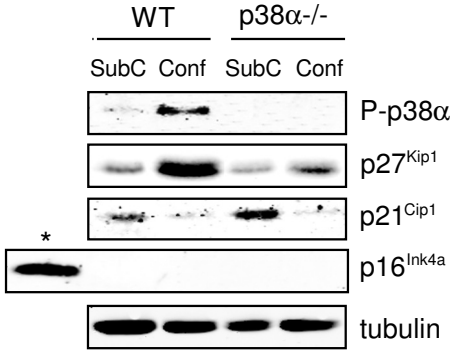

Figure 17. $p27^{Kip1}$ is the major cell cycle inhibitor regulating contact inhibition in premalignant cells. Immunoblot analysis of subconfluent (SubC) and confluent (Confl) WT and p38α-/- MEFs. Primary MEFs were used as a control for $p16^{Ink4a}$ expression (indicated by an asterisk).

1.3. p27^{Kip1} acts downstream of p38α and mediates a G0/G1 proliferation arrest under confluent conditions of growth

To investigate the functional connection between p38α and p27^{Kip1} in confluence, we established cultures of immortalized MEFs lacking p27^{Kip1}. As expected p27^{Kip1}-deficient MEFs also reached higher cellular densities in confluence than their WT counterparts (Figure 18A). Importantly, whereas p38α deficiency impaired both p27^{Kip1} accumulation and contact inhibition, the absence of p27^{Kip1} also resulted in a more relaxed contact inhibition response without significantly affecting p38α activation (Figure 18B), indicating that p27^{Kip1} lays downstream of p38α in the regulation of contact inhibition.

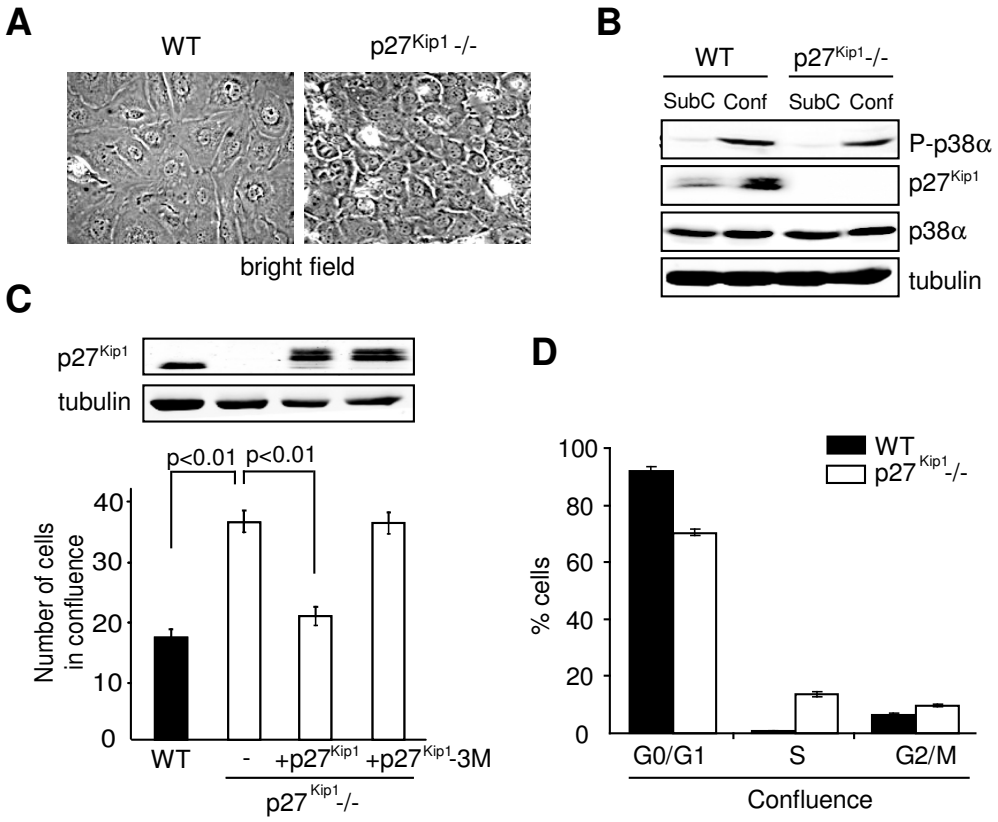

Figure 18. p27^{Kip1} lays downstream of p38α in the regulation of confluence-induced cell cycle arrest. **(A)** Bright field microscopy of overconfluent (C+1) WT and p27^{Kip1}-/- MEFs. **(B)** Immunoblot analysis of cellular lysates from sparse (SubC) and confluent (Conf) WT and p27^{Kip1}-/- MEFs. **(C)** WT and p27^{Kip1}-/- MEFs stably transduced with empty vector (-), p27^{Kip1}-WT or the mutant p27^{Kip1}-3M were grown to confluence and cells were counted in a Neubauer chamber. Number of cells in confluence, number of cells x10^4 . WB analysis shows the expression levels of infected constructs. **(D)** WT, p38α-/- and p27^{Kip1}-/- MEFs were grown to confluence and the percentage of cells in G0/G1, S and G2/M phases were quantified within each population by flow cytometry.

Regarding the mechanism by which p27^{Kip1} regulates contact inhibition, we observed that reconstitution of p27^{Kip1}-/- MEFs with p27^{Kip1} rescued their confluence defect,

whereas expression of the CDK-binding defective triple mutant containing the L32H/P35A/F65A mutations- $p27^{Kip1}$-3M (Martin et al., 2005) did not (Figure 18C). This argues that the cell cycle inhibitory function of $p27^{Kip1}$ is required to implement the contact inhibition response downstream of p38α. In agreement with this idea, both p38α- and $p27^{Kip1}$-deficient cells showed impaired confluence-induced G0/G1 cell cycle arrest (Figure 18D and Figure 11A), which probably explains their ability to reach higher saturation densities than their WT counterparts.

1.4. p38α indirectly regulates $p27^{Kip1}$ protein stability in confluence

Next, we addressed how p38α induces $p27^{Kip1}$ upregulation in confluence. Quantitative reverse transcription-PCR (qRT-PCR) analysis revealed that $p27^{Kip1}$ mRNA levels were lower in confluent p38α-/- than in WT MEFs (Figure 19B), which correlated well with the differences observed in $p27^{Kip1}$ protein accumulation (Figure 19A). However, adding back p38α to p38α-/- MEFs rescued $p27^{Kip1}$ protein levels (Figure 19A) without affecting its mRNA levels (Figure 19B), arguing against the transcriptionally-mediated regulation of $p27^{Kip1}$ by p38α in confluence. Of note, this also indicated that the observed differences in mRNA levels are unspecific and probably due to the process of cell immortalization. We neither observed any significant differences in $p27^{Kip1}$ mRNA stability between confluent WT and p38α-/- MEFs (Figure 19C).

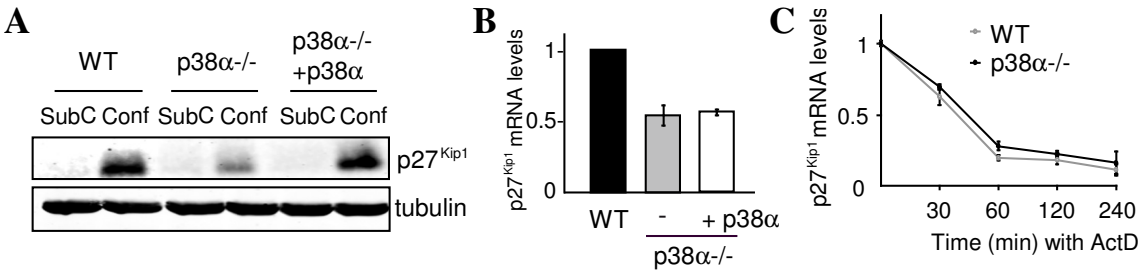

Figure 19. p38α does not regulate $p27^{Kip1}$ mRNA transcription or stability in confluence. (A-B) Subconfluent (SubC) and confluent (Conf) WT, p38α-/- and p38α-/- with p38α added-back MEFs were analyzed by immunoblotting **(A)** and qRT-PCR **(B)**. **(C)** Confluent WT and p38α-/- MEFs were treated with Actinomycin D (2 µg/ml) for the indicated times, harvested and analyzed for $p27^{Kip1}$ mRNA levels by qRT-PCR.

As $p27^{Kip1}$ expression is known to be regulated by phosphorylation (Besson et al., 2008; Bloom and Pagano, 2003), we also investigated the possibility of direct $p27^{Kip1}$

phosphorylation by p38α. We observed that p38α phosphorylated p27^{Kip1} *in vitro* (Figure 20A).

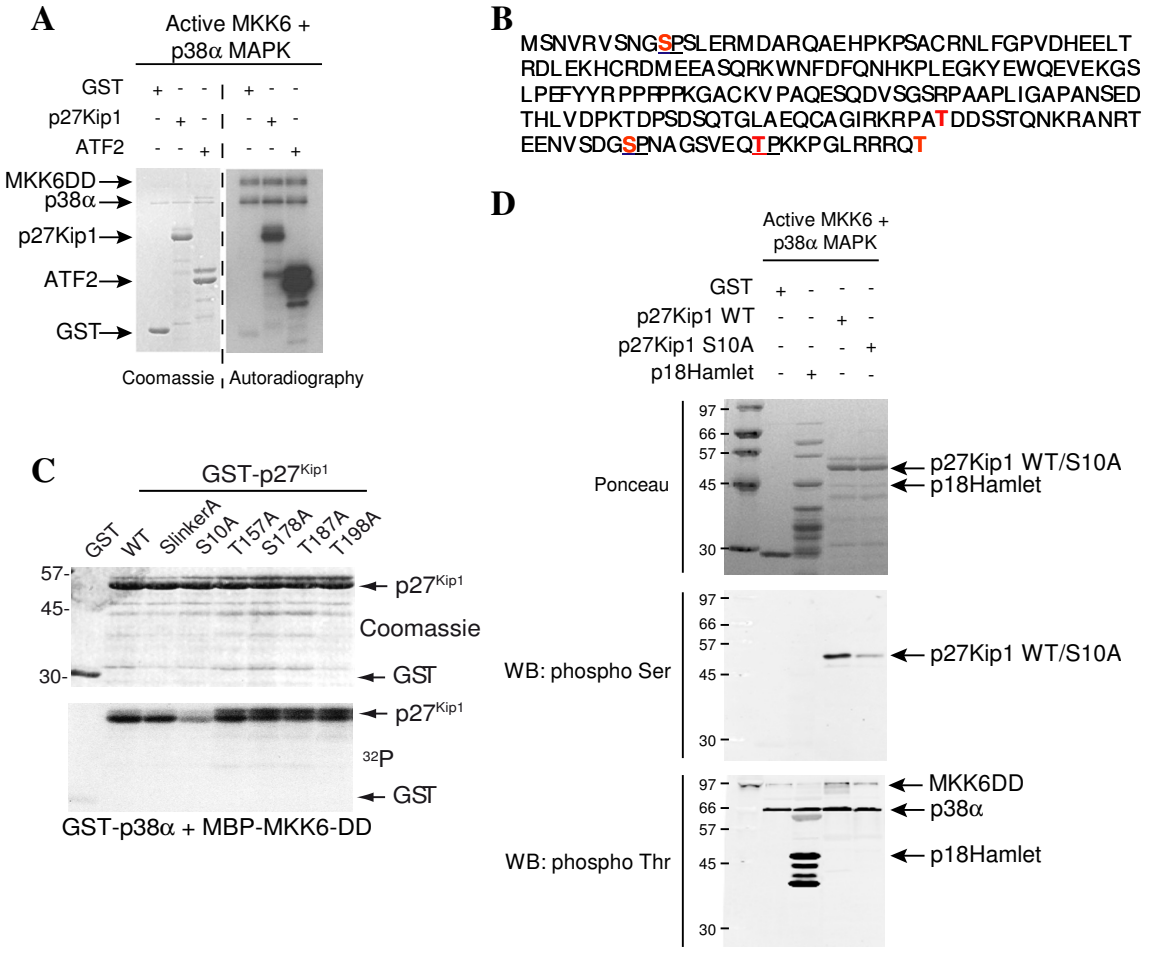

Figure 20. p38α directly phosphorylates p27^{Kip1} on Ser10. (A) *In vitro* kinase assay with MBP-MKK6DD-activated GST-p38α using as a substrate GST-p27^{Kip1} WT. GST alone was used as negative control and ATF2 as a positive control. Proteins were resolved by SDS-PAGE and detected by autoradiography. **(B)** Single point mutations that were used to identify p38α target residues on p27^{Kip1} are indicated in red. **(C)** *In vitro* kinase assay with MKK6-DD-activated GST-p38α using as a substrate GST-p27^{Kip1} WT or the indicated mutants ("Slinker" refers to a Ser present in the linker between GST and p27^{Kip1} (BamHI site)). GST alone was used as negative control. Proteins were resolved by SDS-PAGE and detected by autoradiography. **(D)** GST-tagged p18^{Hamlet}, GST-WT p27^{Kip1} or the mutant S10A were phosphorylated *in vitro* with active p38α and analyzed by immunoblotting.

In order to identify the p38α phosphorylation sites, we mutated to Ala several Ser and Thr residues on human p27^{Kip1}, such as Ser10, Thr157, Thr187 and Thr198 (Figure 20B, red), which have been previously reported to modulate p27^{Kip1} protein stability upon phosphorylation (Ishida et al., 2000; Kossatz et al., 2006; Shin et al., 2002; Tsvetkov et al., 1999), as well as an additional SP-site (consensus site for phosphorylation by p38 composed of the Ser-Pro motif), Ser178 and then used the mutant proteins as p38α

substrates *in vitro*. We found that Ser10 was a major p38α phosphorylation site on $p27^{Kip1}$ (Figure 20C), although some low level of phosphorylation remained in the Ser10A mutant, indicating that other sites are probably phosphorylated by p38α with lower efficiency. Immunoblotting with a generic phospho-Ser antibody (Figure 20D) confirmed the phosphorylation of Ser10 in $p27^{Kip1}$ by p38α, whereas the Thr-phosphorylated p38α substrate $p18^{Hamlet}$ (Cuadrado et al., 2007) was used as a control for threonine phosphorylation.

As Ser10 phosphorylation has been previously associated with $p27^{Kip1}$ protein stabilization (Ishida et al., 2000), we investigated whether phosphorylation of this residue could mediate the accumulation of $p27^{Kip1}$ induced by p38α in confluent cells. We found that both $p27^{Kip1}$ WT and the Ser10A mutant proteins accumulated to similar extents in response to MKK6-DD-induced activation of p38α (Figure 21A). Moreover, $p27^{Kip1}$ WT and the Ser10A mutant were both able to rescue the contact inhibition defect of $p27^{Kip1}$-/- MEFs, and both proteins accumulated to similar extents in confluent cells (Figure 21B). These results suggest that direct phosphorylation by p38α is unlikely to contribute to the upregulation of $p27^{Kip1}$ or its proliferation inhibitory function in confluent cultures.

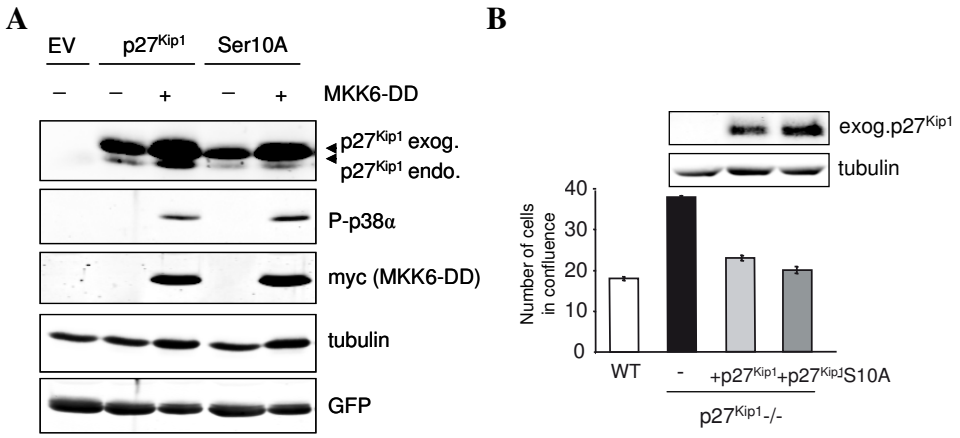

Figure 21. Phosphorylation of $p27^{Kip1}$ on Ser10 does not influence $p27^{Kip1}$ accumulation and contact inhibition. (A) NIH3T3 fibroblasts were transiently transfected with EV (-), $p27^{Kip1}$-WT and $p27^{Kip1}$-Ser10A together with MKK6-DD, as indicated, and analyzed by immunobloting. **(B)** WT and $p27^{Kip1}$-/- MEFs were stably transduced with WT $p27^{Kip1}$, the mutant Ser10A or EV (-), grown to confluence and cells were counted in Neubauer chamber. Number of cells in confluence, number of cells $x10^4$.

In contrast, treatment with cycloheximide showed that $p27^{Kip1}$ was more stable in confluent WT than in p38α-/- MEFs, with half-lives of about 5 h and 2 h, respectively (Figure 22A). Further support for the regulation of $p27^{Kip1}$ protein stability by p38α was obtained by treating p38α-/- MEFs with the proteasome inhibitor MG132, which

increased the stability of p27^{Kip1} to that observed in confluent WT cells (Figures 22B and C). These results suggested that the reduced accumulation of p27^{Kip1} observed in confluent p38α-/- cells was probably due to enhanced proteasome-mediated degradation. Of note, confluent p38α-/- MEFs treated with MG132 contained high amounts of nuclear p27^{Kip1} without any obvious accumulation of p27^{Kip1} in the cytoplasm (Figure 22D), arguing against a role for p38α in the regulation of p27^{Kip1} nucleo-cytoplasmic shuttling.

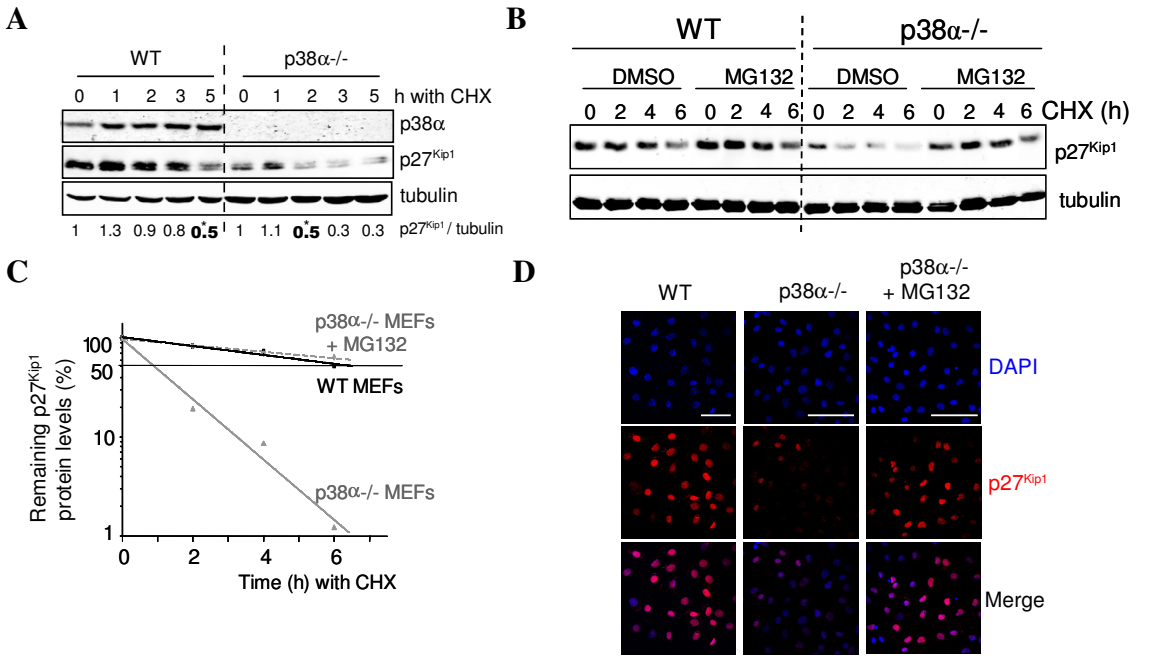

Figure 22. p38α indirectly regulates p27^{Kip1} protein stability in confluent cells. (A) Confluent WT and p38α-/- MEFs were treated with cycloheximide (CHX, 30 μg/ml) for the indicated times and analyzed by immunoblotting. p27^{Kip1} levels were quantified by densitometry and normalized to tubulin. Asterisks indicate p27^{Kip1} half-lives. **(B-C)** Confluent WT and p38α-/- MEFs were treated with CHX for the indicated times in the presence of MG132 (25 μM), where indicated, and cell lysates were analyzed by immunoblotting (B) and quantified by densitometry (C). Tubulin-normalized p27^{Kip1} protein levels are shown (C) as a function of time in a Log_{10} scale. **(D)** Confluent WT, p38α-/- and p38α-/- with p38α added-back MEFs were treated with MG132 or DMSO for 6 h, formalin-fixed, stained with p27^{Kip1} antibody and visualized by confocal microscopy. p27^{Kip1} staining is shown in red and nuclear staining (DAPI) in blue. Bar = 100 μm.

1.5. p38α stabilizes p27^{Kip1} in confluent cells by inhibiting EGF receptor signaling

The enhanced stability of p27^{Kip1} in confluent WT MEFs led us to investigate the nature of the p38α-opposed signals that were responsible for p27^{Kip1} degradation in p38α-deficient cells. The reduced stability of p27^{Kip1} in confluent p38α-/- MEFs could be possibly accounted for by the upregulation of p27^{Kip1} ubiquitin ligases. However, we found no significant differences in the expression of Skp2 and Cdh1, two ubiquitin

ligases related to $p27^{Kip1}$ (Santamaria and Pagano, 2007; Tsvetkov et al., 1999), between confluent p38α-/- and WT MEFs (Figure 23A). In contrast, we found that the levels of Thr187-phosphorylated $p27^{Kip1}$ were higher in confluent p38α-/- than in WT MEFs (Figure 23B). This phosphorylation is known to induce $p27^{Kip1}$ degradation (Tsvetkov et al., 1999) and was recently shown to be stimulated by mitogenic signals downstream of EGF receptor (EGFR) (Chu et al., 2007; Grimmler et al., 2007).

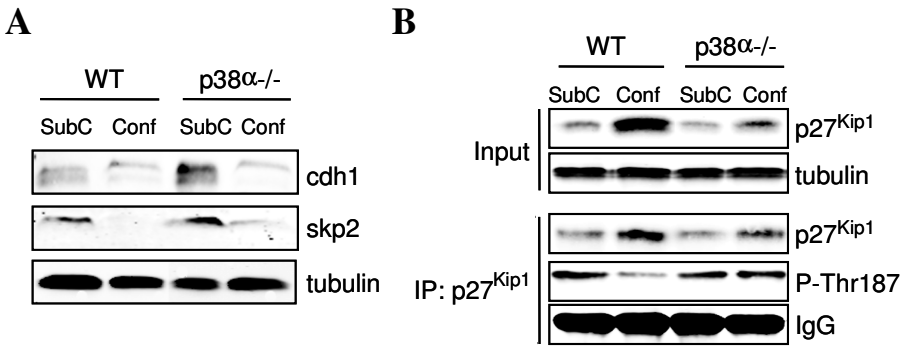

Figure 23. Confluent p38α-/- cells show enhanced phosphorylation on the $p27^{Kip1}$ destabilizing residue Thr187. (A) Immunoblotting of subconfluent (SubC) and confluent (Conf) MEFs. **(B)** $p27^{Kip1}$ immunoprecipitates from sparse (SubC) or confluent (Conf) WT and p38α-/- MEFs were analyzed by immunoblotting.

Along this line, treatment of confluent p38α-/- MEFs with chemical inhibitors of various signaling molecules revealed that EGFR and its downstream effectors Src and MEK1/2, but not PI3K/Akt or GSK3β (Figure 24A), were actually responsible for $p27^{Kip1}$ instability in the absence of p38α. In agreement with the idea that deregulated EGFR signaling was the cause of reduced $p27^{Kip1}$ accumulation in p38α-deficient cells, we found higher levels of active EGFR and its downstream targets Akt, ERK and Src in confluent p38α-/- than in WT cells (Figure 24B). Moreover, $p27^{Kip1}$ upregulation observed upon re-introduction of p38α in p38α-/- MEFs (Figure 16A) correlated with the downregulation of all these signaling pathways (Figure 24B). Accordingly, EGF treatment induced more sustained EGFR signaling in p38α-/- than in WT MEFs, as indicated by the higher levels of phosphorylated EGFR and ERK1/2 at later time points in the absence of p38α (Figure 25A). Importantly, no differences in EGFR activation were observed between WT and p38α-/- MEFs when sparse cultures were stimulated with EGF (Figure 25B), supporting that confluence-induced activation of p38α is required to inhibit EGFR signaling.

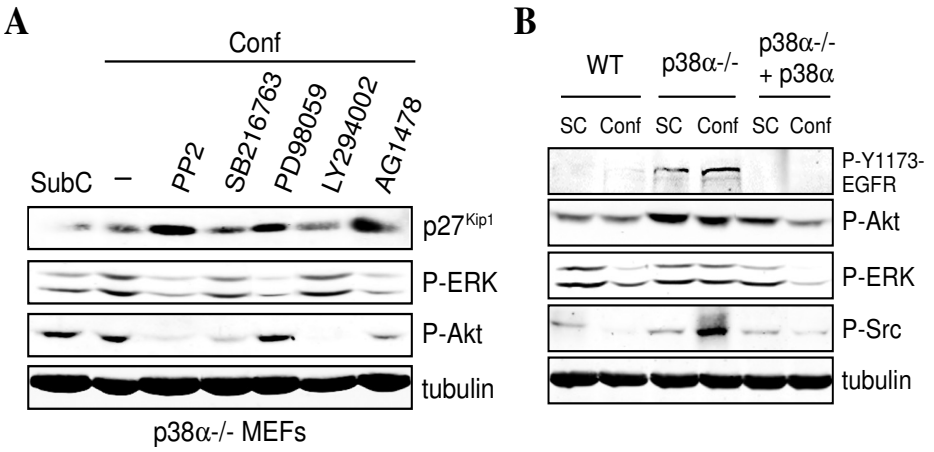

Figure 24. p38α stabilizes p27^{Kip1} by inhibiting EGFR signaling in confluent cells. **(A)** Confluent (Conf) p38α-/- MEFs were incubated 8 h with either DMSO (-) or chemical inhibitors against Src (PP2), GSK3β (SB216763), MEK1/2 (PD98059), PI3K (LY294002) or EGFR (AG1478) and then analyzed by immunoblotting. **(B)** Sparse (SC) and confluent (Conf) WT, p38α-/- and p38α-/- with p38α added-back MEFs were analyzed by immunoblotting.

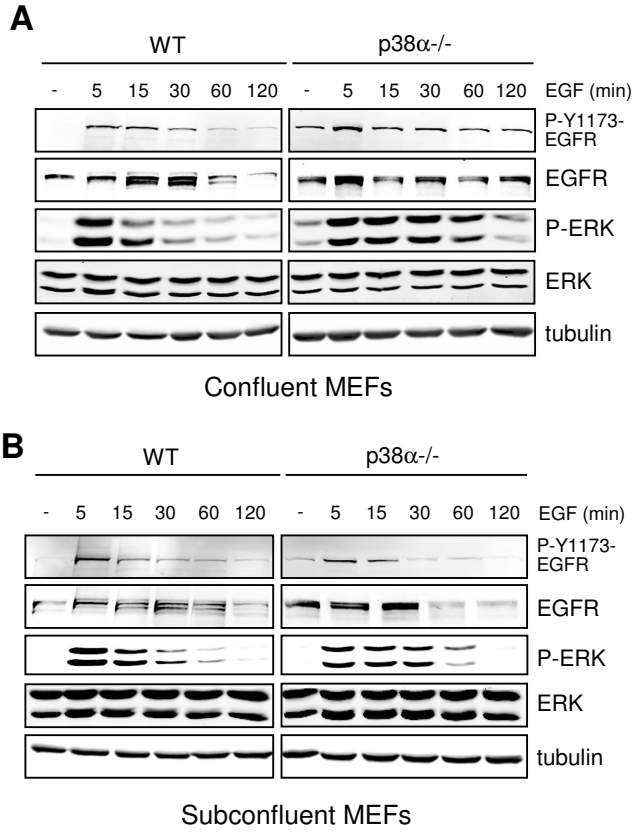

Figure 25. p38α regulates the duration of EGFR-induced mitogenic signaling. **(A-B)** Confluent **(A)** and subconfluent **(B)** WT and p38α-/- MEFs were incubated with EGF (50 ng/ml) for the indicated times and total cell lysates were analyzed by immunoblotting.

Consistently, MKK6-DD-mediated activation of p38α inhibited the EGFR-induced degradation of p27^{Kip1} in NIH3T3 fibroblasts (Figure 26A), whereas treatment of confluent p38α-/- MEFs with the EGFR inhibitor AG1478 not only upregulated p27^{Kip1} to WT levels (Figure 26B), but also rescued their enhanced susceptibility to oncogene-induced lost of contact inhibition (Figure 26C).

Altogether, these results delineate a novel regulatory mechanism in contact inhibition, which involves p38α-mediated downregulation of EGFR signaling and subsequent $p27^{Kip1}$ accumulation. Importantly, whereas SB203580 treatment interferes with the confluent accumulation of $p27^{Kip1}$ in WT cells (Figure 15), this effect was abolished in EGFR-/- MEFs (Figure 26D), which points to EGFR as the key p38α target in the confluent regulation of $p27^{Kip1}$.

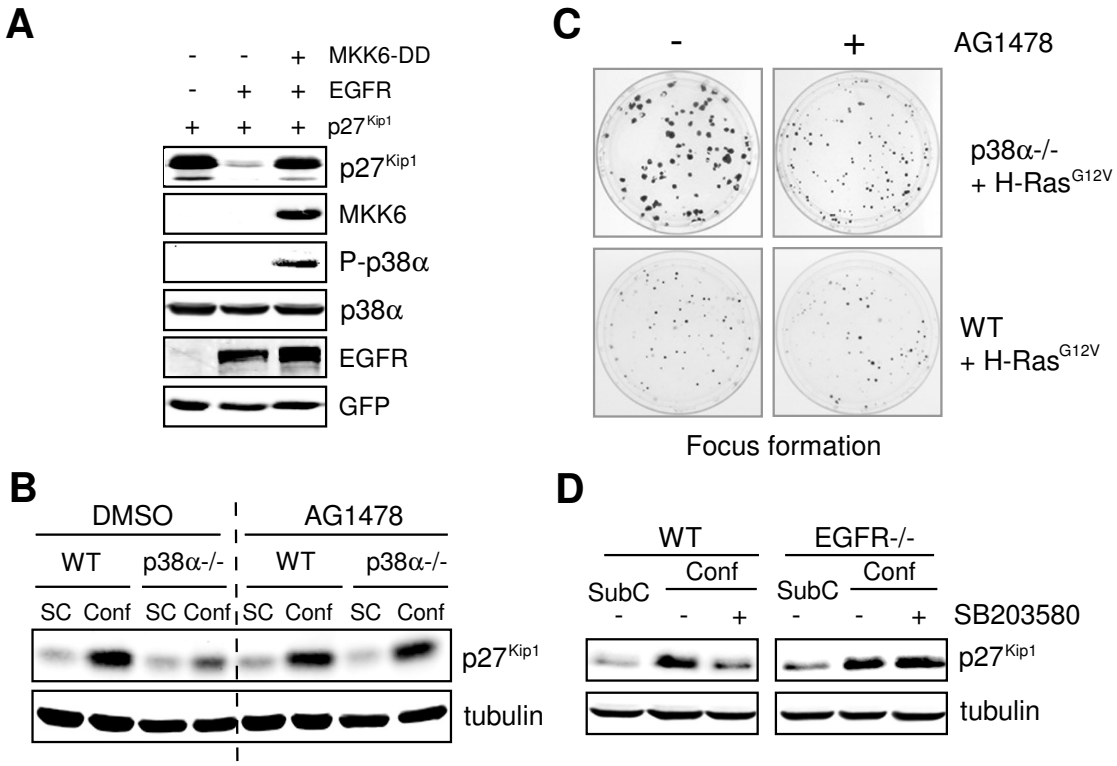

Figure 26. EGFR is the key p38α target in contact inhibition. **(A)** NIH3T3 cells were transiently transfected with EGFR, $p27^{Kip1}$ and the p38 MAPK activator MKK6-DD, as indicated. Cell lysates were analyzed by immunoblotting using GFP as a transfection control. **(B)** Subconfluent (SC) and confluent (Conf) WT and p38α-/- MEFs were incubated 8 h with the EGFR inhibitor AG1478 (10 μM) or with DMSO as indicated, and were analyzed by immunoblotting. **(C)** Focus formation assay using WT and p38α-/- MEFs transiently transduced with $H\text{-}Ras^{G12V}$. Plates were treated daily with the EGFR inhibitor AG1478 (10 μM) as indicated. **(D)** WT and EGFR-/- MEFs were grown to subconfluence (SubC) or confluence (Conf), treated with SB203580 (10 μM) as indicated, and analyzed by immunoblotting.

1.6. Confluent activation of p38α attenuates mitogenic signals by inducing EGFR degradation

Our results indicated that enhanced EGFR signaling was responsible for impaired $p27^{Kip1}$ accumulation and contact inhibition in p38α-/- cells. Thus, we investigated whether p38α could regulate EGFR degradation in confluent cells, since EGFR mutants resistant to degradation are known to display sustained mitogenic signaling (Shtiegman

et al., 2007). We found higher levels of ubiquitinated EGFR, a pre-requisite for EGFR degradation (Grovdal et al., 2004; Levkowitz et al., 1998), in confluent WT than in p38α-/- MEFs (Figure 28A). Furthermore, ligand-induced trafficking of EGFR in WT MEFs resulted in rapid co-localization with the lysosomal marker CD63/LAMP3 (Figure 27, top middle) and this was impaired in p38α-/- MEFs (Figure 27, bottom middle). Conversely, stimulated EGFR in p38α-/- cells was mostly found in transferrin receptor (TFR)-containing early endosomes (Figure 27, bottom right), which are known to serve as platforms for sustained EGFR signaling (Shtiegman et al., 2007), but this hardly occurred in WT cells (Figure 27, top right). These results suggest that p38α regulates the confluence-induced degradation of EGFR by modulating its ubiquitination, which in turn affects the duration of EGFR downstream signals and, as a consequence, $p27^{Kip1}$ protein stability.

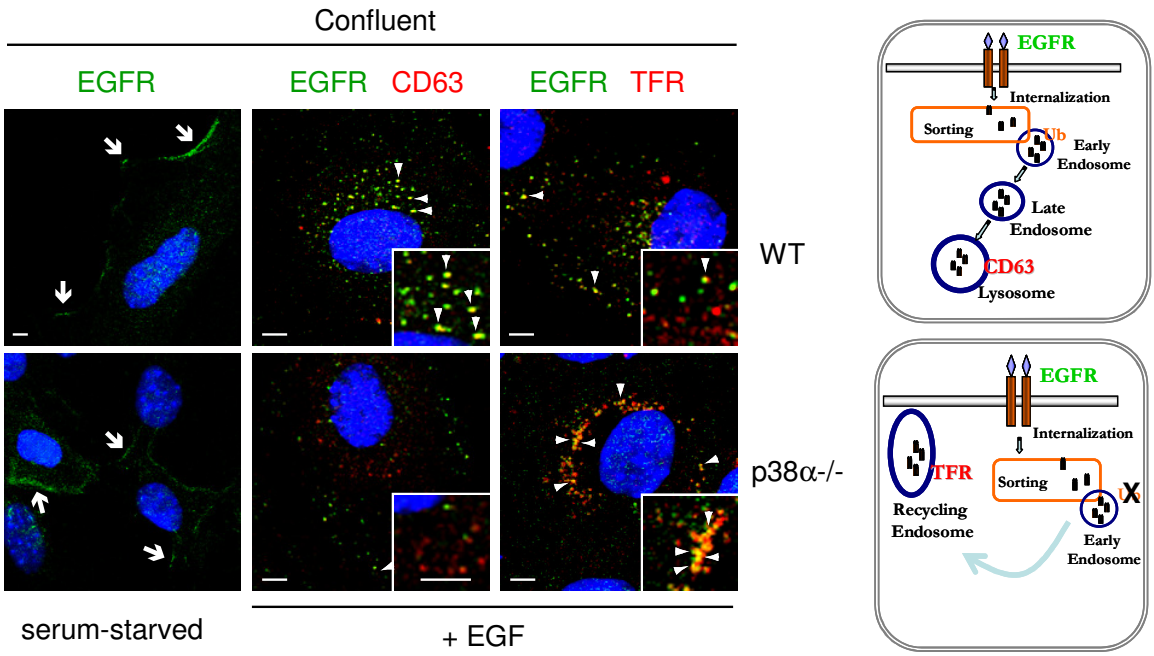

Figure 27. p38α induces confluence-dependent EGFR degradation. (Left)-Confluent WT and p38α-/- MEFs were incubated with 0.5% serum for 48 h and then left non-stimulated or treated with EGF (50 ng/ml) for 40 min. Cells were fixed, stained with antibodies against EGFR (green, left panel), CD63 (red, middle panel) or the transferrin receptor (TFR, red, right panel) and visualized by confocal microscopy. Arrows (left panels) indicate EGFR localization and arrow-heads the co-localization of EGFR with either CD63 (middle panels) or TFR (right panels). Insets show magnifications. Bars = 2 μm. **(Right)**-A scheme representing different fates for active EGFR depending on p38α activity and consequent EGFR ubiquitination.

Accordingly, p38α activation enhanced, whereas SB203580 treatment inhibited, the EGF-induced ubiquitination of EGFR in HEK293 cells as well (Figure 28B). However, we did not observe any effect of p38α on the ligand-induced internalization of EGFR, as confluent p38α-/- and WT MEFs both showed similar co-localization of the internalized

EGFR with clathrin-coated pits following EGF stimulation and no co-localization with caveolin (Figure 29).

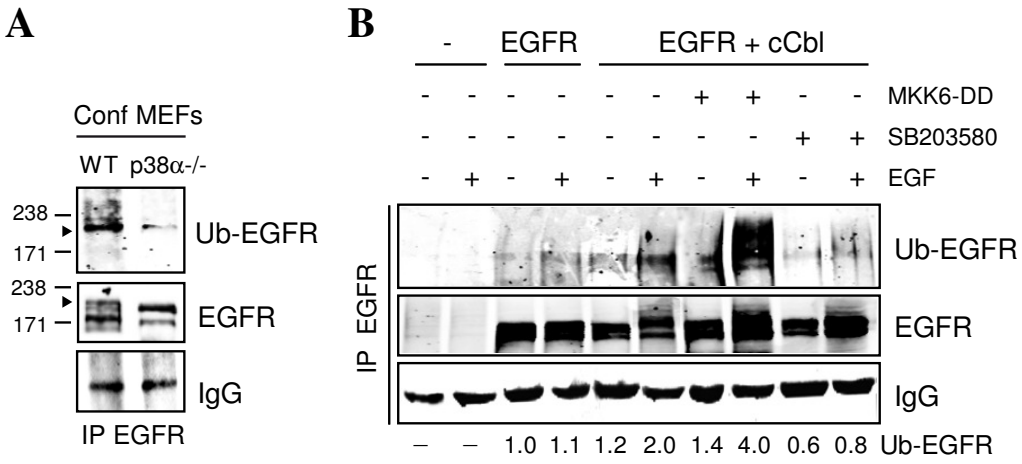

Figure 28. p38α stimulates EGFR ubiquitination in confluent cells. (A) Confluent WT and p38α-/- MEFs were serum starved, treated 15 min with EGF (50 ng/ml) and analyzed for EGFR ubiquitination by immunoprecipitation of the endogenous EGFR followed by immunoblotting. The position of the ubiquitinated EGFR (Ub-EGFR) is indicated with a black arrowhead. Molecular mass markers in kDa are indicated. **(B)** HEK293 cells were transiently transfected with plasmids expressing EGFR, cCbl or MKK6-DD, serum starved and treated 15 min with EGF (50 ng/ml) and SB203580 (10 μM), as indicated. Cell lysates were subjected to EGFR immunoprecipitation 48 h post-transfection and the immunocomplexes were analyzed by immunoblotting. Ubiquitinated EGFR was quantified by densitometry and normalized to the total EGFR levels.

We then evaluated whether p38α might impinge on EGFR ubiquitination by regulating the extent of receptor phosphorylation on Tyr1045 and/or the subsequent recruitment of the E3 ubiquitin ligase cCbl to phospho-Tyr1045 (Levkowitz et al., 1998). We found that whereas p38α did not seem to stimulate EGFR phosphorylation on Tyr1045 (Figure 30A, top panel and Figure 30B), it efficiently enhanced cCbl binding to the receptor, as indicated by the high levels of Tyr-phosphorylated cCbl (Figure 30A, bottom panel; (Levkowitz et al., 1998)). Therefore, we hypothesized that p38α mainly regulates the loading of cCbl onto the Tyr1045-phosphorylated receptor. In agreement with this, p38α activation stimulated EGFR ubiquitination and cCbl binding, which were both impaired after mutation of Tyr1045 (Figure 30C), supporting that p38α probably regulates EGFR ubiquitination through the recruitment of cCbl.

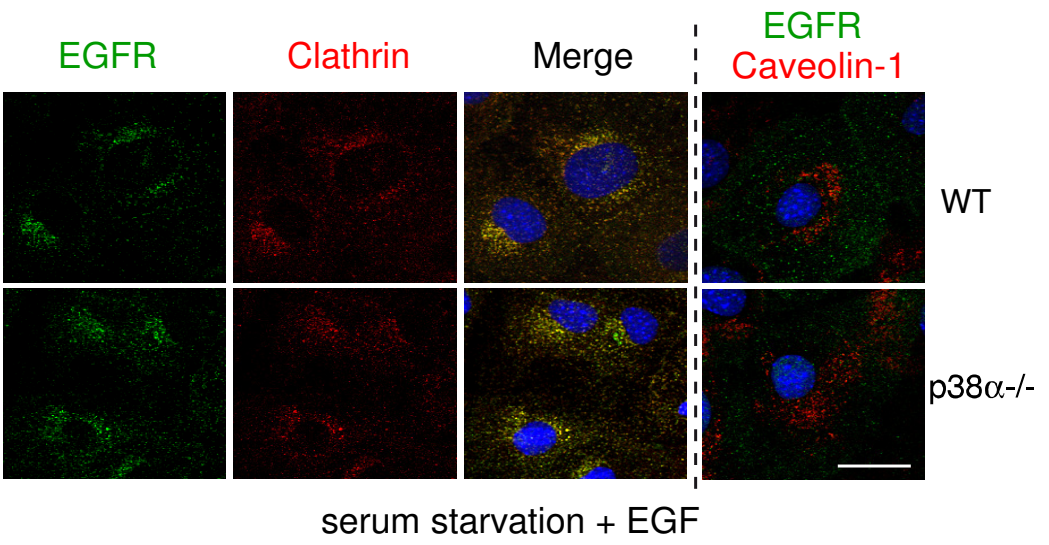

Figure 29. p38α does not regulate EGFR internalization. Confluent WT and p38α-/-MEFs were incubated with 0.5% serum for 48 h and then treated with EGF (50 ng/ml) for 5 min. Cells were fixed, stained with antibodies against EGFR (green, left panel), Clathrin (red, left panel) or Caveolin-1 (red, right panel) and visualized by confocal microscopy. Bar=25 μm.

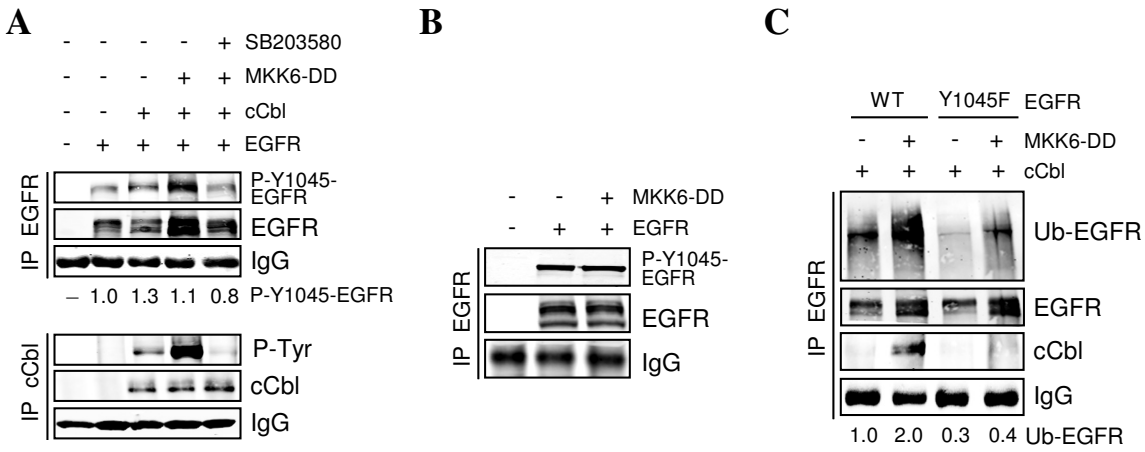

Figure 30. p38α stimulates cCbl ubiquitin ligase activity against EGFR. (A) HEK293 cells were transiently transfected with the indicated plasmids, treated 15 min with EGF (50 ng/ml) and subjected to EGFR (upper panel) or cCbl (lower panel) immunoprecipitation followed by immunoblotting. EGFR phosphorylated on Tyr1045 was quantified by densitometry and normalized to the total EGFR levels. **(B)** HEK293 cells were transiently transfected with EGFR and the p38 activator MKK6-DD, as indicated, treated as in (A) and subjected to EGFR immunoprecipitation followed by immunoblotting. **(C)** HEK293 cells were transiently transfected with WT EGFR or the mutant Y1045F together with cCbl and MKK6-DD, as indicated. EGFR immunoprecipitates were prepared as in (A). Ubiquitinated EGFR was quantified by densitometry and normalized to the total EGFR levels.

1.7. p38α induces EGFR signal termination in confluence by downregulating Sprouty2

While investigating how the association between cCbl and EGFR was regulated by p38α in confluence, we found that Sprouty2 (Spry2), an inhibitor of cCbl-mediated EGFR ubiquitination ((Rubin et al., 2005; Wong et al., 2002); Figure 31A) was highly upregulated in p38α-/- MEFs, which could be rescued to WT levels after reconstitution of p38α into p38α-deficient cells (Figure 31B). This suggested that Spry2 could be functionally implicated in the enhanced EGFR signaling and delayed contact inhibition response of p38α-/- MEFs, which we next evaluated by stably downregulating Spry2 in these cells. As expected Spry2 downregulation rescued $p27^{Kip1}$ levels in various independent clones derived from p38α-/- MEFs (Figure 32). Detailed analysis of clone #4 further revealed that Spry2 downregulation resulted in reduced EGFR signaling concomitant with increased $p27^{Kip1}$ accumulation (Figure 33A) as observed in confluent WT cells. This correlated with a more robust contact inhibition response in p38α-/- MEFs, as indicated by the dramatic decrease in confluent cell numbers upon Spry2 downregulation (Figure 33B) as well as with increased EGFR ubiquitination (Figure 33C) and enhanced resitance to oncogene-induced foci formation (Figure 33D), that phenocopied the effect of inhibiting EGFR in p38α-/- MEFs (Figure 26C).

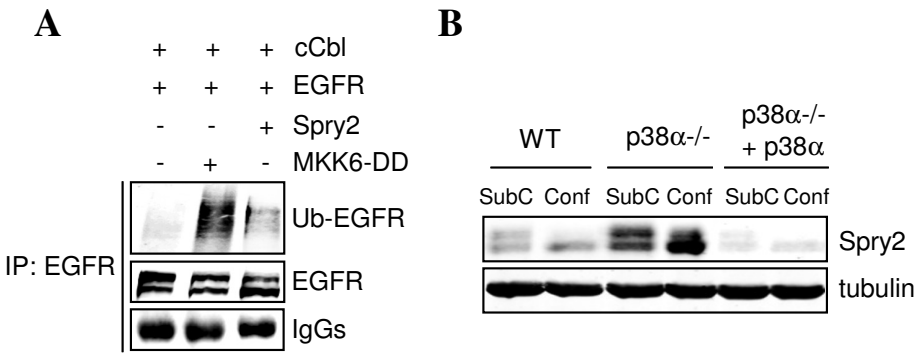

Figure 31. The cCbl inhibitor Spry2 is upregulated in confluent p38α-deficient MEFs and inhibits EGFR ubiquitination. (A) HEK293 cells were transiently transfected with cCbl, EGFR, Spry2 and MKK6-DD, as indicated. After 48 h EGFR was immunoprecipitated from 1 mg of total lysates and the immunoprecipitates were analyzed by immunoblotting. **(B)** Subconfluent (SubC) and confluent (Conf) WT, p38α-/- and p38α-/- with p38α added-back MEFs were analyzed by immunoblotting.

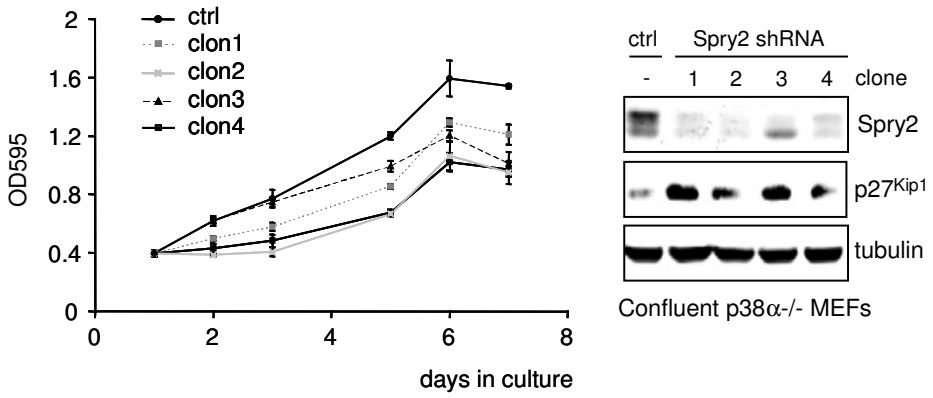

Figure 32. Contact inhibition response of various independent clones of p38α-/- MEFs interfered with Spry2 shRNAs. p38α-/- MEFs were stably transduced with shRNA lentiviral vector encoding either scrambled (ctrl) or Spry2-directed hairpins. Several stable cell clones were isolated and analyzed by MTT assay **(left panel)**. Cells were harvested at day 7 and analyzed by immunoblotting **(right panel)**. Clone number 4 was used for further experiments.

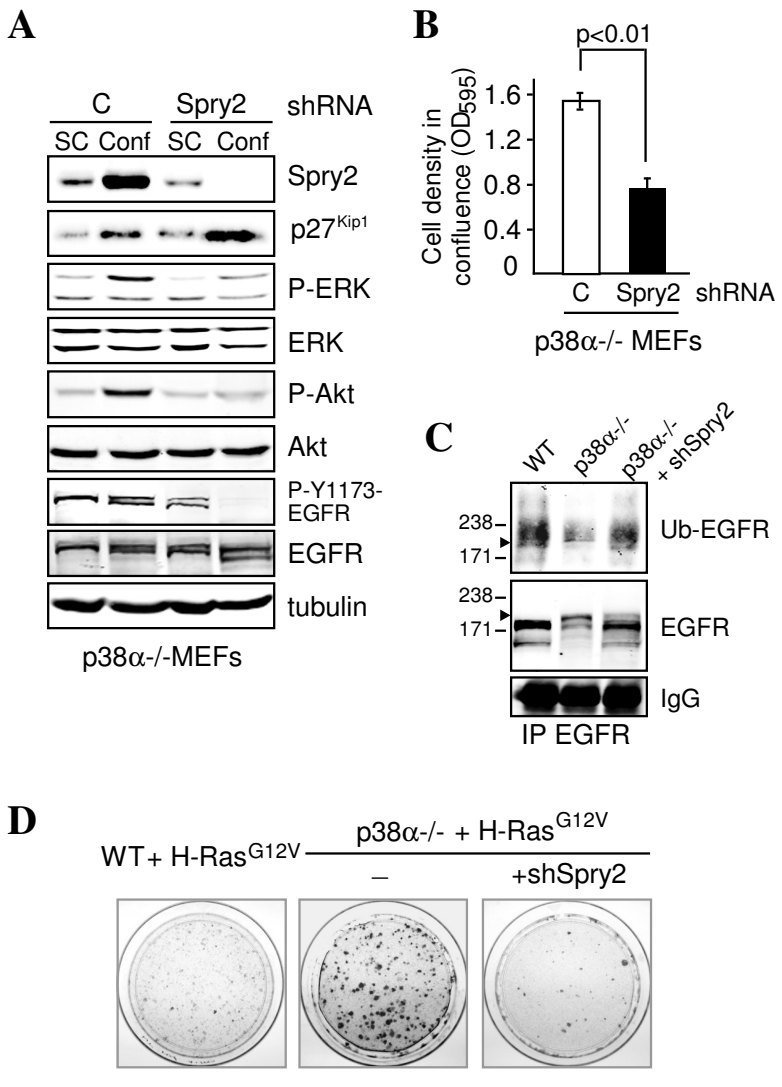

Figure 33. Spry2 mediates the p38α-induced inhibition of EGFR signaling and p27Kip1 accumulation in confluent cells. **(A)** Subconfluent (SC) and confluent (Conf) p38α-/- MEFs were stably transduced with scrambled (C) or Spry2-directed shRNAs and total lysates were analyzed by immunoblotting. **(B)** Overconfluent cell densities of p38α-/- MEFs expressing shRNAs as in (A) were determined by MTT assays. **(C)** Confluent WT, p38α-/- and Spry2 shRNA-expressing p38α-/- MEFs were serum starved, treated with EGF and analyzed for EGFR ubiquitination by immunoprecipitation of the endogenous EGFR followed by immunoblotting. **(D)** H-RasG12V-induced focus formation assay using WT MEFs and p38α-/- MEFs expressing scrambled (-) or Spry2-directed (shSpry2) shRNAs.

In line with high Spry2 levels being the likely cause of enhanced EGFR signaling in confluent p38α-/- cells, we observed increased binding of Spry2 to immunoprecipitated cCbl in confluent p38α-/- MEFs (Figure 34), which correlated with reduced cCbl-mediated ubiquitination and degradation of EGFR in these cells (Figure 27 and Figure 28B). Furthermore, whereas inhibition of p38α activity in confluent cells resulted in Spry2 accumulation and reduced levels of $p27^{Kip1}$ (Figure 35A), MKK6-DD-induced activation of p38α had the opposite effect (Figure 35B), which confirmed the results oberved in MEFs (Figure 31A), indicating an inverse correlation between p38α activity and Spry2 protein levels. Accordingly, Spry2 was much more stable in p38α-/- deficient MEFs (Figure 35C), pointing towards Spry2 as a key p38α target to induce $p27^{Kip1}$ accumulation via cCbl-dependent EGFR degradation.

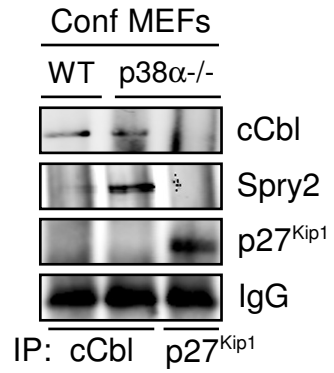

Figure 34. p38α inhibits Spry2 binding to cCbl. Cell lysates from confluent WT and p38α-/- MEFs were subjected to cCbl immunoprecipitation and then analyzed by immunoblotting. Anti-$p27^{Kip1}$ antibody was used as an IP control.

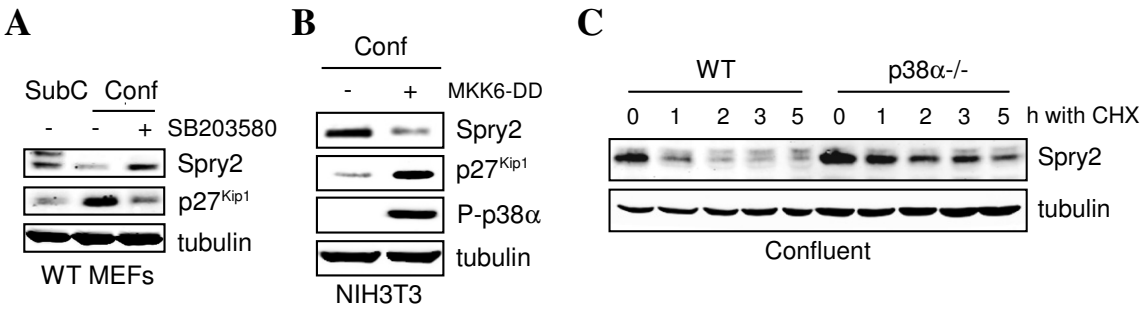

Figure 35. p38α regulates confluence by inhibiting Spry2. (A) Subconfluent (SubC) or confluent (Conf) WT MEFs were incubated 12 h with SB203580 or DMSO (-) and then analyzed by immunoblotting. **(B)** NIH3T3 cells (90% confluence) were transiently transfected with MKK6-DD or empty vector (-), harvested when they were confluent and analyzed by immunoblotting. **(C)** Confluent WT and p38α-/- MEFs were treated with CHX for the indicated times and analyzed by immunoblotting.

1.8. p38α downregulates Spry2 in confluence through the ubiquitin ligase Siah2

The difference in Spry2 protein stability between confluent WT and p38α-/- MEFs prompted us to explore whether p38α could regulate cCbl or Siah2, two ubiquitin ligases that have been shown to regulate Spry2 (Hall et al., 2003; Nadeau et al., 2007). Although Spry2 interacted with cCbl in confluent p38α-/- MEFs (Figure 34), we found that cCbl was a poor Spry2 ubiquitin ligase, as co-transfection with cCbl only slightly decreased Spry2 protein levels (Figure 36A). In contrast, co-transfection with Siah2 caused a strong downregulation of Spry2 (Figure 36A). In line with Siah2, but not cCbl, being responsible for the p38α-induced downregulation of Spry2 in confluence, we observed that the Spry2-Y55F mutant, which is impaired in cCbl binding (Mason et al., 2004), was downregulated as efficiently as Spry2-WT in confluent cells (Figure 36B).

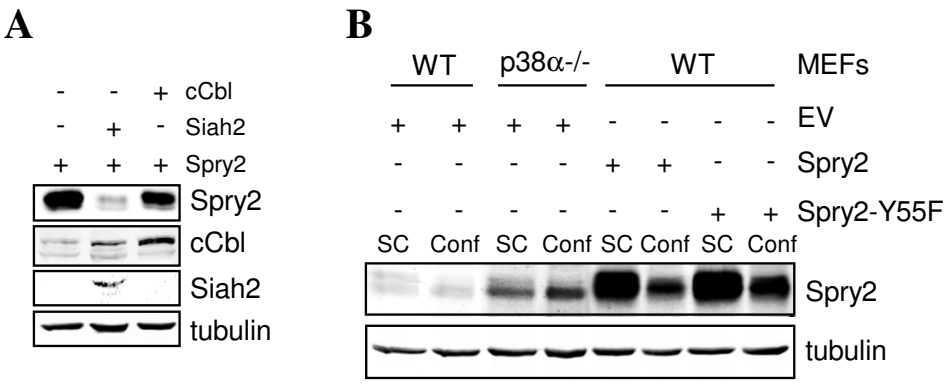

Figure 36. cCbl is a poor ubiquitin ligase of Spry2. (A) NIH3T3 cells were transiently transfected with plasmids encoding Spry2, Siah2 and cCbl, as indicated, and were analyzed by immunoblotting. **(B)** WT MEFs stably expressing WT Spry2 or the mutant Y55F as well as WT and p38α-/- MEFs transduced with the empty vector (EV) were grown to sparse (SC) or confluent (Conf) conditions and cell lysates were analyzed by immunoblotting.

As p38α has been reported to regulate Siah2 activity in the context of hypoxia signaling (Khurana et al., 2006), we investigated whether Siah2 could also function downstream of p38α in contact inhibition by regulating Spry2 stability in confluent MEFs. Indeed, we found that high cellular density increased Siah2 expression in WT but not in p38α-/- MEFs (Figure 37A), which inversely correlated with Spry2 expression in these cells (Figure 31B). To evaluate the causality of this correlation in the regulation of $p27^{Kip1}$ by p38α, we co-expressed Spry2 together with Siah2 in the presence of MKK6-DD or SB203580 and monitored $p27^{Kip1}$ levels (Figure 37B). Activation of p38α by MKK6-DD increased Siah2 levels, which correlated with both Spry2 downregulation and $p27^{Kip1}$ upregulation, pointing to Siah2 as a p38α target that indirectly regulates $p27^{Kip1}$ protein

levels through Spry2. This was confirmed by treatment with the inhibitor SB203580 that reversed the effect of p38α activation on the Siah2-Spry2-p27^{Kip1} axis (Figure 37B).

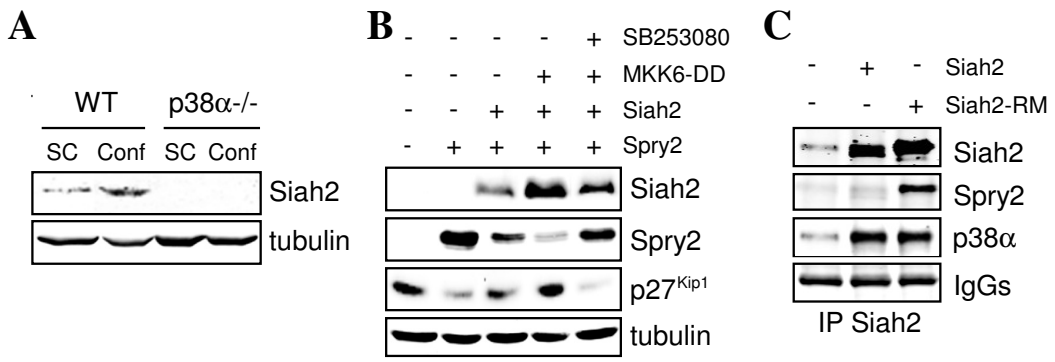

Figure 37. p38α downregulates Spry2 through the ubiquitin ligase Siah2. **(A)** Cell lysates from sparse (SC) and confluent (Conf) WT and p38α-/- MEFs were analyzed by immunoblotting. **(B)** NIH3T3 cells were transiently transfected with Spry2, Siah2 and MKK6-DD and 36 h later were treated with either SB203580 or DMSO for another 12 h, as indicated. Cell lysates were analyzed by immunoblotting. **(C)** Siah2 was immunoprecipitated from lysates of HEK293 cells transfected with plasmids encoding WT Siah2 or the mutant Siah2-RM and the immunocomplexes were analyzed by immunoblotting.

Furthermore, we were able to co-immunoprecipitate Spry2 together with endogenous p38α in a complex with the catalytic inactive mutant Siah2-RM (Figure 37C), suggesting that p38α can modulate Spry2 stability by directly binding to and regulating Siah2. Of note, we could also see an interaction between endogenous p38α and WT Siah2 (Figure 37C), despite Spry2 not being present in the complex, most likely due to the strong ubiquitin ligase activity of Siah2 on Spry2 (Figure 36), which indicates that p38α binds Siah2 independently of Spry2. Interestingly, the stability effect observed on Siah2 (Figure 37B) correlates with increased Ser/Thr phosphorylation on Siah2 upon p38α activation by MKK6-DD (Figure 38A), suggesting that p38α is likely to stabilize Siah2 in confluence by phosphorylation. Accordingly, we found that Thr24 and Ser29, two sites that have been previously reported to regulate Siah2 stability and its ubiquitin-ligase activity in hypoxia signaling (Khurana et al., 2006), were the main residues targeted by p38α on Siah2 in contact inhibition as well (Figure 38C).

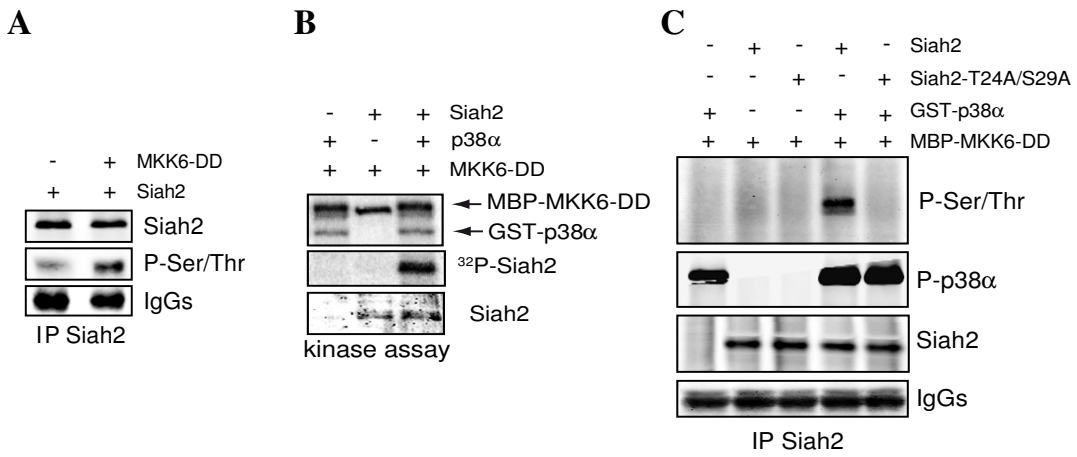

Figure 38. p38α directly phosphorylates Siah2. (A) HEK293 cells were transiently transfected with Siah2 and MKK6-DD, as indicated, incubated for 30 h and then treated with MG132 for 6 h more. Total lysates were immunoprecipitated with Siah2 antibody and were analyzed by immunoblotting. **(B)** HEK293 cells were transiently transfected with Siah2-WT and the total lysates were immunoprecipitated with Siah2 antibody. Immunocomplexes were used as substrates for *in vitro* phosphorylation with MKK6-DD-activated GST-p38α or MKK6-DD alone and subsequently analyzed by autoradiography. **(C)** HEK293 cells were transiently transfected with Siah2-WT or the Siah2-T24A/S29A double mutant and the total lysates were immunoprecipitated with Siah2 antibody. Immunocomplexes were used as substrates for *in vitro* phosphorylation with MKK6-DD-activated GST-p38α or MKK6-DD alone and subsequently analyzed by immunoblotting with the indicated antibodies.

1.9. p38α negatively regulates oncogene-induced transformation through contact inhibition and this function is impaired in transformed cell lines

We previously reported (Dolado et al., 2007) that p38α-/- MEFs probably lose contact inhibition upon oncogene expression more efficiently than WT cells, as indicated by the bigger size of the foci produced by oncogenes in confluent p38α-/- cultures (Figure 39). Noteworthy, H-Ras^{V12} (H-Ras^{GV12})-transformed WT and p38α-deficient MEFs proliferated with similar rates in confluence (Figure 40).

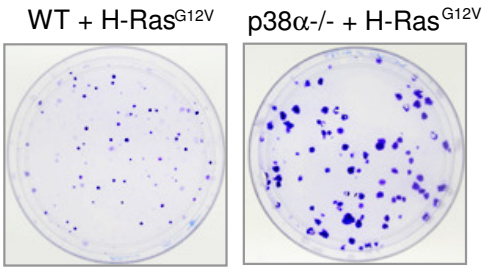

Figure 39. p38α-/- MEFs are more susceptible to the oncogene-induced loss of contact inhibition. Confluent WT and p38α-/- MEFs were transiently transduced with H-Ras^{V12} and allowed to form foci.

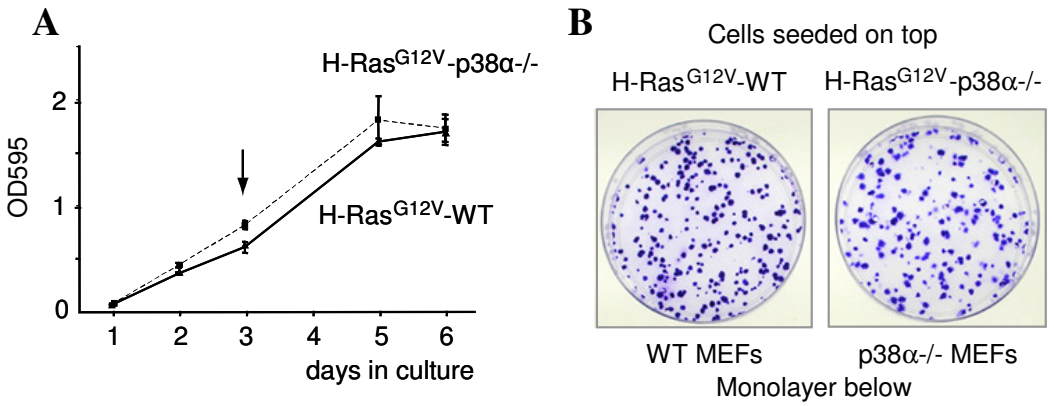

Figure 40. H-Ras^{V12}-transformed WT and p38α-/- MEFs similarly proliferate in confluence. **(A)** MTT cell proliferation curves of H-Ras^{V12}-transformed WT and p38α-/- MEFs. The arrow indicates the onset of confluence. **(B)** H-Ras^{V12}-transformed WT and p38α-/- MEFs (500 cells) were seeded on top of confluent monolayers of contact inhibited MEFs of the same genotype (without H-Ras^{V12}) and allowed to form foci.

As loss of contact inhibition is considered a hallmark of cell transformation (Abercrombie, 1979; Hanahan and Weinberg, 2000; Pollack et al., 1968), we next investigated whether malfunctioning of the p38α-p27^{Kip1} axis could underline the impaired contact inhibition response of transformed cells. With this aim, we expressed oncogenic H-Ras^{V12} in MEFs and analyzed their contact inhibition response in terms of p38α activation and p27^{Kip1} accumulation. In agreement with previous reports (Leone et al., 1997; Takuwa and Takuwa, 1997), we found that H-Ras^{V12} expression abolished contact inhibition, as cells did not arrest in confluence (Figure 40A) and p27^{Kip1} failed to accumulate in such conditions (Figure 41A). Noteworthy, confluent activation of p38α was also impaired upon oncogene expression, suggesting that transformed cells most likely deregulate signaling upstream of p38α to prevent the confluence-induced activation of p38α and subsequent p27^{Kip1} accumulation. Consistent with this idea, we confirmed that forced activation of p38α by expression of MKK6-DD strongly increased p27^{Kip1} protein levels in H-Ras^{V12}-transformed cells (Figure 41B), suggesting that although transformation uncouples the confluence state from p38α activation, this pathway is still potentially functional.

Altogether, these results point towards the p38α-p27^{Kip1} axis as a key inhibitor in the onset of cell transformation through the regulation of contact inhibition, which nonetheless seems to be under negative selective pressure in the early transformed cell, most likely in order to evade proliferative constraints and progress towards malignancy.

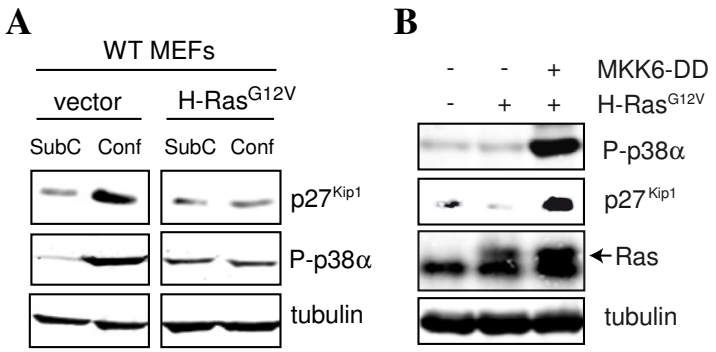

Figure 41. p38α-mediated regulation of contact inhibition is impaired in transformed cells. **(A)** Total lysates from subconfluent (SubC) and confluent (Conf) empty vector- or H-Ras^{V12}-transduced MEFs were analyzed by immunobloting. **(B)** NIH3T3 cells transiently transfected with H-Ras^{V12} alone or together with MKK6-DD were analyzed by immunoblotting.

2. Regulation of gene expression by p38α MAPK in malignant cell transformation

2.1. Comparison of the transformed phenotype between WT and p38α-/- fibroblasts expressing H-Ras^{V12}

WT and p38α-/- MEFs were stably transduced with H-Ras^{V12} and subsequently compared in terms of proliferation, morphology, contact inhibition and extracellular matrix-independent growth. We found that immortalized WT and p38α-/- MEFs proliferated with comparable rates (Figure 11B), although p38α-/- MEFs proliferated slightly faster than WT MEFs upon H-Ras^{V12} transduction (Figure 42A, see also Figure 40A above). Furthermore, H-Ras^{V12}-expressing p38α-/- MEFs acquired a more refringent morphology when compared to WT MEFs (Figure 42B) and also formed more colonies in soft agar (Figure 42C). Importantly, the differences between WT and p38α-/- MEFs could be rescued by re-introduction of p38α in H-Ras^{V12} expressing p38α-/- cells (Figure 42D and 42E), meaning that the observed differences were directly related to the absence of p38α.

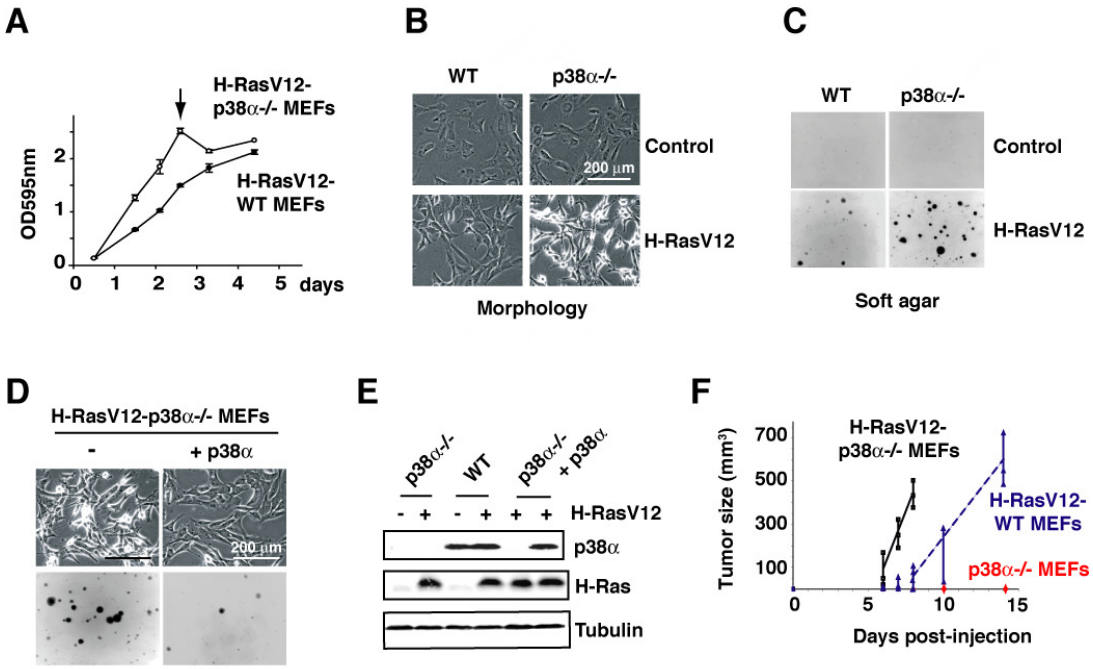

Figure 42. p38α negatively regulates H-Ras^{V12}-induced malignant transformation. **(A)** Proliferation rates of H-Ras^{V12}-expressing WT and p38α-/- MEFs. The arrow indicates when H-Ras^{V12}-expressing p38α-/- cells achieved confluence. **(B-C)** H-Ras^{V12}-expressing WT and p38α-/- MEFs, as well as control cells transduced with an empty vector, were selected with puromycin (1.5 μg/ml) for 1 week and then compared in terms of **(B)** morphology and **(C)** anchorage-independent growth in soft agar. **(D-E)** p38α-/- MEFs were rescued by forced expression of p38α and then analyzed for **(D)** anchorage-independent growth and morphology, as well as by **(E)** immublotting with the indicated antibodies. **(F)** Nude mice were injected subcutaneously with control p38α-/- (red) and H-Ras^{V12}-expressing WT (blue) or p38α-/- (black) MEFs, and tumor size was measured periodically.

In agreement with a recent report (Bulavin and Fornace, 2004), our results indicate that the tumor-suppressive effect displayed by p38α is likely independent of p53, whose expression was undetectable in our cell system under any condition. The *in vivo* relevance of these observations was confirmed by injecting nude mice subcutaneously with H-Ras^{V12}-transformed p38α-/- MEFs, which gave rise to tumors significantly faster than H-Ras^{V12}-transformed WT MEFs (Figure 42F).

2.2. Gene expression profiling of H-Ras^{V12}-transformed WT and p38α-/- fibroblasts

In order to identify new transcriptional targets of p38α in the regulation of oncogene-induced transformation, RNA from exponentially proliferating H-Ras^{V12}-transformed WT and p38α-/- MEFs was extracted in triplicates, labeled and analyzed with the Amersham Codelink® 20K platform. Statistical filtering, retaining only genes with an increased or decreased expression greater than ±1.5-fold between both cell lines with an adjusted p-value < 0.01, revealed 202 genes that were significantly deregulated between WT and p38α-/- MEFs (Appendix Table 2). Among them, 139 genes (69%) were upregulated and 63 (31%) were downregulated in H-Ras^{V12}-p38α-/- fibroblasts (Figure 43A).

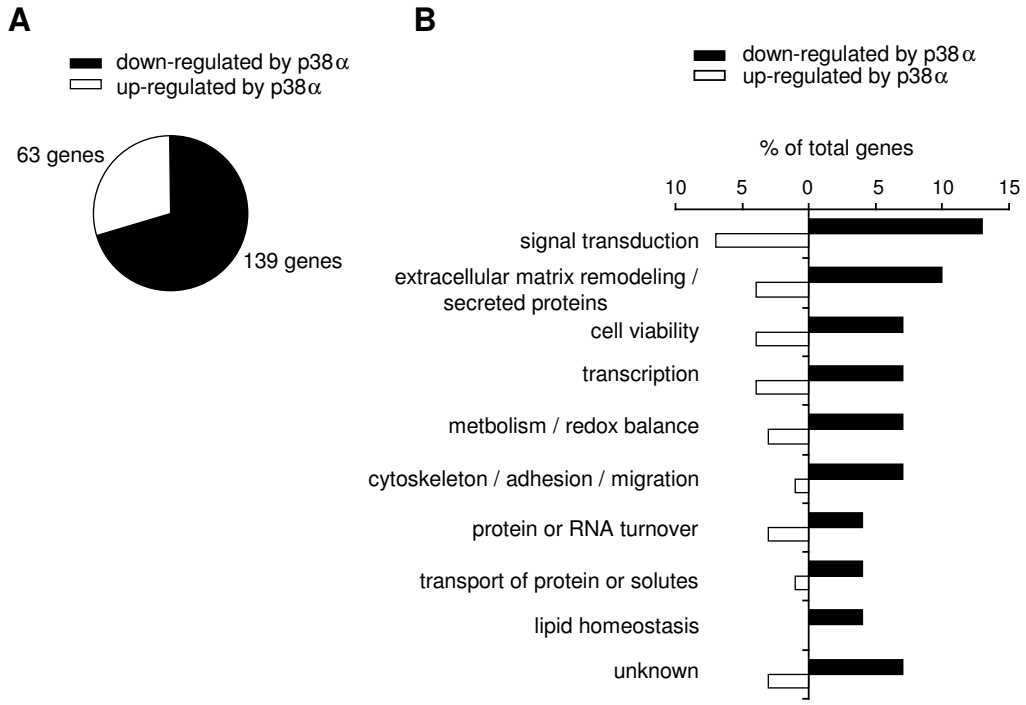

Figure 43. Functional categories of the differentially expressed genes between H-Ras^{V12}-expressing p38α-/- and WT MEFs. (A) Representation of the total number of genes (202) found to be upregulated (white) or downregulated (black) by p38α in the microarray analysis comparing H-Ras^{V12}-p38α-/- and H-Ras^{V12}-WT MEFs. **(B)** Number of genes (as percentage of 202 genes) within each functional category that are up- (black) or down-regulated (white) in H-Ras^{V12}-p38α-/- MEFs.

Genes were subsequently clustered according to their biological function using Gene Ontology (GO)-based approaches (Figure 43B and Appendix Table 3). The majority of biological functions represented were related to signal transduction (20% of the genes) and matrix remodelling (14%). Another 30% of the genes were shared at equal parts by functions regarding the regulation of cell viability (11%), transcription (11%) and metabolism/redox regulation (10%). There were five additional functional categories representing the rest of the genes, including functions dealing with cytoskeleton dynamics and migration (8%), protein/RNA turn-over (7%), protein/solute transport (5%), lipid homeostasis (4%) and other unknown functions (10%) (Appendix Table 3).

2.3. Validation of gene expression in cultured cells by semiquantitative RT-PCR

To validate microarray gene expression data, we selected 31 out of the 202 genes found to be regulated by p38α (Appendix Table 4) and performed semiquantitative RT-PCR. Gene selection was based on the difference in mRNA expression levels (fold-change) between H-Ras^{V12}-p38α-/- and H-Ras^{V12}-WT MEFs, as well as on the putative involvement of each gene in oncogenic Ras transformation or p38α signaling. 19 out of the 31 genes were up-regulated in H-Ras^{V12}-p38α-/- MEFs whereas the other 12 were downregulated in these cells. Most of the genes selected could be categorized into 5 functional groups, which are signal transduction (*Arhgdib*, *Rab3b*, *Ralgds*, *Nck2*, *Ramp3*, *Cd9, Dock8, Cxcl1*), cell viability (*Pmp22*, *Egln3*, *Nr4a1*, *Rtn4*, *Traf1*), metabolism/redox regulation (*Sardh*, *Gstm2*), matrix remodeling (*Loxl1*, *Mmp3*, *Ctsl*, *Ctsh*, *Dpep1*) and transcription (*Foxd1, Snf1lk*).

In order to dissect the individual contribution of p38α and H-Ras^{V12} to gene expression, we used two different cellular systems to perform gene expression validation. The first consisted of established WT and p38α-/- MEFs constitutively expressing H-Ras^{V12} for at least two weeks (Alfonso et al., 2006; Dolado et al., 2007), which allowed the evaluation of gene expression under conditions of chronic, steady-state H-Ras^{V12} signaling in both cell lines. The second were WT and p38α-/- MEFs expressing a 4-hydroxytamoxifen (OHT)-inducible, estrogen receptor (HBD-ER)-tagged form of H-Ras^{V12} (ER-HRas^{V12}) ((Dolado et al., 2007); Figure 44). This allowed monitoring of gene expression in the absence of H-Ras^{V12} signaling as well as early (24 h) after its acute activation, hence permitting to establish the timeline for the observed differences in gene expression between H-Ras^{V12}-transformed p38α-/- and WT MEFs.

We observed that all the genes analyzed by semiquantitative RT-PCR were deregulated between stable H-Ras^{V12}-expressing WT and p38α-/- MEFs (Figures 45B and C, right panels) in a manner that completely mirrored the microarray results, at least qualitatively (note microarray fold change values to the right).

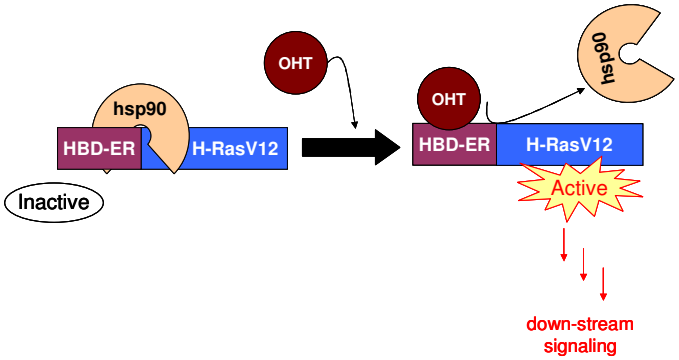

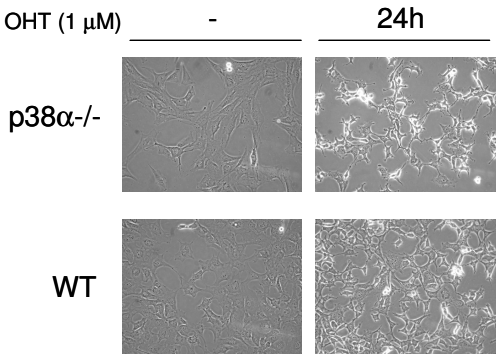

Figure 44. 4-hydroxytamoxifen (OHT)-inducible system of H-Ras^{V12}. (Top) - The ER-HRas^{V12} construct consists of a N-terminal fusion of the hormone-binding domain of the human estrogen receptor (HBD-ER) in frame with H-Ras^{V12}. It allows the controlled expression of H-Ras^{V12} after addition of OHT to the culture media. **(Bottom) -** Morphological transformation of ER-HRas^{V12}-expressing MEFs after treatment with 1 µM OHT for 24 h.

Of note, we could not detect expression of 5 out of the 31 genes, namely *Stac2, Rom1, Dpep1, Traf1* and *Lzts2*. Concerning the other 26 genes, the analysis of the RNA extracted from ER-HRas^{V12}-expressing WT and p38α-/- MEFs, bearing the H-Ras^{V12} inducible system, revealed that approximately half of the 26 genes analyzed were already deregulated in the parental lines due to the absence of p38α (Figure 45B, left panel, indicated by an asterisk), whereas the other half were additionally influenced by H-Ras^{V12} signaling (Figure 45C, left panel, indicated by an asterisk). Interestingly, the effect of H-Ras^{V12} on gene expression in the latter case was already clear 24 h after the onset of H-Ras^{V12} signaling (i.e. 24 h of OHT treatment) and afterwards remained during the transformation process (i.e. compare with MEFs stably expressing H-Ras^{V12}). Importantly, those genes deregulated between H-Ras^{V12}-expressing WT and p38α-/- MEFs due to p38α deficiency (Figure 45B, left panel, see WT (-) and p38α-/- (-)) could be rescued by re-introduction of p38α into p38α-/- MEFs (control cells, without H-Ras^{V12}) (Figure 45D). This argues that the observed changes in gene expression in the parental cells are directly due to the absence of p38α and not to secondary genetic alterations.

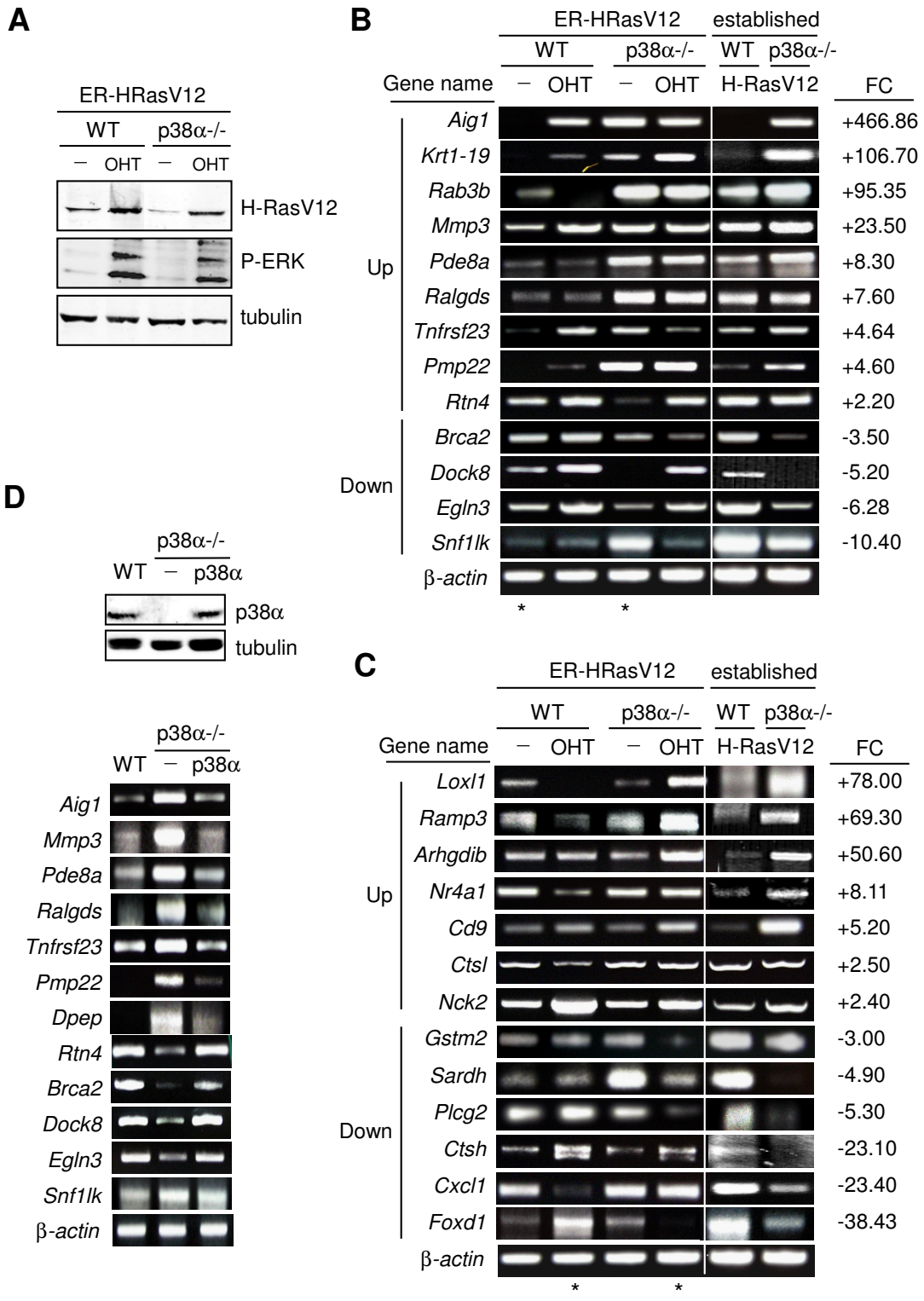

Figure 45. Semiquantitative RT-PCR validation of 26 genes selected from the microarray analysis. **(A)** Immunoblotting of cell extracts from ER-HRas^{V12}-expressing WT and p38α-/- MEFs stimulated with OHT (1 μM) for 24 h. **(B)** Genes deregulated between H-Ras^{V12}-expressing p38α-/- and WT MEFs by virtue of p38α deficiency. The two lines to the right represent established H-Ras^{V12}-expressing MEFs. The first 4 lines to the left correspond to WT and p38α-/- MEFs bearing the ER-HRas^{V12} system. Treatment with OHT (1 μM) for 24 h is indicated. Asterisks indicate changes dependent on p38α. Up – upregulated in p38α-/- MEFs, Down – downregulated in p38α-/- MEFs. **(C)** Genes deregulated between H-Ras^{V12}-expressing p38α-/- and WT MEFs by the combined effect of p38α and H-Ras^{V12} signaling. Samples as in **(B)**. Asterisks indicate changes caused mainly by H-Ras^{V12} expression. **(D)** p38α immublotting in WT, p38α-/- and p38α add-back p38α-/- MEFs (top) followed by semiquantitative RT-PCR (bottom) against genes found to be dependent on p38α expression (see **(B)**). FC, microarray fold-change (log_2 ratio) in H-Ras^{V12}-p38α-/- *versus* H-Ras^{V12}-WT MEFs.

2.4. Gene expression validation in cultured cells and mouse tumors by quantitative RT-PCR

In order to assess the relevance of the observed gene expression changes between WT and p38α-/- MEFs for *in vivo* tumorigenesis, some genes were also analyzed by quantitative RT-PCR (qRT-PCR) in H-Ras^{V12}-expressing WT and p38α-/- MEFs, as well as in tumors derived from these cells in nude mice ((Dolado et al., 2007); see Figure 42F above). Additionally, we also analyzed the expression of these genes in mouse lung tumors bearing activated K-Ras^{V12}, either WT or p38α-/- (Ventura et al., 2007). Interestingly, all the genes analyzed were similarly deregulated in a p38α-dependent manner in MEFs, MEF-derived tumors and lung tissue in accordance with the results obtained in the microarray analysis (Figure 46). This suggests that p38α might indeed modulate tumorigenesis *in vivo* by regulating the expression of genes involved in cell transformation. Although the microarray-based profiling and qRT-PCR analysis did not result in identical quantitative changes, fold-changes were qualitatively maintained for all of the genes analyzed in the different *in vitro* and *in vivo* biological models (Figure 46 and Appendix Table 5).

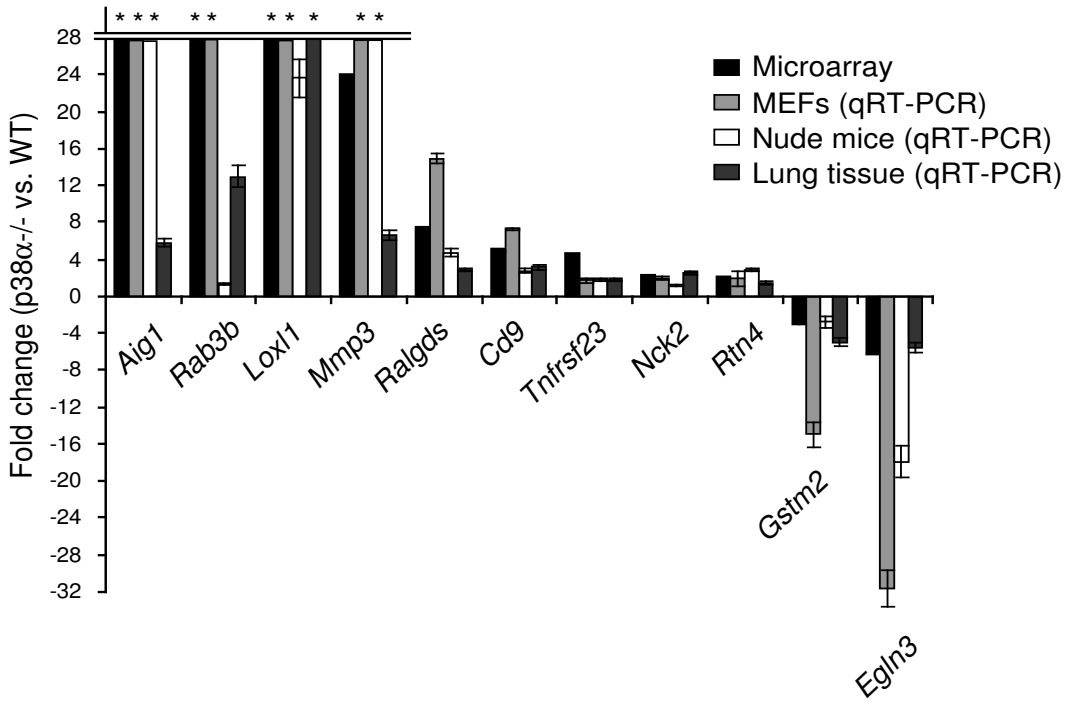

Figure 46. Quantitative RT-PCR (qRTPCR) analysis of gene expression in various *in vitro* and *in vivo* biological models. qRT-PCR analysis was performed on RNA extracted from exponentially proliferating, H-Ras^{V12}-expressing WT and p38α-/- MEFs (light gray), subcutaneous xenografts in nude mice derived from these same cells (white), or K-Ras^{V12}-induced lung tumors in WT and p38α-/- mice (dark grey). qRT-PCR results for each gene are plotted side-by-side with the respective microarray fold change value (black). The asterisks indicate fold changes greater than 28. All qRT-PCR values together with their coresponding standard deviations are listed in Appendix Table 5.

2.5. Selection of genes differentially expressed between H-Ras^{V12}-transformed WT and p38α-/- MEFs for functional validation

Next, we randomly selected 9 out of the 26 genes validated by semiquantitative RT-PCR to perform functional assays, which was done based on their level of deregulation between H-Ras^{V12}-expressing WT and p38α-/- MEFs (fold-change) as well as on their putative connection with the process of cell transformation. These were *Aig1*, *Mmp3*, Ctsh, *Cd9*, *Pmp22*, *Nck2*, *Rtn4*, *Gstm2*, and *Egln3* (Table 4).

Table 4. Differentially expressed genes between H-Ras^{V12}-transformed p38α-/- and WT MEFs selected for functional validation

Genebank Accession Number	Gene symbol	Fold change*	Gene name
NM_025446	*Aig1*	+466.86	Androgen induced-1
NM_010809	*Mmp3*	+23.50	Matrix metallopeptidase 3
NM_007657	*Cd9*	+5.20	CD9 antigen
NM_008885	*Pmp22*	+4.60	Peripheral myelin protein
NM_010879	*Nck2*	+2.40	Non-catalytic region of tyrosine kinase adaptor protein 2
NM_024226	*Rtn4*	+2.20	Reticulon 4
NM_008183	*Gstm2*	-3.00	Glutathione S-transferase, mu 2
NM_028133	*Egln3*	-6.28	EGL nine homolog 3, PHD3
NM_007801	*Ctsh*	-23.40	Cathepsin H

*, microarray-based fold change (log_2 ratio) in H-Ras^{V12}-p38α-/- *versus* H-Ras^{V12}-WT MEFs

The first three genes, *Aig1*, *Mmp3* and *Ctsh*, codify for membrane (*Aig1*) or extracellular matrix proteins (*Mmp3, Ctsh*) (Buhling et al., 2002; Seo et al., 2001; Sternlicht and Werb, 2001) and were mostly selected due to their acute deregulation in H-Ras^{V12}-p38α-/- *versus* H-Ras^{V12}-WT MEFs, which ranges from +468-fold for *Aig1* to -23 -fold for *Ctsh*. Little is known about *Aig1*, also known as androgen-induced 1, in the context of malignant transformation, but we were tempted to validate this gene due to its high level of expression in the highly transfomed H-Ras^{V12}-p38α-/- MEFs. As for *Mmp3*, this gene is upregulated 23-fold in H-Ras^{V12}-p38α-/- *versus* H-Ras^{V12}-WT MEFs and codifies for a matrix remodeling enzyme called matrix metalloproteinase (MMP)-3 or stromelysin (Str)-1. As with many other MMPs, which are involved in extracellular matrix

breakdown in physiological and disease conditions (i.e. cancer) (Overall and Dean, 2006; Werb and Chin, 1998), MMP-3 has been well established as a promoter of tumor progression, which seems to be accounted for by its pro-invasive activity as well as by its ability to promote cell proliferation and inhibit apoptosis (Radisky et al., 2005; Si-Tayeb et al., 2006; Sternlicht et al., 1999). The third gene within this group, *Ctsh* (cathepsin H or Ctsh), codifies for a lysosomal protein of the family of cathepsin proteases that have recently emerged as an important class of proteolytic enzymes in cancer (Palermo and Joyce, 2008). Accordingly, emerging evidence suggests that Ctsh participates in tumor progression (Reinheckel et al., 2005; Schweiger et al., 2004).

Six other genes were selected based on their potential connection with the process of oncogenic transformation as well as with Ras or p38 MAPK signaling. These are the metabolic genes *Gstm2* and *Egln3*, the tyrosine kinase signaling-modulating genes *Cd9* and *Nck2*, the anti-proliferative *Pmp22* and the pleiotropic gene *Rtn4*, which is involved in various processes ranging from migration and cytoskeleton dynamics to apoptosis (Table 4). Out of them, *Cd9*, *Nck2*, *Rtn4* and *Pmp22* were upregulated in the more transformed H-Ras^{V12}-p38α-/- MEFs, whereas *Gstm2* and *Egln3* were downregulated in these cells, suggesting that the first four may play tumor promoting activities. Accordingly, some among them have been described to be upregulated in tumor *versus* normal tissue and be potentially associated with tumor progression. For instance, *Cd9*, encoding for CD9 antigen or motility related protein (Mrp)-1 of the tetraspanin family, has been widely associated with cell adhesion and motility (Mhawech et al., 2004). Furthermore, CD9 has been described as a membrane scaffold protein that mediates activation of EGFR by transforming growth factor-α (TGF-α), hence promoting cell proliferation and tumor development (Imhof et al., 2008; Shi et al., 2000). Similarly, *Nck2*, which stands for non-catalytic region of tyrosine kinase adaptor protein (Nck) 2, also known as Grb4 or Nckβ, has been shown to act as an intracellular adaptor protein linking receptor tyrosine kinases to downstream signaling pathways via its SH2 domain, hence promoting cell proliferation (Frese et al., 2006; Ruusala et al., 2008) and tumor progression (Chou et al., 1992; Li et al., 1992). Conversely, *Rtn4*, which codifies for proteins of the neurite outgrowth inhibitor family Nogo, has not been that widely implicated in malignant transformation as *Cd9* or *Nck2*, although it may regulate tumor cell survival in certain conditions (Oertle et al., 2003). Interestingly, the Nogo isoform Nogo-B has been shown to be directly phosphorylated by the p38 MAPK downstream kinase MAPKAPK-2 (Rousseau et al., 2005), which might be relevant for the regulation of cell migration by p38α. In contrast to *Rtn4*, no functional or molecular connection currently exists linking p38 and the *Pmp22* gene product, namely peripheral myelin protein 22 (Pmp22) or growth arrest specific (Gas)-3, also a member of the tetraspanin

protein family (Mobley et al., 2007). The fact that this gene is upregulated in the more transformed H-Ras^{V12}-p38α-/- MEFs is intriguing, as it would not be expected for an anti-proliferative (Zoidl et al., 1995) and pro-apoptotic gene (Brancolini et al., 1999; Fabbretti et al., 1995) to drive tumor promoting activities.

Of the other 2 genes downregulated in H-Ras^{V12}-p38α-/- MEFs, *Gstm2*, which codifies for the second member of the mamalian Mu-class of cytosolic glutathione S-transferases (GSTs) (Nebert and Vasiliou, 2004), emerged as an attractive candidate to challenge functionally. Indeed, Gstm2 has been shown to modulate the cell response to oxidative stress via detoxification of oxygen radicals (Zhou et al., 2008) as well as through inhibition of apoptotic pathways (Cho et al., 2001). Its implication in oxidative stress, made it a potentially interesting protein regulated by p38α in the context of cell transformation, since oxidative stress and oncogenic signaling have been shown to cooperate in cancer progression (Mitsushita et al., 2004; Woo and Poon, 2004). Concerning *Egln3*, this gene codifies for the third member of the prolyl hydroxylase (PHD) family, namely Egln3 or PHD3, which acts as an oxygen sensor that inhibits angiogenic responses in normoxia via degradation of the hypoxia inducible factor (HIF)-1 (Metzen, 2007). Furthermore, PHD3 has been also shown to have a strong pro-apoptotic activity (Lee et al., 2005), which might explain its downregulation in the more transformed H-Ras^{V12}-p38α-/- MEFs. Of note, p38α has been recently shown to regulate PHD3 expression by post-translational means (Khurana et al., 2006). Curiously, PHD3 has been recently reported to mediate the process of skeletal muscle differentiation (Fu et al., 2007), a process where p38α plays a critical role (Perdiguero et al., 2007), although no link has been established yet between p38α and PHD3 in this process.

2.6. Functional validation of genes deregulated between H-Ras^{V12}-expressing WT and p38α-/- fibroblasts

The ability to grow anchorage-independently is the most predictive *in vitro* phenotype for *in vivo* tumorigenesis (Shin et al., 1975). Thus, we set a functional assay based on this particular trait of the cancer cell to study the effect of selected microarray candidates on the inhibitory role of p38α against oncogenic H-Ras^{V12} transformation. The assay consisted in a transient (2-3 days) co-infection of WT and p38α-/- MEFs with oncogenic H-Ras^{V12} alone or in combination with each microarray candidate of interest, followed by a 10/15-day soft agar assay. We wanted to analyze how each gene affected the ability of oncogenic H-Ras^{V12} to induce anchorage-independent growth, which is enhanced in the absence of p38α (Dolado et al., 2007). Technically, we overexpressed in p38α-/- MEFs the microarray genes (Figure 42C) that were upregulated in the less transformed H-

Ras^{V12}-WT MEFs (i.e. *Ctsh*, *Gstm2*, *Egln3*) (Table 4), expecting that they would inhibit anchorage-independent growth if they were effectors the tumor suppressor effect of p38α in WT cells. Conversely, genes found to be upregulated in H-Ras^{V12}-p38α-/- MEFs were overexpressed in WT cells (i.e. *Aig1*, *Mmp3*, *Cd9*, *Nck2*, *Rtn4*, *Pmp22*) (Table 4). In the second case, we foresaw that gene overexpression might enhance soft agar growth in WT MEFs, which would explain why these genes were upregulated in the first place in the more transformed H-Ras^{V12}-p38α-/- MEFs. In addition to soft agar, proliferation rates were also measured in parallel.

After cloning the selected gene candidates in retroviral vectors and stable transduce them in MEFs, we first evaluated the effect of overexpressing in WT MEFs those genes found to be upregulated in H-Ras^{V12}-p38α-/- cells, namely *Aig1*, *Mmp3*, *Cd9*, *Nck2*, *Rtn4* and *Pmp22* (Table 4). Their steady-state levels of overexpression were checked before functional validation by immunoblotting or RT-PCR (Figure 47A), depending on the availability of antibodies. Interestingly, overexpression of *Mmp*3, *Cd9* and *Rtn4* enhanced the transformed phenotype of H-Ras^{V12}-WT MEFs to levels that mirrored the behaviour of H-Ras^{V12}-p38α-/- cells, both at the level of proliferation (Figure 47B) and capability to grow anchorage-independently (Figure 47C). Similarly, *Nck2* stimulated the proliferation of WT MEFs to p38α-/- levels (Figure 47B), although it did not have any effect on H-Ras^{V12}-induced soft agar growth (Table 5), suggesting that p38α might regulate different traits of the cancer cell (i.e. proliferation, anchorage-independent growth) through distinct transcriptional targets. Overall, our results suggest that p38α may normally attenuate H-Ras^{V12}-induced transformation in MEFs by transcriptionally downregulating the expression of these four genes. In contrast, no conclusions could be drawn on *Aig1* since we did not manage to ectopically express this gene, whereas *Pmp22* overexpression in H-Ras^{V12}-WT MEFs unexpectedly decreased, rather than enhanced, their transformed phenotype (Figure 48A). Although this would be in agreement with the pro-apoptotic and anti-proliferative functions ascribed to *Pmp22* (Brancolini et al., 1999; Fabbretti et al., 1995; Zoidl et al., 1995), it raises the question of whether endogenous *Pmp22* is actually functional in p38α-/- MEFs, specially since *Pmp22* overexpression in these cells (where it is already upregulated compared to WT cells) attenuates their transformed phenotype as well (Figure 48A).

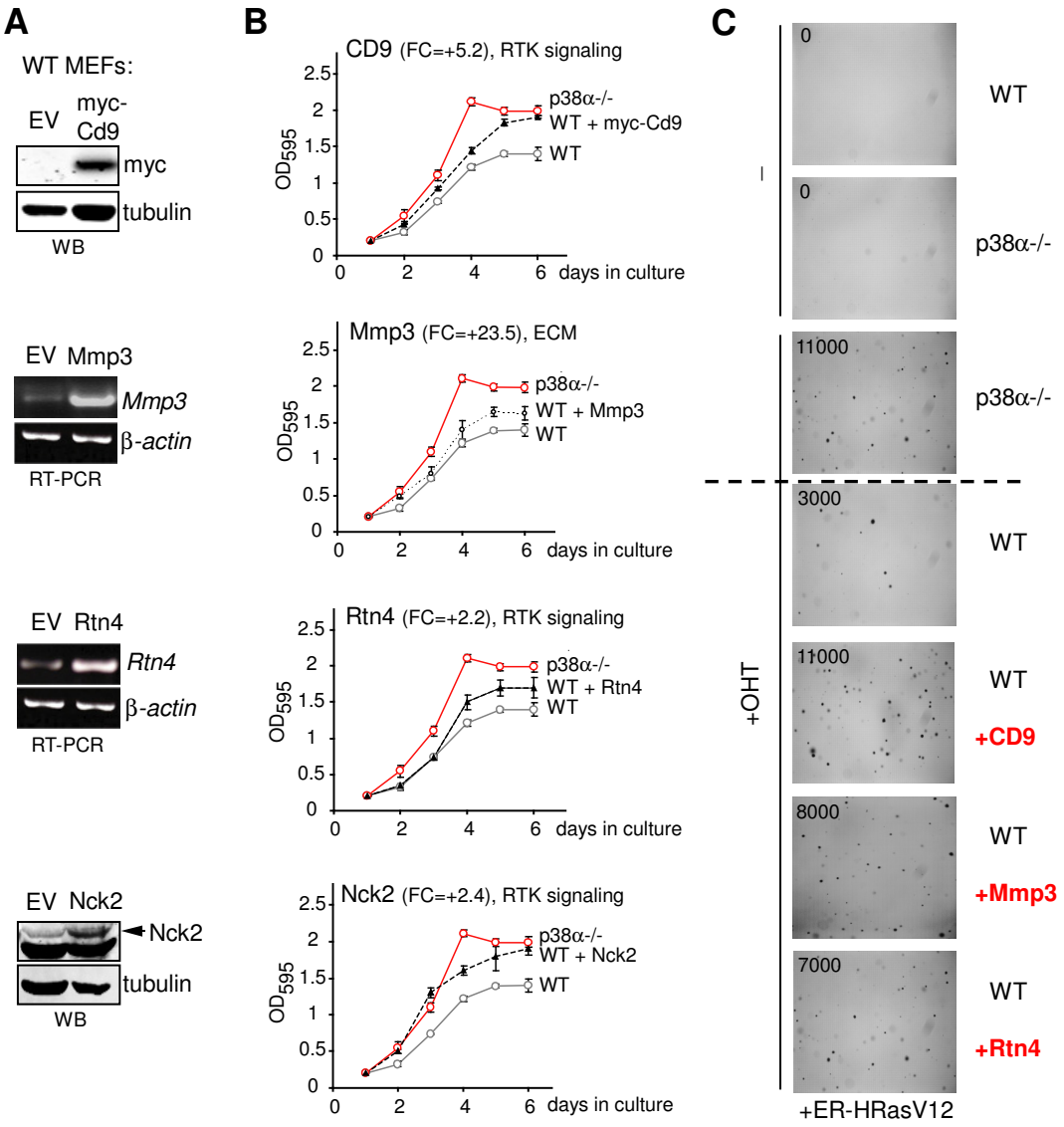

Figure 47. Effect of the overexpression of genes upregulated in H-Ras^{V12}-p38α-/- MEFs on the proliferation and anchorage- independent growth (soft agar) of H-Ras^{V12}-expressing WT MEFs. (A) Immunoblot or semiquantitative RT-PCR analyses of unstimulated ER-HRas^{V12}-WT MEFs after being stably transduced with retroviruses encoding an empty vector (EV) or each gene of interest. **(B)** MTT proliferation charts of OHT-stimulated ER-HRas^{V12}-expressing WT and p38α-/- MEFs. WT cells additionally expressed each gene of interest where indicated (dashed black line). **(C)** Anchorage-independent growth (soft agar) assays of unstimulated or OHT-stimulated ER-HRas^{V12}-expressing WT and p38α-/- MEFs. WT cells expressed each gene of interest where indicated (below dashed line). FC, microarray fold-change (log_2 ratio) in H-Ras^{V12}-p38α-/- *versus* H-Ras^{V12}-WT MEFs.

Complementary to the above, we overexpressed in H-Ras^{V12}-p38α-/- MEFs the three genes, *Egln3*, *Ctsh* and *Gstm2,* found to be upregulated in H-Ras^{V12}-WT cells. After checking their expression levels in established cell lines (Figure 49A), we found that forced expression of *Egln3* in H-Ras^{V12}-p38α-/- MEFs attenuated their transformed phenotype to WT levels (Figure 49B and 49C), which may explain its low expression levels in H-Ras^{V12}-p38α-/- MEFs (FC=-6.28), in accordance with its reported pro-

apoptotic activity (Lee et al., 2005). In contrast, *Ctsh* expression did not affect neither proliferation (Figure 49B) nor soft agar colony formation (Table 5) in H-Ras^{V12}-p38α-/- MEFs. This is in agreement with *Ctsh* coding for a matrix remodeling protein that is likely to regulate tumor cell invasion rather than cell autonomous traits such as proliferation or anchorage-independent growth.

Table 5. Effect of candidate gene overexpression in H-Ras^{V12}-induced proliferation and anchorage-independent growth (soft agar)

Gene symbol	Expression in p38α-/- vs WT MEFs*	Proliferation[1]	Soft agar[2]
Aig1	Upregulated	Not expressed	Not expressed
Mmp3	Upregulated	Enhanced in WT	Enhanced in WT
Cd9	Upregulated	Enhanced in WT	Enhanced in WT
Rtn4	Upregulated	Enhanced in WT	Enhanced in WT
Nck2	Upregulated	Enhanced in WT	No effect
Pmp22	Upregulated	Reduced in p38α-/-	Reduced in p38α-/-
Gstm2	Downregulated	Enhanced in WT	Enhanced in WT
Egln3	Downregulated	Reduced in p38α-/-	Reduced in p38α-/-
Ctsh	Downregulated	No effect	No effect

*, microarray fold-change. **1**, effect of gene overexpression in H-Ras^{V12}-induced proiferation. **2**, effect of gene overexpression in H-Ras^{V12}-induced soft agar growth.

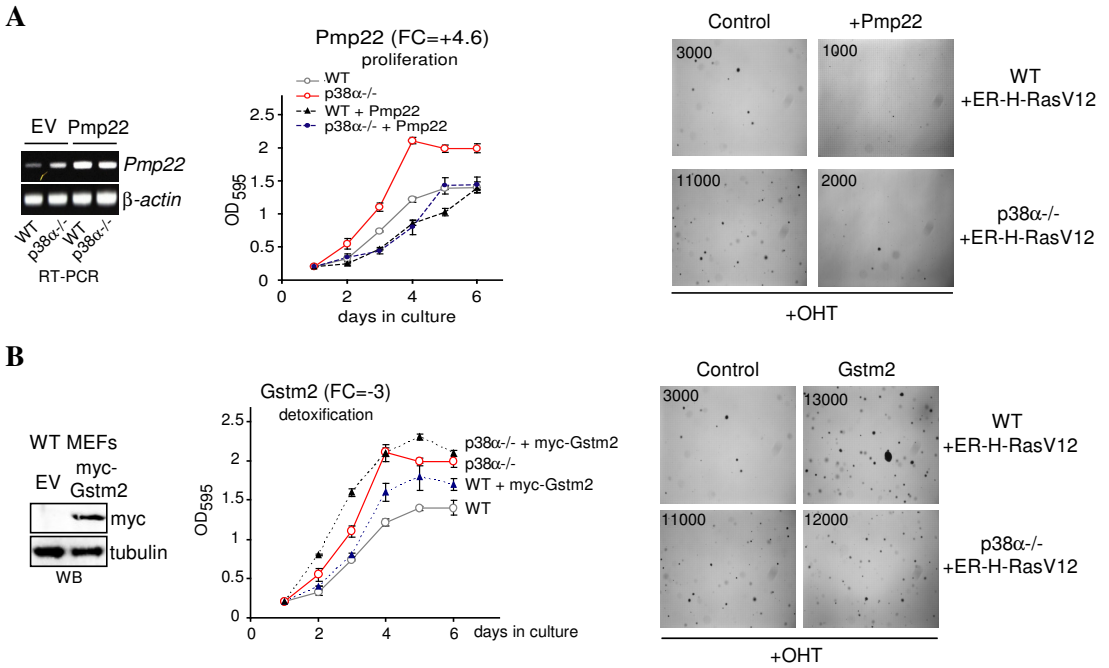

Figure 48. Effect of the overexpression of *Pmp22* and *Gstm2* on the proliferation and anchorage-independent growth of H-Ras^{V12}-expressing MEFs. (A-B) Immunoblot analysis, proliferation and soft agar assays were performed as inFigure 47. FC, microarray fold-change (log_2 ratio) in H-Ras^{V12}-p38α-/- *versus* H-Ras^{V12}-WT MEFs.

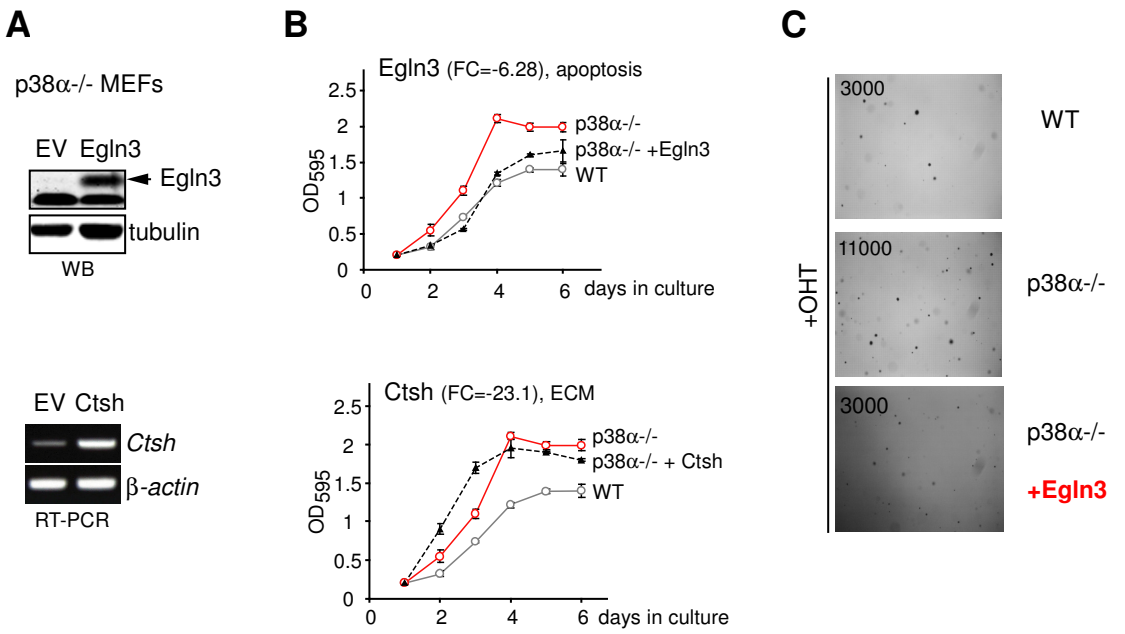

Figure 49. Effect of the overexpression of genes upregulated in H-Ras^{V12}-WT MEFs on the proliferation and anchorage- independent growth (soft agar) of H-Ras^{V12}-expressing p38α-/- MEFs. **(A)** Immunoblot or semiquantitative RT-PCR analyses of unstimulated ER-HRas^{V12} p38α-/- MEFs after being stably transduced with retroviruses encoding an empty vector (EV) or each gene of interest. **(B)** MTT proliferation charts of OHT-stimulated ER-HRas^{V12}-expressing WT and p38α-/- MEFs. p38α-/- cells additionally expressed each gene of interest where indicated (dashed black line). **(C)** Anchorage-independent growth (soft agar) assays of unstimulated or OHT-stimulated ER-HRas^{V12}-expressing WT and p38α-/- MEFs. p38α-/- cells additionally expressed each gene of interest where indicated. FC, microarray fold-change (log_2 ratio) in H-Ras^{V12}-p38α-/- *versus* H-Ras^{V12}-WT MEFs.

Strikingly, the *Gstm2* overexpression did not have any significant effect on the transformed phenotype of H-Ras^{V12}-p38α-/- MEFs (Figure 48B), whereas greatly enhanced proliferation and soft agar growth of WT MEFs (Figure 48B), in spite of being upregulated in the latter (Table 4). Noteworthy, we recently found that *Gstm2* is actually connected to malignant transformation in MEFs, which seems to be accounted for by its ability to increase cell survival in response to oxidative stress via inhibition of the pro-apoptotic activity of p38α (Dolado et al., 2007). Namely, cells with high *Gstm2* expression desensitize p38α from oxidative stress, which results in the accumulation of high levels of carcinogenic oxygen radicals and the acquisition of a more transformed phenotype. Consequently, *Gstm2* has no effect in H-Ras^{V12}-p38α-/- MEFs, since these cells already contain high levels of oxidative stress and do not have p38α (Dolado et al., 2007). In contrast, *Gstm2* overexpression greatly enhances the transformed phenotype of H-Ras^{V12}-WT MEFs via p38α inhibition and subsequent accumulation of oxidative stress (Dolado et al., 2007), in accordance with Figure 48B. Thus, it is possible that *Gstm2* upregulation in H-Ras^{V12}-WT MEFs may respond to an adaptative response

induced by H-Ras^{V12} in these cells (as there are no differences in *Gstm2* expression between WT and p38α-/- control cells (Figure 45C)) in order to impair the apoptotic activity of p38α in response to H-Ras^{V12}-induced oxidative stress and favour malignant progression.

2.7. EGFR signaling is transcriptionally regulated by p38α in malignant transformation through a substantial gene network

Recent evidence in our laboratory suggests that EGFR is an important transcriptional target of p38α for the *in vivo* regulation of tumorigenesis (Ventura et al., 2007), in agreement with previous *in vitro* studies (Frey et al., 2006; Vergarajauregui et al., 2006; Winograd-Katz and Levitzki, 2006; Zwang and Yarden, 2006). Accordingly, we have confirmed that EGFR activity is enhanced in the absence of p38α and is functionally implicated in the more transformed phenotype of H-Ras^{V12}-p38α-/- MEFs, since chemical inhibition of EGFR in these cells phenocopies the behaviour of H-Ras^{V12}-WT levels (Figures 24B, 25A and 26C). Consequently, we made a special effort to identify new genes regulated by p38α that could be in turn linked to EGFR signaling. We found that approximately 10% of all the genes significantly deregulated between H-Ras^{V12}-expressing WT and p38α-/- MEFs (Appendix Table 2) are connected to EGFR signaling (Table 6). Most of them codify for proteins that enhance EGFR signaling and are up-regulated in H-Ras^{V12}-p38α-/- MEFs (Table 6), that is negatively regulated by p38α. This suggests that an important function of p38α in the negative regulation of cell transformation may lay at the level of EGFR signaling. These include, among others, *Cd9*, a plasma membrane protein that stimulates EGFR activity by facilitating the interaction of the receptor with its ligands ((Murayama et al., 2002; Yang et al., 2006); (Figure 47)); *Areg*, a mitogenic ligand of EGFR previously associated to malignant cell transformation (Castillo et al., 2006); *Klf5*, a transcription factor that stimulates EGFR expression (Yang et al., 2007); *Hck*, a Src-family kinase that participates in EGFR recycling and signal rely as well as cell survival (Zhang et al., 2007); and *Eps8*, a tyrosine kinase substrate that amplifies EGFR signaling following mitogenic stimulation (Matoskova et al., 1995).

Table 6. EGFR-related genes regulated by p38α

	Genebank Acc. No.	Gene symbol	Gene name / function	Effect on EGFR signaling
Downregulated by p38α[1]	NM_010407	*Hck*	Hemopoietic cell kinase / EGFR activation, EGFR signal rely	Enhaces (Zhang et al., 2007)
	NM_009704	*Areg*	Amphiregulin / EGFR ligand	Enhances (Castillo et al., 2006)
	NM_007657	*Cd9*	CD9 antigen / EGFR paracrine activation	Enhances (Fujiwara et al., 2000)
	NM_009769	*Klf5*	Kruppel-like factor 5 / EGFR transcription	Enhances (Yang et al., 2007)
	NM_007945	*Eps8*	EGFR pathway substrate 8 / EGFR signaling	Enhances (Matoskova et al., 1995)
	NM_011101	*Prkca*	Protein kinase C, alpha / EGFR activation, EGFR signal rely	Enhances (Stewart and O'Brian, 2005)
	NM_010718	*Limk2*	LIM motif-containing protein kinase 2 / EGFR effector	Enhances (Wang et al., 2006)
	NM_025445	*Arfgap3*	ADP-ribosylation factor GTPase activating protein 3 / EGFR endocytosis	Enhances (Nie et al., 2006)
	NM_010879	*Nck2*	Non-catalytic region of tyrosine kinase adaptor protein 2 / EGFR SH2-domain adaptor protein	Enhances (Hehlgans et al., 2007)
	NM_009984	*Ctsl*	Cathepsin L / EGFR recycling	Enhances (Reinheckel et al., 2005)
	NM_021454	*Cdc42ep5*	Cdc42 effector protein (Rho GTPase binding) 5 / EGFR degradation	Enhances (Hirsch and Wu, 2007)
	MN_013473	*Anxa8*	Annexin A8 / EGFR internalization	Enhances(Radke et al., 2004)
	NM_010685	*Lamp2*	Lysosomal membrane glycoprotein 2 / EGFR endocytosis	Enhances (Warren et al., 1998)
	NM_010809	*Mmp3*	Matrix metallopeptidase 3 / EGFR downstream signaling	Enhances (Uttamsingh et al., 2008)
	NM_009058	*Ralgds*	Ral guanine nucleotide dissociation stimulator / EGFR signaling	Enhances (Wolthuis et al., 1998)
Upregulated by p38α[2]	NM_010453	*Hoxa5*	Homeo box A5 / transcription of EGFR regulatory proteins	Inhibits (Henderson et al., 2006)
	NM_009421	*Traf1*	TNFR-associated factor 1 / modulates EGFR expression	Enhances (Miller et al., 1998)
	NM_009701	*Aqp5*	Aquaporin 5 / EGFR signaling	Enhances(Herrlich et al., 2004)
	NM_172285	*Plcg2*	Phospholipase C, gamma 2 / EGFR signal rely	Enhances (Bianco et al., 2007)
	NM_008176	*Cxcl1*	Chemokine (C-X-C motif) ligand 1 / EGFR signaling	Enhances (Ueda et al., 2006)

1, upregulated in H-Ras^{V12}-p38α-/- MEFs; **2**, downregulated in H-Ras^{V12}- p38α-/- MEFs.

Interestingly, qRT-PCR validation showed that expression of most of these genes in H-Ras^{V12}-p38α-/- *versus* H-Ras^{V12}-WT MEFs completely mirrored the microarray results,

at least qualitatively (Figure 50), supporting the high biological reproducibility of our microarray data set.

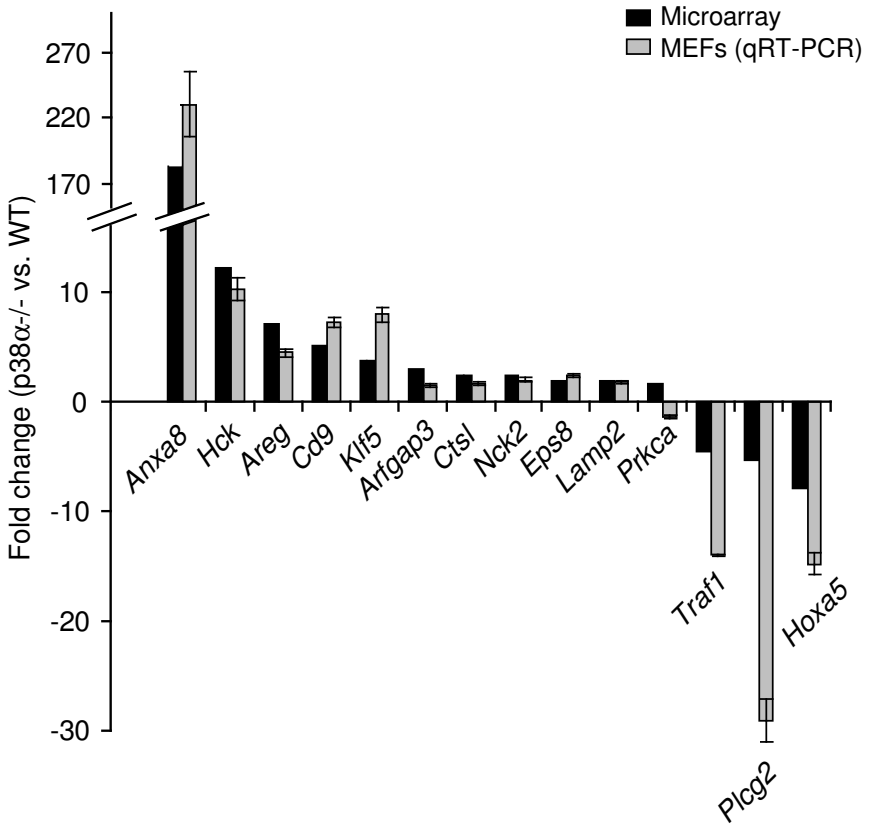

Figure 50. Quantitative RT-PCR validation of EGFR-related genes. EGFR-related genes were validated by qRT-PCR in exponentially proliferating H-Ras^{V12}-p38α-/- *versus* H-Ras^{V12}-WT MEFs (grey) and plotted beside the microarray fold change for each gene (black).

Furthermore, overexpression of *Cd9* as an example, in H-Ras^{V12}-WT MEFs not only rescued their transformed phenotype to p38α-/- levels (Figures 47B and C), but also greatly activated EGFR kinase activity, as indicated by the high levels of P-EGFR-Y1068 (Figure 51A, bottom panel), as well as its downstream signaling pathways ERK1/2 and Akt (Figure 51A, upper panel). This argues that p38α negatively regulates cell transformation, at least in part, by inhibiting EGFR signaling via the downregulation of several genes that stimulate EGFR activity. In agreement with this, chemical inhibition of p38α in WT MEFs led to increased expression of *Cd9* (Figure 51B). Of note, the interplay between EGFR and p38α in cell transformation might not only be limited to a cluster of EGFR-regulating genes, but also to the transcriptional regulation of EGFR itself by p38α (Ventura et al., 2007). Indeed, EGFR mRNA is upregulated in the absence of p38α in all biological systems analyzed, from MEFs in culture to subcutaneous xenografts derived from H-Ras^{V12}-expressing WT and p38α-/- MEFs, or K-Ras^{V12}-induced lung tumors in

WT and p38α-/- mice (Figure 52A). Accordingly, chemical inhibition of p38α in WT MEFs resulted in increased EGFR mRNA levels (Figure 52B).

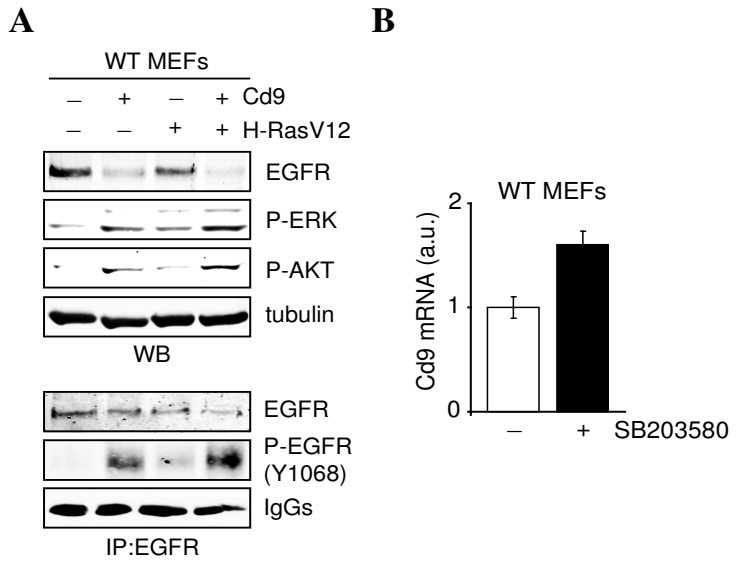

Figure 51. Cd9 expression enhances EGFR signaling. (A) Control or H-Ras^{V12}-expressing WT MEFs were transduced with an empty vector (-) or mouse Cd9 and subsequently analyzed biochemically for the level of activity of EGFR downstream pathways (upper panel), as well as for the extent of active EGFR (Y1068) following immunoprecipitation (lower panel). **(B)** Cd9 mRNA was quantified by qRT-PCR in extractes from exponentially proliferating H-Ras^{V12}-WT MEFs treated with DMSO or SB203580 (10 µM) for 12 h.

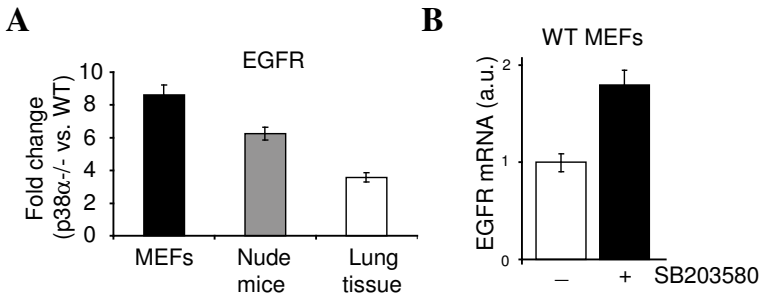

Figure 52. EGFR mRNA expression is regulated by p38α in various cell types. (A) qRT-PCR analysis of the EGFR mRNA in exponentially proliferating H-Ras^{V12}-p38α-/- *versus* H-Ras^{V12}-WT MEFs (black), in tumor xenografts derived from these same cells in nude mice (grey), as well as in K-Ras^{V12}-induced lung tumors in p38α-/- mice *versus* WT mice (white). **(B)** EGFR mRNA expression was quantified by qRT-PCR in RNA extracted from exponentially proliferating H-Ras^{V12}-WT MEFs treated with DMSO or SB203580 (10 µM) for 12 h.

Discussion

1. Multi-level regulation of cell transformation by p38α

Cancer is a genetic disease characterized by the simultaneous disruption of several cellular traits required for organism homeostasis (Hanahan and Weinberg, 2000). At the molecular level, there are several hypotheses to explain the origin and progression of this malignancy, but they all agree that deregulated cell proliferation and suppressed apoptosis together set the founding for neoplastic progression (Evan and Vousden, 2001). In this respect, p38α MAPK has been established in recent years as an efficient inhibitor of cell transformation, as it can negatively regulate proliferation and survival of the transformed cell (Dolado and Nebreda, 2008; Han and Sun, 2007). In addition, p38α can also protect normal cells against oncogenic insults by maintaining their differentiated state (Ventura et al., 2007) or irreversibly driving them into senescence (Wang et al., 2002). p38α has been shown to coordinate all these cellular processes by impinging on the activity of multiple nuclear cell cycle regulators and transcription factors (Bulavin and Fornace, 2004; Perdiguero, 2008), presumably by direct phosphorylation in most cases.

This work, shows that p38α regulates another key aspect of tissue homeostasis (Carter, 1968), the process of contact inhibition, which upon deregulation leads to cell transformation *in vitro* and hyperplasia *in vivo* (Rubin, 2008). Indeed, evidence is provided supporting a novel, multi-step mechanism engaged by p38α at high cellular density, which involves the inhibition of EGFR-induced mitogenic signals that destabilize $p27^{Kip1}$ (Figure 53). We found that confluent activation of p38α stimulates the cCbl-mediated ubiquitination and degradation of EGFR, which in turn shut-downs mitogenic signals, such as those relied by the Src non-receptor tyrosine kinase and the ERK1 and ERK2 MAPKs (Balmanno and Cook, 1999; Chu et al., 2007); (Grimmler et al., 2007; Weber et al., 1997), and this indirectly results in $p27^{Kip1}$ upregulation and cell cycle arrest. Our data indicate that p38α does not regulate cCbl protein levels *per se*, but through phosphorylation and stabilization of the ubiquitin ligase Siah2, which induces degradation of the cCbl inhibitor Spry2 and facilitates the loading of the ubiquitin ligase cCbl onto EGFR. This has important functional implications, as p38α protects normal cells against transformation through the regulation of contact inhibition (Figure 54). In contrast, already transformed, non-contact inhibited cells fail to activate p38α and upregulate $p27^{Kip1}$ in confluence, which points towards the p38α-$p27^{Kip1}$ axis as a safe-guard mechanism that transformed cells must by-pass in their course to malignancy.

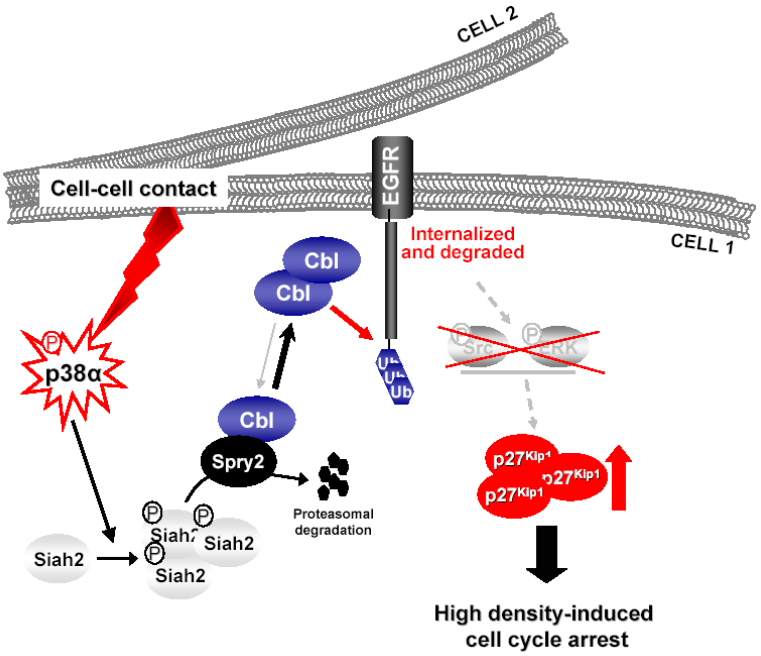

Figure 53. Proposed model for the regulation of contact inhibition by p38α. Confluent cell-to-cell contacts activate p38α, which induces Siah2-mediated downregulation of Spry2 and subsequent dissociation of cCbl, triggering EGFR ubiquitination and degradation. Termination of EGFR-induced mitogenic signaling results in $p27^{Kip1}$ accumulation and cell cycle arrest.

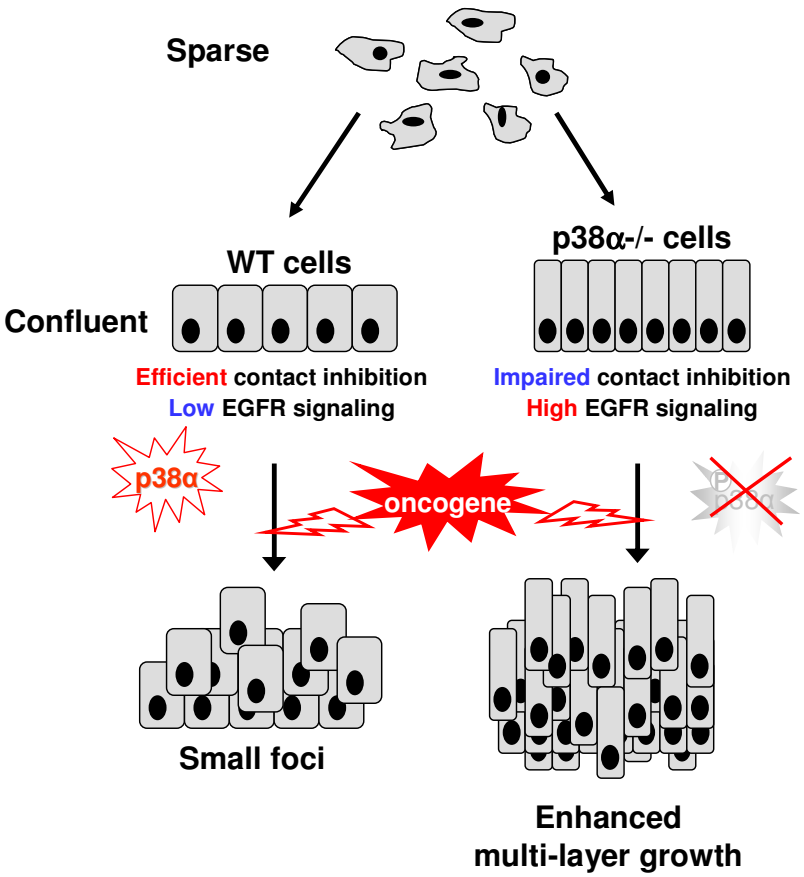

Figure 54. Impaired contact inhibition results in enhanced oncogenic transformation. The absence of p38α results in a higher saturation density of confluent cell cultures that sensitizes the cells to oncogene-induced transformation.

As mentioned above, the regulation of contact inhibition by p38α occurs mostly by post-translational means. However, the development and progression of cancer are known to be normally accompanied by many changes in gene expression (Levine and Tjian, 2003). This prompted us to characterize the differences in gene expression between oncogene-transformed WT and p38α-/- MEFs, with the aim of unveiling new transcriptional mediators of the tumor suppressor activity of p38α. Interestingly, we have found several genes not previously connected to p38α signaling that seem to mediate its tumor suppressor effect against H-Ras^{V12}-induced transformation.

Taken together, our results provide a mechanistic explanation on how p38α inhibits cell proliferation to avoid transformation at high cellular densities. We have also found that an important role of p38α to inhibit oncogene-induced transformation may be at the level of regulating the expression of several transformation-associated genes.

2. Contact inhibition at the molecular level

Deregulation of contact inhibition is one of the first steps to be accomplished in the process of cell transformation (Abercrombie, 1979), as it facilitates tumor progression by providing the incipient transformed cell with unrestrained proliferative capabilities. However, the molecular pathways responsible for the maintenance or deregulation of the contact inhibition response are still poorly understood.

2.1. Role of cell cycle inhibitors

It is assumed that upon direct contacts with neighbouring cells (Schutz and Mora, 1968), non-transformed cells rely on yet not well characterized membrane proteins to trigger intracellular signals ultimately leading to cell cycle arrest. Further downstream, the cell cycle regulators inhibiting proliferation in confluent mammalian cells have been long known, namely p27^{Kip1}, p16^{Ink4a} and p21^{Cip1}. Noteworthy, although these proteins have been consistently associated with the contact inhibition response (Cho et al., 2008; Polyak et al., 1994; Wieser et al., 1999), an open question concerns their degree of functional redundancy. For instance, p16^{Ink4a} is known to play a key role in the regulation of primary cell proliferation, as primary MEFs upregulate p16^{Ink4a} but not p27^{Kip1} in confluence (Appendix, Figure 1) and p16^{Ink4a} ablation predisposes primary murine cultures to immortalization (Sharpless et al., 2001). In contrast, genetic deletion of p27^{Kip1} in primary MEFs does not affect their contact inhibition response, neither predisposes to immortalization (Nakayama et al., 1996), whereas p16^{Ink4a}-deficient, immortalized MEFs readily accumulate p27^{Kip1} in confluence and depend on p27^{Kip1} for contact inhibition (Faust et al., 2005). Altogether, these results suggest that whereas p16^{Ink4a} may play an

important anti-proliferative role in confluent primary cells, $p27^{Kip1}$ likely compensates for the absence of $p16^{Ink4a}$ in immortalized cultures, hence constituting a second-line barrier for premalignant cells to by-pass in order to evade contact inhibition and progress towards malignancy. In agreement with this, we have found that inhibition of $p27^{Kip1}$ accumulation in $p16^{Ink4a}$-deficient, immortalized MEFs (via chemical inhibition of p38α) impairs their contact inhibition response and facilitates their malignant conversion. Of note, we have ruled out $p16^{Ink4a}$ as a mediator of p38α function in confluence since p38α regulates contact inhibition in immortalized MEFs and NIH3T3 fibroblasts that both lack $p16^{Ink4a}$ expression.

2.2. The interplay between p38α and $p27^{Kip1}$ in contact inhibition

A long-pursued issue in the field of contact inhibition has been the elucidation of the signaling pathways linking membrane receptor engagement in confluence with cell cycle inhibitor function in the nucleus. In this regard, we previously identified p38 MAPK as a signaling molecule implicated in the process, since p38α is activated in confluence and correlates with $p27^{Kip1}$ upregulation, whereas its deficiency results in reduced $p27^{Kip1}$ accumulation and impaired contact inhibition (Faust et al., 2005). Now, we have established a causal link between p38α and $p27^{Kip1}$ that points towards $p27^{Kip1}$ as the main cell cycle inhibitor downstream of p38α in contact inhibition. Namely, confluent activation of p38α results in the accumulation of $p27^{Kip1}$, but not $p16^{Ink4a}$ or $p21^{Cip1}$, and $p27^{Kip1}$-deficient cells fail to properly inhibit proliferation in confluence, despite appropriate activation of p38α. Mechanistically, we have found that p38α does not impinge on $p27^{Kip1}$ function through direct phosphorylation, neither by regulating $p27^{Kip1}$ mRNA, subcellular localization or expression of $p27^{Kip1}$ ubiquitin ligases, but it rather indirectly regulates $p27^{Kip1}$ protein stability by opposing EGFR-derived signals that degrade $p27^{Kip1}$. Of note, we have found that p38α can directly phosphorylate $p27^{Kip1}$ *in vitro* on its stabilizing residue Ser10 (Ishida et al., 2000), although this has unclear functional implications for contact inhibition, since p38α still regulates confluent levels of $p27^{Kip1}$ and cell cycle arrest in the absence of S10 phosphorylation.

2.3. How is p38α activated in contact inhibition?

An intriguing question is how p38α is activated when cells reach confluence. Two possible membrane initiators of the intracellular signals engaged by direct cell-cell contacts are mammalian N-cadherin (Levenberg et al., 1999) and *Drosophila* proto-cadherin Fat (Zeng and Hong, 2008). Nevertheless, solid evidence linking these proteins to contact inhibition is missing and no ortholog for *Drosophila´*s Fat has been characterized in mammals yet. Thus whether p38α may lay downstream of N-Cadherin

or Fat in confluent mammalian cells needs to be further addressed. Additionally, several members of the Ste20 family of kinases that link membrane receptors with MAPK pathways have been shown to activate p38α in response to various stimuli. It would be interesting to investigate whether the Ste20 kinase Hippo/Mst, which has been implicated in contact inhibition through the inhibition of YAP-mediated transcription (Zhao et al., 2007), also regulates p38α activation in confluence. Namely, Hippo kinase activation arrests proliferation in confluence by relocating the mitogenic transcription factor YAP from the nucleus to the cytoplasm, which prevents YAP from transcriptionally inducing mitogenic proteins such as cyclin E. Of note, we have observed that p38α affects neither the cytoplasmic accumulation of YAP nor the expression of the YAP target cyclin E in confluent MEFs, (Appendix, Figures 2 and 3) suggesting that the Hippo-YAP and p38α signaling pathways are likely to function as parallel regulators of contact inhibition in mammalian cells. This might explain why contact inhibition is impaired, but not fully abolished, in p38α-/- cells, as the Hippo pathway may partially compensate for p38α deficiency in confluent cells via YAP regulation. Whether p38α may act as a Hippo effector parallel to YAP in contact inhibition thus needs further investigation.

2.4. EGFR as a new p38α target in contact inhibition

Recent evidence generated in our laboratory has unveiled EGFR as a potential new target of p38α in the early stages of tumor development (Ventura et al., 2007), since p38α-deficient mice display more intense EGFR signaling in the lungs than their WT littermates and this correlates with a higher susceptibility of the former to oncogene-induced tumorigenesis. Along these results, we show here that such an inverse correlation between p38α and EGFR signaling also exists in cultured fibroblasts *in vitro*. Namely, p38α-/- MEFs show higher levels of EGFR signaling and cell numbers in confluence than WT cells, the latter being accounted for by an impaired accumulation of the cell cycle inhibitor $p27^{Kip1}$ in confluence. Interestingly, mimicking the *in vivo* results (Ventura et al., 2007), the enhanced EGFR signaling observed in p38α-/- MEFs seems to set the cells in a leap-forward position for oncogene-induced transformation. Accordingly, EGFR inhibition in p38α-deficient cells sets them back to a contact-inhibited phenotype and rescues their oncogene-induced focus formation capability to WT levels.

But, how does p38α mechanistically regulate EGFR in contact inhibition? Actually, few reports to date have addressed mechanistically how p38α regulates malignant cell transformation other than through direct modulation of cell cycle inhibitors. It was only in 2006 that EGFR was proposed as a new p38 MAPK target in the context of cancer cell chemotherapy (Winograd-Katz and Levitzki, 2006). Two subsequent studies

(Vergarajauregui et al., 2006; Zwang and Yarden, 2006) showed that p38α can directly phosphorylate EGFR after stress or cytotoxic stimuli, which was sufficient for rapid receptor internalization in the absence of growth factors. In turn, this likely prevented future mitogenic activation of EGFR and decreased cell survival by sequestering the receptor away from the plasma membrane in early endosomes. Interestingly, this p38α role in EGFR internalization was mediated not only by EGFR phosphorylation, but also by activation through phosphorylation of the early endosome protein EEA1, in agreement with previous results on G-protein coupled receptor endocytosis (Mace et al., 2005). Noteworthy, both studies (Vergarajauregui et al., 2006; Zwang and Yarden, 2006) showed that p38α was not required for EGFR internalization if growth factors were present, as EGF apparently induces EGFR internalization through a poorly characterized, p38α-independent mechanism. Actually, if p38α would still induce EGFR internalization in the presence of mitogens, hence sequestering the active EGFR in early endosomes, the effect of p38α activity would be likely oncogenic, according to the strong mitogenic effect of the active EGFR when located in early endosomes (Pennock and Wang, 2003; Vieira et al., 1996). In agreement with these results, we have found p38α to inhibit EGFR signaling in confluent, serum-cultured MEFs by modulating receptor ubiquitination and degradation but not internalization. Namely, whereas EGFR gets similarly internalized upon EGF treatment in confluent WT and p38α-/- MEFs, it rapidly traffics to the lysosomes and is degraded in WT MEFs but recycles to the plasma membrane and keeps mitogenic signaling in p38α-/- cells. Consequently, $p27^{Kip1}$ rapidly accumulates in confluent WT cells and induces cell cycle arrest, whereas the sustained mitogenic signaling of p38α-/- cells impairs $p27^{Kip1}$ accumulation and contact inhibition.

As degradation rather than internalization seems to underlie the confluent regulation of EGFR by p38α, we next explored how p38α could modulate receptor degradation. Noteworthy, it has been recently reported that p38α can engage the EGFR degradation pathway in epithelial cells by indirectly inducing phosphorylation of the receptor on Tyr1045 by an unknown mechanism (Frey et al., 2006), which subsequently induces receptor degradation by recruiting the E3 ubiquitin ligase cCbl. However, we have not observed that p38α activation in confluent cells results in higher EGFR phospho-Tyr1045 levels. In contrast, we have found p38α activity to regulate the interaction between cCbl and EGFR through a distict mechanism, that is by negatively regulating the expression of the cCbl inhibitor Spry2. Actually, Spry2 is a well established EGFR activator as it competes with the receptor for binding with the ubiquitin ligase cCbl (Fong et al., 2003; Haglund et al., 2005), so that high Spry2 levels normally result in sustained EGFR signaling due to impaired receptor ubiquitination and degradation (Wong et al., 2002). Accordingly, we have observed that the high levels of Spry2 expression in confluent

p38α-/- MEFs led to reduced loading of cCbl on EGFR in confluent conditions of growth, along with impaired receptor degradation, which was reversed by forced p38α re-expression. The fact that the shRNA-mediated downregulation of Spry2 in p38α-/- MEFs rescued the accumulation of $p27^{Kip1}$, cell numbers in confluence, and EGFR mitogenic signaling to WT levels, further demonstrates that p38α regulates contact inhibition through downregulation of EGFR signalling in a Spry2/cCbl-dependent manner. Of note, Spry2 has also been described to inhibit in some cases, instead of activate, signaling downstream of the EGFR by interfering with Ras activity. However, this is a topic of current debate, since the interplay between Spry2 and Ras seems to be highly dependent on the cellular context as well as on the transformed status of the cell (Lito et al., 2008; Mason et al., 2006).

As for the mechanism of Spry2 regulation by p38α, it is worth mentioning that Spry2 activity has been previously shown to be regulated in a phosphorylation-dependent manner by the p38 downstream kinase Mnk1 (DaSilva et al., 2006). Surprisingly, Mnk1 was reported to stabilize Spry2, whereas p38α activation correlates with a more unstable Spry2 protein, arguing that Mnk1 does not likely act downstream of p38α in contact inhibition since they have opposite effects on Spry2 expression. In contrast, we have found the Spry2 ubiquitin ligase Siah2 to be phosphorylated and stabilized in confluence by p38α, which correlates with the observed downregulation of Spry2 following confluent activation of p38α. This indicates that p38α activation leads to cCbl-mediated inhibition of EGFR and subsequent $p27^{Kip1}$ accumulation via Spry2 degradation by Siah2, which we have found in a ternary complex with Spry2 and p38α in cells. Of note, although both cCbl and Siah2 ubiquitin ligases can bind Spry2, only Siah2 but not cCbl can efficiently degrade it. This provides a mechanistic explanation for the sustained effect of Spry2 on EGFR activation by means of cCbl sequestration, which would not likely occur if Spry2 was efficiently degraded by cCbl as well.

3. New potential p38α transcriptional effectors in tumor suppression

p38α deficiency in MEFs normally results in enhanced transformation following oncogene transduction (Dolado et al., 2007), as reflected by the greater alteration of H-Ras^{V12}-p38α-/- MEFs in cell transformation markers such as increased proliferation and survival, refringent morphology, loss of contact inhibition and anchorage-independent growth. Not surprisingly, we have found a large number of genes that stimulate cell proliferation and survival which are negatively regulated by p38α. Conversely, various genes stimulating apoptosis were found upregulated in the less transformed H-Ras^{V12}-WT MEFs.

Apart from survival and proliferation, p38α has also been shown to regulate other traits of the tumor cell that are likely regulated by signals relied from plasma membrane proteins, such as cell morphology, contact inhibition and anchorage-independent growth. Interestingly, when going over the list of genes deregulated between H-Ras^{V12}-expressing WT and p38α-/- MEFs, it is easy to immediately pinpoint various p38α-regulated genes encoding membrane-associated proteins that may be involved in such processes. These include *Ezr*, encoding the cytoskeleton protein Ezrin shown to be important for the regulation of contact inhibition of growth and tumorigenesis (Okada et al., 2007; Pang et al., 2004; Tran Quang et al., 2000), as well as various genes encoding transmembrane proteins such as the tetraspanin *Tspan13* or the protocadherins *Pcdh7* and *Pcdh10*. Of note, certain protocadherins (i.e. Fat1) are emerging as key regulators of contact inhibition (Tanoue and Takeichi, 2004; Zhao et al., 2007). Future functional studies with these membrane proteins should unveil whether they act as effectors of p38α in the regulation of membrane-mediated cellular processes linked to transformation, such as contact inhibition or cell competition (Moreno, 2008).

Beyond gene identification, we have validated by RT-PCR the expression of 26 selected genes to be regulated by p38α not only in MEFs, but also in two different tumor models. Importantly, as the cellular phenotype is determined not by the mRNA, but by the protein translated from the mRNA, we have analyzed the endogenous protein expression levels of some of these genes in MEFs, and have confirmed that protein levels correlate with mRNA levels in all cases. Functional overexpression experiments have allowed us to establish a functional connection between these genes and p38α in the context of H-Ras^{V12}-induced transformation. Two particular genes, *Gstm2* and *Cd9*, have been further characterized and their mechanism of action as inhibitors of the tumor suppressor activity of p38α have been addressed.

3.1. New mediators of the apoptotic response of p38α MAPK in tumor suppression

In agreement with the well established role of p38α as an inducer of apoptosis, various genes related to apoptosis/survival have been found in our microarray study. Examples of these include *Ralgds*, which is downregulated by p38α and encodes a Ras effector shown to promote tumorigenesis by increasing cell survival (Gonzalez-Garcia et al., 2005); *Tnfrsf23*, a putative tumor necrosis factor (TNF) receptor (R) decoy that may inhibit apoptosis by interfering with TNFR signaling (Bridgham and Johnson, 2004), also downregulated by p38α; and *Egln3*, a gene with a strong pro-apoptotic activity (Maxwell, 2005) found to be upregulated in H-Ras^{V12}-WT cells, in line with the importance of the apoptotic activity of p38α for tumor suppression (Dolado et al., 2007). Furthermore, we

have also identified the gene *Gstm2*, which encodes a member of the glutathione-S-transferase (GST) family of phase II detoxification enzymes, as a key regulator of the pro-apoptotic activity of p38α in malignant transformation (Dolado et al., 2007). Mechanistic characterization has unveiled Gstm2 as a potent inhibitor of the p38α-mediated apoptotic response under stress conditions, such as following oncogenic H-Ras^{V12}-induced ROS. Gstm2 and other Gstm-family members (i.e. Gstm1) are able to inhibit the ability of p38α to detect oxidative stress accumulation early in the process of oncogenic transformation (Dolado et al., 2007). Mechanistically, this seems to be accounted for by the inhibitory activity of Gstm proteins on the MAPKKK Ask1, which prevents Ask1 activation by ROS and subsequent signal relay downstream to p38α MAPK (Figure 55). This, in turn, has important implications for tumorigenesis since *Gstm2* overexpression in H-Ras^{V12}-transformed WT cells mimics the enhanced transformed phenotype of p38α-deficient cells. Furthermore, cancer cells have developed a way to uncouple the activation of p38α by ROS, namely by increasing the expression levels of Gstm2, and this provides them with greater *in vitro* tumorigenicity. Thus, our results suggest that drugs targeting particular GST proteins may enhance the tumor suppressor activity of p38α by restoring its pro-apoptotic function upon ROS detection. Future experiments will have to confirm whether GSTs can be considered as oncogenes in certain cancer stages and if GST-targeting drugs might be used as anti-cancer agents for certain tumors.

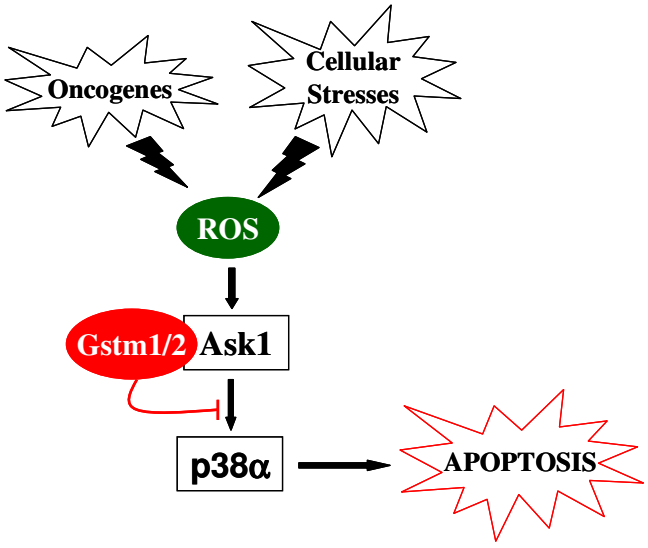

Figure 55. Proposed mode of action for Gstm1 and Gstm2 in the inhibiton of p38α MAPK activation by oxidative stress. ROS can be produced within the cell by several stimuli, including signaling from oncogenes as well as following stress treatments. One of the main pathways transducing oxidative stress consists of the Ask1-p38α axis, which usually results in the induction of apoptosis. Gstm1 and Gstm2 interfere with this process most likely by binding to and inhibiting Ask1.

3.2. Transcriptional regulation of EGFR-related genes by p38α

We have also identified approximately 20 EGFR-related genes regulated by p38α that may potentially modulate cell survival and proliferation through EGFR signaling. This

is already a good indication that EGFR may be a key p38α target in cell transformation not only at the protein level (i.e. Spry2/cCbl-mediated degradation), but also at the transcriptional one. These include p38α-downregulated genes that generally stimulate EGFR signaling, such as the Src-family member *Hck*, the EGFR ligand *Areg*, or the EGFR-activating tetraspanin *Cd9*; as well as genes reported to inhibit EGFR signaling, such as the transcription factor *Hoxa5*, which we have found upregulated by p38α.

In addition, we have started to characterize *Cd9*, which encodes a trans-membrane protein (CD9) of the tetraspanin family that has been previously implicated in a large variety of cellular processes such as cell differentiation (Tachibana and Hemler, 1999), EGFR signaling (Higashiyama et al., 1995; Inui et al., 1997; Shi et al., 2000), as well as cell adhesion and migration (Le Naour et al., 2006). Of particular relevance for this project is the fact that CD9 expression has been positively correlated with tumorigenesis, which might be accounted for by its stimulatory role on EGFR signaling (Shi et al., 2000) and its association with certain adhesion molecules and proteases (i.e. ADAM10) (Le Naour et al., 2006). CD9 has been also found overexpressed in human carcinomas (Cajot et al., 1997; Huang et al., 1998), which correlates with its higher expression levels (+5.2-fold) in the more transformed H-Ras^{V12}-p38α-/- than in H-Ras^{V12}-WT MEFs. As there is previous evidence showing an inverse correlation between p38α activity and EGFR signaling in cancer (Ventura et al., 2007; Zwang and Yarden, 2006), we have focused on CD9 as a new potential target of p38α to regulate EGFR activity in tumorigenesis. In this regard, we have found that CD9 overexpression in H-Ras^{V12}-WT MEFs enhances their transformed phenotype and EGFR signaling levels as in H-Ras^{V12}-p38α-/- cells, which suggests that CD9 may be downregulated by p38α in order to attenuate oncogenic H-Ras^{V12}-induced transformation via EGFR inhibition.

Future experiments addressing the mechanisms of EGFR activation by CD9 and how they might be regulated by p38 MAPK should be performed. Indeed, although CD9 has been shown to activate EGFR by inducing the shedding of its ligands in a juxtacrine manner (Shi et al., 2000), we have preliminary evidence indicating that CD9 may as well activate EGFR in a cell-autonomous manner by inducing receptor processing, as it has been previously shown for the TACE-mediated processing of EGFR-4 (Rio et al., 2000) or more recently for HER2 (Pedersen et al., 2009). CD9-transduced WT MEFs should be used to study the effect that CD9 overexpression has on EGFR shedding, and how this might be modulated by H-Ras^{V12} signaling and/or p38α activity.

4. EGFR as a nodal p38α target in the regulation of cell transformation

Different traits of the transformed cell seem to be regulated by p38α through partially independent mechanisms. Thus, the effect of p38α on the proliferation, focus formation or anchorage-independent growth capabilities of transformed cells depends on the particular oncogene expressed (Dolado et al., 2007). For instance, the inhibition of anchorage-independent growth relies on the pro-apoptotic activity of p38α in response to the intracellular accumulation of ROS induced by oncogenes such as H- or N-Ras (Dolado et al., 2007). In contrast, there was no mechanistic basis so far for the inhibitory effect of p38α on foci formation induced by oncogenes that do not signal primarily through ROS, such as Raf (Dolado et al., 2007).

Evidence obtained in this work indicates that the regulation of contact inhibition through the Spry2-EGFR-$p27^{Kip1}$ network may be an important mechanism for p38α to specifically inhibit oncogene-induced foci formation, independently of ROS sensing. In particular, enhanced levels of EGFR signaling, due to Spry2 upregulation, sensitize p38α-/- cells to malignant transformation by H-Ras, and high Spry2 seem to be also required for Raf to efficiently induce foci formation in p38α-deficient MEFs (Appendix, Figure 4). Accordingly, efficient transformation by H-Ras has been shown to require EGFR signaling through a positive feed-back loop involving Spry2 (Lito et al., 2008), in agreement with previous reports highlighting the importance of EGFR for Ras-induced tumorigenesis (Sibilia et al., 2000). In summary, it appears that the downregulation of EGFR signaling by p38α negatively regulates the initiation of tumorigenesis by inhibiting proliferation at high cellular densities. Accordingly, early transformed cells uncouple confluent growth from p38α activation, suggesting that the role of p38α in contact inhibition is probably under negative selective pressure in transformation in order to evade anti-proliferative constraints and facilitate progression towards malignancy.

In line with EGFR playing a central role in the regulation of malignant transformation by p38α, we have found the regulation of EGFR by p38α to go beyond the post-translational level. Indeed, we have identified a large number of genes coding for positive regulators of EGFR signaling whose expression is negatively regulated by p38α. Interestingly, functional validation of one of them, *Cd9*, has shown that its overexpression not only stimulates EGFR signaling in H-Ras^{V12}-WT cells, but also rescues their transformed phenotype to H-Ras^{V12}-p38α-/- levels. This suggests that an important tumor suppressor function of p38α may function at the level of transcriptionally-inhibiting EGFR signaling, as previously suggested (Ventura et al., 2007). The upcoming characterization of more EGFR-related genes might uncover a plethora of transcriptional targets of p38α that impinge on EGFR signaling in cancer.

Taken together, we have characterized two different mechanisms orchestrated by p38α to inhibit EGFR signaling in malignant transformation, that is through the cCbl-dependent degradation of the receptor or by downregulating the expression of genes that stimulate EGFR signaling. Although the relative contribution of each mechanism to the overall tumor suppressor effect of p38α is not well understood, this may well depend on the transformed state of the cell, the cell cycle phase or the temporal scope of the response induced by p38α. For instance, p38α activity regulates EGFR transcription in proliferating, H-Ras^{V12}-transformed MEFs, but we found no differences in EGFR mRNA levels between contact-inhibited, non-transformed WT and p38α-/- MEFs. It is also possible that whereas the post-translational regulation of EGFR by p38α in contact inhibition is aimed at eliciting a fast response, the long-term inhibition of H-Ras^{V12} transformation by p38α requires tuning of the steady-state transcriptional level of genes that in turn impinge on EGFR signaling.

Conclusions

1. p38α negatively regulates different traits of the transformed cell through distinct molecular mechanisms. Regulation of contact inhibition requires p38α to sense cell-cell contacts and to induce an anti-proliferative response.

2. Premalignant cells require both p38α and $p27^{Kip1}$ for contact inhibition. $p27^{Kip1}$ lays downstream of p38α, hence confluent accumulation of $p27^{Kip1}$ to induce a G0/G1-proliferation arrest needs p38α activity.

3. p38α does not affect $p27^{Kip1}$ transcription, mRNA stability or subcellular localization in confluence, but indirectly enhances $p27^{Kip1}$ protein stability.

4. p38α stabilizes $p27^{Kip1}$ through the inhibition of EGF receptor (EGFR) signaling, since confluent activation of p38α induces EGFR ubiquitination and degradation.

5. p38α indirectly induces EGFR degradation in confluence by downregulating Sprouty2 - an enhancer of EGFR signaling and stability- via the ubiquitin ligase Siah2.

6. The p38α effect on confluent $p27^{Kip1}$ upregulation and cell cycle arrest is impaired in tumorigenic cells, but can be rescued by forced activation of p38α.

7. p38α negatively regulates oncogene-induced cell transformation not only at the post-translational level, but also by transcriptional means.

8. Analysis of gene expression patterns, as well as functional studies, suggest that p38α may regulate tumorigenesis by modulating the expression of genes that impinge on cell transformation.

9. A significant gene cluster regulated by p38α consist of genes capable of activating EGFR signaling whose expression is negatively regulated by p38α. This indicates that p38α may inhibit EGFR signaling also by transcriptional means.

10. EGFR is regulated at multiple levels by p38α, indicating its likely implication in significant part of the tumor suppressor effect of p38α in cell transformation.

Conclusiones

1. p38α inhibe diferentes características de la célula maligna a través de mecanismos bien diferenciados. La regulación de la inhibición al contacto requiere que p38α sienta los contactos célula-célula e induzca una respuesta anti-proliferativa.

2. Las células premalignas requieren p38α y $p27^{Kip1}$ para la inhibición al contacto. $p27^{Kip1}$ actúa como sustrato de p38α, así que el aumento en sus niveles de expresión en confluencia, que lleva a una parada proliferativa en G0/G1, necesita de la actividad de p38α.

3. p38α no afecta la transcripción, estabilidad del ARNm o localización subcelular de $p27^{Kip1}$ en confluencia, sino que aumenta la estabilidad de la proteína $p27^{Kip1}$ de forma indirecta.

4. p38α estabiliza a $p27^{Kip1}$ a través de la inhibición de la señalización del receptor de EGF (EGFR, *epidermal growth factor receptor*), ya que la activación de p38α en confluencia induce la ubiquitinación y degradación de EGFR.

5. p38α indirectamente induce la degradación de EGFR en confluencia al disminuir la expresión de Sprouty2 -un estimulador de la estabilidad y señalización de EGFR- a través de la ubiquitina ligasa Siah2.

6. El efecto de p38α en la acumulación confluente de $p27^{Kip1}$ y la posterior parada proliferativa no es operativo en células tumorigénicas, aunque se puede reactivar en las mismas a través de la activación forzada de p38α.

7. p38α inhibe la transformación maligna inducida por oncogenes no sólo a un nivel post-traduccional, sino también por medios transcripcionales.

8. Análisis de los patrones de expresión génica, junto con estudios funcionales, sugieren que p38α podría regular el proceso de carcinogénesis al modular la expresión de genes determinantes del fenotipo transformado celular.

9. Un grupo génico significativo regulado por p38α consiste en genes con la capacidad de activar la señalización de EGFR, cuya expresión se encuentra regulada negativamente por p38α. Esto indica que p38α podría inhibir la señalización de EGFR también a un nivel transcripcional.

10. EGFR está regulado negativamente por p38α a varios niveles, sugiriendo que podría mediar una parte significativa del efecto supresor tumoral de p38α en el proceso de transformación celular.

Bibliography

Abercrombie, M. (1979). Contact inhibition and malignancy. Nature *281*, 259-262.

Adams, R. H., Porras, A., Alonso, G., Jones, M., Vintersten, K., Panelli, S., Valladares, A., Perez, L., Klein, R., and Nebreda, A. R. (2000). Essential role of p38alpha MAP kinase in placental but not embryonic cardiovascular development. Mol Cell *6*, 109-116.

Alepuz, P. M., de Nadal, E., Zapater, M., Ammerer, G., and Posas, F. (2003). Osmostress-induced transcription by Hot1 depends on a Hog1-mediated recruitment of the RNA Pol II. Embo J *22*, 2433-2442.

Alfonso, P., Dolado, I., Swat, A., Nunez, A., Cuadrado, A., Nebreda, A. R., and Casal, J. I. (2006). Proteomic analysis of p38alpha mitogen-activated protein kinase-regulated changes in membrane fractions of RAS-transformed fibroblasts. Proteomics *6 Suppl 1*, S262-271.

Allen, M., Svensson, L., Roach, M., Hambor, J., McNeish, J., and Gabel, C. A. (2000). Deficiency of the stress kinase p38alpha results in embryonic lethality: characterization of the kinase dependence of stress responses of enzyme-deficient embryonic stem cells. J Exp Med *191*, 859-870.

Ambrosino, C., Mace, G., Galban, S., Fritsch, C., Vintersten, K., Black, E., Gorospe, M., and Nebreda, A. R. (2003). Negative feedback regulation of MKK6 mRNA stability by p38alpha mitogen-activated protein kinase. Molecular and cellular biology *23*, 370-381.

Aouadi, M., Bost, F., Caron, L., Laurent, K., Le Marchand Brustel, Y., and Binetruy, B. (2006). p38 mitogen-activated protein kinase activity commits embryonic stem cells to either neurogenesis or cardiomyogenesis. Stem Cells *24*, 1399-1406.

Arteaga, C. L. (2002). Overview of epidermal growth factor receptor biology and its role as a therapeutic target in human neoplasia. Semin Oncol *29*, 3-9.

Balmanno, K., and Cook, S. J. (1999). Sustained MAP kinase activation is required for the expression of cyclin D1, p21Cip1 and a subset of AP-1 proteins in CCL39 cells. Oncogene *18*, 3085-3097.

Beardmore, V. A., Hinton, H. J., Eftychi, C., Apostolaki, M., Armaka, M., Darragh, J., McIlrath, J., Carr, J. M., Armit, L. J., Clacher, C.*, et al.* (2005). Generation and characterization of p38beta (MAPK11) gene-targeted mice. Molecular and cellular biology *25*, 10454-10464.

Bensaad, K., and Vousden, K. H. (2005). Savior and slayer: the two faces of p53. Nat Med *11*, 1278-1279.

Besson, A., Dowdy, S. F., and Roberts, J. M. (2008). CDK inhibitors: cell cycle regulators and beyond. Dev Cell *14*, 159-169.

Bianco, A., Poukkula, M., Cliffe, A., Mathieu, J., Luque, C. M., Fulga, T. A., and Rorth, P. (2007). Two distinct modes of guidance signalling during collective migration of border cells. Nature *448*, 362-365.

Bloom, J., and Pagano, M. (2003). Deregulated degradation of the cdk inhibitor p27 and malignant transformation. Semin Cancer Biol *13*, 41-47.

Bogoyevitch, M. A., and Court, N. W. (2004). Counting on mitogen-activated protein kinases--ERKs 3, 4, 5, 6, 7 and 8. Cell Signal *16*, 1345-1354.

Bost, F., Aouadi, M., Caron, L., and Binetruy, B. (2005). The role of MAPKs in adipocyte differentiation and obesity. Biochimie *87*, 51-56.

Brancho, D., Tanaka, N., Jaeschke, A., Ventura, J. J., Kelkar, N., Tanaka, Y., Kyuuma, M., Takeshita, T., Flavell, R. A., and Davis, R. J. (2003). Mechanism of p38 MAP kinase activation in vivo. Genes Dev *17*, 1969-1978.

Brancolini, C., Marzinotto, S., Edomi, P., Agostoni, E., Fiorentini, C., Muller, H. W., and Schneider, C. (1999). Rho-dependent regulation of cell spreading by the tetraspan membrane protein Gas3/PMP22. Mol Biol Cell *10*, 2441-2459.

Bridgham, J. T., and Johnson, A. L. (2004). Alternatively spliced variants of Gallus gallus TNFRSF23 are expressed in the ovary and differentially regulated by cell signaling pathways. Biol Reprod *70*, 972-979.

Buhling, F., Waldburg, N., Kruger, S., Rocken, C., Wiesner, O., Weber, E., and Welte, T. (2002). Expression of cathepsins B, H, K, L, and S during human fetal lung development. Dev Dyn *225*, 14-21.

Bulavin, D. V., Amundson, S. A., and Fornace, A. J. (2002a). p38 and Chk1 kinases: different conductors for the G(2)/M checkpoint symphony. Curr Opin Genet Dev *12*, 92-97.

Bulavin, D. V., Demidov, O. N., Saito, S., Kauraniemi, P., Phillips, C., Amundson, S. A., Ambrosino, C., Sauter, G., Nebreda, A. R., Anderson, C. W.*, et al.* (2002b). Amplification of PPM1D in human tumors abrogates p53 tumor-suppressor activity. Nat Genet *31*, 210-215.

Bulavin, D. V., and Fornace, A. J., Jr. (2004). p38 MAP kinase's emerging role as a tumor suppressor. Adv Cancer Res *92*, 95-118.

Bulavin, D. V., Higashimoto, Y., Popoff, I. J., Gaarde, W. A., Basrur, V., Potapova, O., Appella, E., and Fornace, A. J., Jr. (2001). Initiation of a G2/M checkpoint after ultraviolet radiation requires p38 kinase. Nature *411*, 102-107.

Bulavin, D. V., Kovalsky, O., Hollander, M. C., and Fornace, A. J., Jr. (2003). Loss of oncogenic H-ras-induced cell cycle arrest and p38 mitogen-activated protein kinase activation by disruption of Gadd45a. Molecular and cellular biology *23*, 3859-3871.

Bulavin, D. V., Phillips, C., Nannenga, B., Timofeev, O., Donehower, L. A., Anderson, C. W., Appella, E., and Fornace, A. J., Jr. (2004). Inactivation of the Wip1 phosphatase inhibits mammary tumorigenesis through p38 MAPK-mediated activation of the p16(Ink4a)-p19(Arf) pathway. Nat Genet *36*, 343-350.

Bulavin, D. V., Saito, S., Hollander, M. C., Sakaguchi, K., Anderson, C. W., Appella, E., and Fornace, A. J., Jr. (1999). Phosphorylation of human p53 by p38 kinase coordinates N-terminal phosphorylation and apoptosis in response to UV radiation. Embo J *18*, 6845-6854.

Cai, B., Chang, S. H., Becker, E. B., Bonni, A., and Xia, Z. (2006). p38 MAP kinase mediates apoptosis through phosphorylation of BimEL at Ser-65. J Biol Chem *281*, 25215-25222.

Cajot, J. F., Sordat, I., Silvestre, T., and Sordat, B. (1997). Differential display cloning identifies motility-related protein (MRP1/CD9) as highly expressed in primary compared to metastatic human colon carcinoma cells. Cancer Res *57*, 2593-2597.

Carter, A. B., Knudtson, K. L., Monick, M. M., and Hunninghake, G. W. (1999). The p38 mitogen-activated protein kinase is required for NF-kappaB-dependent gene expression. The role of TATA-binding protein (TBP). J Biol Chem *274*, 30858-30863.

Carter, A. B., Tephly, L. A., and Hunninghake, G. W. (2001). The absence of activator protein 1-dependent gene expression in THP-1 macrophages stimulated with phorbol esters is due to the lack of p38 mitogen-activated protein kinase activation. J Biol Chem *276*, 33826-33832.

Carter, S. B. (1968). Tissue homeostasis and the biological basis of cancer. Nature *220*, 970-974.

Casanovas, O., Jaumot, M., Paules, A. B., Agell, N., and Bachs, O. (2004). P38SAPK2 phosphorylates cyclin D3 at Thr-283 and targets it for proteasomal degradation. Oncogene *23*, 7537-7544.

Casanovas, O., Miro, F., Estanyol, J. M., Itarte, E., Agell, N., and Bachs, O. (2000). Osmotic stress regulates the stability of cyclin D1 in a p38SAPK2-dependent manner. J Biol Chem *275*, 35091-35097.

Castillo, J., Erroba, E., Perugorria, M. J., Santamaria, M., Lee, D. C., Prieto, J., Avila, M. A., and Berasain, C. (2006). Amphiregulin contributes to the transformed phenotype of human hepatocellular carcinoma cells. Cancer Res *66*, 6129-6138.

Chambers, A. F., Groom, A. C., and MacDonald, I. C. (2002). Dissemination and growth of cancer cells in metastatic sites. Nat Rev Cancer *2*, 563-572.

Chen, G., Hitomi, M., Han, J., and Stacey, D. W. (2000). The p38 pathway provides negative feedback for Ras proliferative signaling. J Biol Chem *275*, 38973-38980.

Chen, P., Xie, H., Sekar, M. C., Gupta, K., and Wells, A. (1994). Epidermal growth factor receptor-mediated cell motility: phospholipase C activity is required, but mitogen-activated protein kinase activity is not sufficient for induced cell movement. The Journal of cell biology *127*, 847-857.

Cho, S. G., Lee, Y. H., Park, H. S., Ryoo, K., Kang, K. W., Park, J., Eom, S. J., Kim, M. J., Chang, T. S., Choi, S. Y*., et al.* (2001). Glutathione S-transferase mu modulates the stress-activated signals by suppressing apoptosis signal-regulating kinase 1. J Biol Chem *276*, 12749-12755.

Cho, Y. S., Bae, J. M., Chun, Y. S., Chung, J. H., Jeon, Y. K., Kim, I. S., Kim, M. S., and Park, J. W. (2008). HIF-1alpha controls keratinocyte proliferation by up-regulating p21(WAF1/Cip1). Biochim Biophys Acta *1783*, 323-333.

Chou, M. M., Fajardo, J. E., and Hanafusa, H. (1992). The SH2- and SH3-containing Nck protein transforms mammalian fibroblasts in the absence of elevated phosphotyrosine levels. Molecular and cellular biology *12*, 5834-5842.

Chu, I., Sun, J., Arnaout, A., Kahn, H., Hanna, W., Narod, S., Sun, P., Tan, C. K., Hengst, L., and Slingerland, J. (2007). p27 phosphorylation by Src regulates inhibition of cyclin E-Cdk2. Cell *128*, 281-294.

Cobb, M. H., Hepler, J. E., Cheng, M., and Robbins, D. (1994). The mitogen-activated protein kinases, ERK1 and ERK2. Semin Cancer Biol *5*, 261-268.

Comoglio, P. M., and Trusolino, L. (2005). Cancer: the matrix is now in control. Nat Med *11*, 1156-1159.

Coulombe, P., and Meloche, S. (2006). Atypical mitogen-activated protein kinases: Structure, regulation and functions. Biochim Biophys Acta.

Crump, N., Han, Y., and Mahadevan, L.C. (2007). Stress-activated MAP kinases in chromatin and gene regulation. Top Curr Genet *19*.

Cuadrado, A., Lafarga, V., Cheung, P. C., Dolado, I., Llanos, S., Cohen, P., and Nebreda, A. R. (2007). A new p38 MAP kinase-regulated transcriptional coactivator that stimulates p53-dependent apoptosis. Embo J *26*, 2115-2126.

Cuenda, A., and Cohen, P. (1999). Stress-activated protein kinase-2/p38 and a rapamycin-sensitive pathway are required for C2C12 myogenesis. J Biol Chem *274*, 4341-4346.

Cuenda, A., and Rousseau, S. (2007). p38 MAP-kinases pathway regulation, function and role in human diseases. Biochim Biophys Acta *1773*, 1358-1375.

Curto, M., Cole, B. K., Lallemand, D., Liu, C. H., and McClatchey, A. I. (2007). Contact-dependent inhibition of EGFR signaling by Nf2/Merlin. The Journal of cell biology *177*, 893-903.

Curto, M., and McClatchey, A. I. (2008). Nf2/Merlin: a coordinator of receptor signalling and intercellular contact. Br J Cancer *98*, 256-262.

Daniel, C., Schroder, O., Zahn, N., Gaschott, T., and Stein, J. (2004). p38 MAPK signaling pathway is involved in butyrate-induced vitamin D receptor expression. Biochem Biophys Res Commun *324*, 1220-1226.

DaSilva, J., Xu, L., Kim, H. J., Miller, W. T., and Bar-Sagi, D. (2006). Regulation of sprouty stability by Mnk1-dependent phosphorylation. Molecular and cellular biology *26*, 1898-1907.

Datta, S. R., Dudek, H., Tao, X., Masters, S., Fu, H., Gotoh, Y., and Greenberg, M. E. (1997). Akt phosphorylation of BAD couples survival signals to the cell-intrinsic death machinery. Cell *91*, 231-241.

De Chiara, G., Marcocci, M. E., Torcia, M., Lucibello, M., Rosini, P., Bonini, P., Higashimoto, Y., Damonte, G., Armirotti, A., Amodei, S*., et al.* (2006). Bcl-2 Phosphorylation by p38 MAPK: identification of target sites and biologic consequences. J Biol Chem *281*, 21353-21361.

de Melker AA, v. d. H. G., Borst J. (2004). Ubiquitin ligase activity of c-Cbl guides the epidermal growth factor receptor into clathrin-coated pits by two distinct modes of Eps15 recruitment. J Biol Chem *279(53)*, 55465-55473.

De Vita, G., Bauer, L., da Costa, V. M., De Felice, M., Baratta, M. G., De Menna, M., and Di Lauro, R. (2005). Dose-dependent inhibition of thyroid differentiation by RAS oncogenes. Mol Endocrinol *19*, 76-89.

Diehl, N. L., Enslen, H., Fortner, K. A., Merritt, C., Stetson, N., Charland, C., Flavell, R. A., Davis, R. J., and Rincon, M. (2000). Activation of the p38 mitogen-activated protein kinase pathway arrests cell cycle progression and differentiation of immature thymocytes in vivo. J Exp Med *191*, 321-334.

Dietrich, C., Scherwat, J., Faust, D., and Oesch, F. (2002). Subcellular localization of beta-catenin is regulated by cell density. Biochem Biophys Res Commun *292*, 195-199.

Dolado, I., and Nebreda, A. R. (2008). Regulation of tumorigenesis by p38alpha MAP kinase. In Stress-Activated Protein Kinases, S.B. Heidelberg, ed., pp. 99-128.

Dolado, I., Swat, A., Ajenjo, N., De Vita, G., Cuadrado, A., and Nebreda, A. R. (2007). p38alpha MAP kinase as a sensor of reactive oxygen species in tumorigenesis. Cancer Cell *11*, 191-205.

Duan, L., Miura, Y., Dimri, M., Majumder, B., Dodge, I. L., Reddi, A. L., Ghosh, A., Fernandes, N., Zhou, P., Mullane-Robinson, K*., et al.* (2003). Cbl-mediated ubiquitinylation is required for lysosomal sorting of epidermal growth factor receptor but is dispensable for endocytosis. J Biol Chem *278*, 28950-28960.

Eagle, H., and Levine, E. M. (1967). Growth regulatory effects of cellular interaction. Nature *213*, 1102-1106.

Edlund, S., Bu, S., Schuster, N., Aspenstrom, P., Heuchel, R., Heldin, N. E., ten Dijke, P., Heldin, C. H., and Landstrom, M. (2003). Transforming growth factor-beta1 (TGF-beta)-induced apoptosis of prostate cancer cells involves Smad7-dependent activation of p38 by TGF-beta-activated kinase 1 and mitogen-activated protein kinase kinase 3. Mol Biol Cell *14*, 529-544.

Evan, G. I., and Vousden, K. H. (2001). Proliferation, cell cycle and apoptosis in cancer. Nature *411*, 342-348.

Fabbretti, E., Edomi, P., Brancolini, C., and Schneider, C. (1995). Apoptotic phenotype induced by overexpression of wild-type gas3/PMP22: its relation to the demyelinating peripheral neuropathy CMT1A. Genes Dev *9*, 1846-1856.

Farley, N., Pedraza-Alva, G., Serrano-Gomez, D., Nagaleekar, V., Aronshtam, A., Krahl, T., Thornton, T., and Rincon, M. (2006). p38 mitogen-activated protein kinase mediates the Fas-induced mitochondrial death pathway in CD8+ T cells. Molecular and cellular biology *26*, 2118-2129.

Fassetta, M., D´Alessandro, L., Coltella, N., Di Renzo, M. F., and Rasola, A. (2006). Hepatocyte growth factor installs a survival platform for colorectal cancer cell invasive growth and overcomes p38 MAPK-mediated apoptosis. . Cell Signal *in press*.

Faust, D., Dolado, I., Cuadrado, A., Oesch, F., Weiss, C., Nebreda, A. R., and Dietrich, C. (2005). p38alpha MAPK is required for contact inhibition. Oncogene *24*, 7941-7945.

Feng, X. (2005). RANKing intracellular signaling in osteoclasts. IUBMB Life *57*, 389-395.

Finn, G. J., Creaven, B. S., and Egan, D. A. (2004). Daphnetin induced differentiation of human renal carcinoma cells and its mediation by p38 mitogen-activated protein kinase. Biochem Pharmacol *67*, 1779-1788.

Foley, K. P., and Eisenman, R. N. (1999). Two MAD tails: what the recent knockouts of Mad1 and Mxi1 tell us about the MYC/MAX/MAD network. Biochim Biophys Acta *1423*, M37-47.

Folkman, J., and Moscona, A. (1978). Role of cell shape in growth control. Nature *273*, 345-349.

Fong, C. W., Leong, H. F., Wong, E. S., Lim, J., Yusoff, P., and Guy, G. R. (2003). Tyrosine phosphorylation of Sprouty2 enhances its interaction with c-Cbl and is crucial for its function. J Biol Chem *278*, 33456-33464.

Forte, G., Minieri, M., Cossa, P., Antenucci, D., Sala, M., Gnocchi, V., Fiaccavento, R., Carotenuto, F., De Vito, P., Baldini, P. M.*, et al.* (2006). Hepatocyte growth factor effects on mesenchymal stem cells: proliferation, migration, and differentiation. Stem Cells *24*, 23-33.

Frese, S., Schubert, W. D., Findeis, A. C., Marquardt, T., Roske, Y. S., Stradal, T. E., and Heinz, D. W. (2006). The phosphotyrosine peptide binding specificity of Nck1 and Nck2 Src homology 2 domains. J Biol Chem *281*, 18236-18245.

Frey, M. R., Dise, R. S., Edelblum, K. L., and Polk, D. B. (2006). p38 kinase regulates epidermal growth factor receptor downregulation and cellular migration. Embo J *25*, 5683-5692.

Fu, J., Menzies, K., Freeman, R. S., and Taubman, M. B. (2007). EGLN3 prolyl hydroxylase regulates skeletal muscle differentiation and myogenin protein stability. J Biol Chem *282*, 12410-12418.

Fujiwara, Y., Sugita, Y., Nakamori, S., Miyamoto, A., Shiozaki, K., Nagano, H., Sakon, M., and Monden, M. (2000). Assessment of Stanniocalcin-1 mRNA as a molecular marker for micrometastases of various human cancers. Int J Oncol *16*, 799-804.

Fuse, T., Tanikawa, M., Nakanishi, M., Ikeda, K., Tada, T., Inagaki, H., Asai, K., Kato, T., and Yamada, K. (2000). p27Kip1 expression by contact inhibition as a prognostic index of human glioma. J Neurochem *74*, 1393-1399.

Garner, A. P., Weston, C. R., Todd, D. E., Balmanno, K., and Cook, S. J. (2002). Delta MEKK3:ER* activation induces a p38 alpha/beta 2-dependent cell cycle arrest at the G2 checkpoint. Oncogene *21*, 8089-8104.

Gauthier, M. L., Pickering, C. R., Miller, C. J., Fordyce, C. A., Chew, K. L., Berman, H. K., and Tlsty, T. D. (2005). p38 regulates cyclooxygenase-2 in human mammary epithelial cells and is activated in premalignant tissue. Cancer Res *65*, 1792-1799.

Ghatan, S., Larner, S., Kinoshita, Y., Hetman, M., Patel, L., Xia, Z., Youle, R. J., and Morrison, R. S. (2000). p38 MAP kinase mediates bax translocation in nitric oxide-induced apoptosis in neurons. The Journal of cell biology *150*, 335-347.

Goloudina, A., Yamaguchi, H., Chervyakova, D. B., Appella, E., Fornace, A. J., Jr., and Bulavin, D. V. (2003). Regulation of human Cdc25A stability by Serine 75 phosphorylation is not sufficient to activate a S phase checkpoint. Cell Cycle *2*, 473-478.

Gonzalez-Garcia, A., Pritchard, C. A., Paterson, H. F., Mavria, G., Stamp, G., and Marshall, C. J. (2005). RalGDS is required for tumor formation in a model of skin carcinogenesis. Cancer Cell *7*, 219-226.

Gradl, G., Faust, D., Oesch, F., and Wieser, R. J. (1995). Density-dependent regulation of cell growth by contactinhibin and the contactinhibin receptor. Curr Biol *5*, 526-535.

Grethe, S., Ares, M. P., Andersson, T., and Porn-Ares, M. I. (2004). p38 MAPK mediates TNF-induced apoptosis in endothelial cells via phosphorylation and downregulation of Bcl-x(L). Exp Cell Res *298*, 632-642.

Grethe, S., Coltella, N., Di Renzo, M. F., and Porn-Ares, M. I. (2006). p38 MAPK downregulates phosphorylation of Bad in doxorubicin-induced endothelial apoptosis. Biochem Biophys Res Commun *347*, 781-790.

Grimmler, M., Wang, Y., Mund, T., Cilensek, Z., Keidel, E. M., Waddell, M. B., Jakel, H., Kullmann, M., Kriwacki, R. W., and Hengst, L. (2007). Cdk-inhibitory activity and stability of p27Kip1 are directly regulated by oncogenic tyrosine kinases. Cell *128*, 269-280.

Grovdal, L. M., Stang, E., Sorkin, A., and Madshus, I. H. (2004). Direct interaction of Cbl with pTyr 1045 of the EGF receptor (EGFR) is required to sort the EGFR to lysosomes for degradation. Exp Cell Res *300*, 388-395.

Gumbiner, B. M. (2000). Regulation of cadherin adhesive activity. The Journal of cell biology *148*, 399-404.

Guy, G. R., Wong, E. S., Yusoff, P., Chandramouli, S., Lo, T. L., Lim, J., and Fong, C. W. (2003). Sprouty: how does the branch manager work? J Cell Sci *116*, 3061-3068.

Hacohen, N., Kramer, S., Sutherland, D., Hiromi, Y., and Krasnow, M. A. (1998). sprouty encodes a novel antagonist of FGF signaling that patterns apical branching of the Drosophila airways. Cell *92*, 253-263.

Haglund, K., Schmidt, M. H., Wong, E. S., Guy, G. R., and Dikic, I. (2005). Sprouty2 acts at the Cbl/CIN85 interface to inhibit epidermal growth factor receptor downregulation. EMBO Rep *6*, 635-641.

Hall, A. B., Jura, N., DaSilva, J., Jang, Y. J., Gong, D., and Bar-Sagi, D. (2003). hSpry2 is targeted to the ubiquitin-dependent proteasome pathway by c-Cbl. Curr Biol *13*, 308-314.

Han, J., and Sun, P. (2007). The pathways to tumor suppression via route p38. Trends Biochem Sci *32*, 364-371.

Hanahan, D., and Weinberg, R. A. (2000). The hallmarks of cancer. Cell *100*, 57-70.

Haq, R., Brenton, J. D., Takahashi, M., Finan, D., Finkielsztein, A., Damaraju, S., Rottapel, R., and Zanke, B. (2002). Constitutive p38HOG mitogen-activated protein kinase activation induces permanent cell cycle arrest and senescence. Cancer Res *62*, 5076-5082.

Hehlgans, S., Haase, M., and Cordes, N. (2007). Signalling via integrins: implications for cell survival and anticancer strategies. Biochim Biophys Acta *1775*, 163-180.

Heimark, R. L., and Schwartz, S. M. (1985). The role of membrane-membrane interactions in the regulation of endothelial cell growth. The Journal of cell biology *100*, 1934-1940.

Henderson, G. S., van Diest, P. J., Burger, H., Russo, J., and Raman, V. (2006). Expression pattern of a homeotic gene, HOXA5, in normal breast and in breast tumors. Cell Oncol *28*, 305-313.

Hengst, L., Dulic, V., Slingerland, J. M., Lees, E., and Reed, S. I. (1994). A cell cycle-regulated inhibitor of cyclin-dependent kinases. Proc Natl Acad Sci U S A *91*, 5291-5295.

Herrlich, A., Leitch, V., and King, L. S. (2004). Role of proneuregulin 1 cleavage and human epidermal growth factor receptor activation in hypertonic aquaporin induction. Proc Natl Acad Sci U S A *101*, 15799-15804.

Higashiyama, S., Iwamoto, R., Goishi, K., Raab, G., Taniguchi, N., Klagsbrun, M., and Mekada, E. (1995). The membrane protein CD9/DRAP 27 potentiates the juxtacrine growth factor activity of the membrane-anchored heparin-binding EGF-like growth factor. The Journal of cell biology *128*, 929-938.

Hirsch, D. S., and Wu, W. J. (2007). Cdc42: an effector and regulator of ErbB1 as a strategic target in breast cancer therapy. Expert Rev Anticancer Ther *7*, 147-157.

Holbro, T., Civenni, G., and Hynes, N. E. (2003). The ErbB receptors and their role in cancer progression. Exp Cell Res *284*, 99-110.

Holley, R. W., and Kiernan, J. A. (1968). "Contact inhibition" of cell division in 3T3 cells. Proc Natl Acad Sci U S A *60*, 300-304.

Hou, S. T., Xie, X., Baggley, A., Park, D. S., Chen, G., and Walker, T. (2002). Activation of the Rb/E2F1 pathway by the nonproliferative p38 MAPK during Fas (APO1/CD95)-mediated neuronal apoptosis. J Biol Chem *277*, 48764-48770.

Houde, M., Laprise, P., Jean, D., Blais, M., Asselin, C., and Rivard, N. (2001). Intestinal epithelial cell differentiation involves activation of p38 mitogen-activated protein kinase that regulates the homeobox transcription factor CDX2. J Biol Chem *276*, 21885-21894.

Houghton, J., Morozov, A., Smirnova, I., and Wang, T. C. (2006). Stem cells and cancer. Semin Cancer Biol.

Huang, C. I., Kohno, N., Ogawa, E., Adachi, M., Taki, T., and Miyake, M. (1998). Correlation of reduction in MRP-1/CD9 and KAI1/CD82 expression with recurrences in breast cancer patients. Am J Pathol *153*, 973-983.

Huang, H., Ryu, J., Ha, J., Chang, E. J., Kim, H. J., Kim, H. M., Kitamura, T., Lee, Z. H., and Kim, H. H. (2006). Osteoclast differentiation requires TAK1 and MKK6 for NFATc1 induction and NF-kappaB transactivation by RANKL. Cell Death Differ *13*, 1879-1891.

Hunter, T. (1984). The epidermal growth factor receptor gene and its product. Nature *311*, 414-416.

Hynes, N. E., Horsch, K., Olayioye, M. A., and Badache, A. (2001). The ErbB receptor tyrosine family as signal integrators. Endocr Relat Cancer *8*, 151-159.

Ichijo, H. (1999). From receptors to stress-activated MAP kinases. Oncogene *18*, 6087-6093.

Imhof, I., Gasper, W. J., and Derynck, R. (2008). Association of tetraspanin CD9 with transmembrane TGF{alpha} confers alterations in cell-surface presentation of TGF{alpha} and cytoskeletal organization. J Cell Sci *121*, 2265-2274.

Inui, S., Higashiyama, S., Hashimoto, K., Higashiyama, M., Yoshikawa, K., and Taniguchi, N. (1997). Possible role of coexpression of CD9 with membrane-anchored heparin-binding EGF-like

growth factor and amphiregulin in cultured human keratinocyte growth. J Cell Physiol *171*, 291-298.

Ishida, N., Kitagawa, M., Hatakeyama, S., and Nakayama, K. (2000). Phosphorylation at serine 10, a major phosphorylation site of p27(Kip1), increases its protein stability. J Biol Chem *275*, 25146-25154.

Ito, K., Hirao, A., Arai, F., Takubo, K., Matsuoka, S., Miyamoto, K., Ohmura, M., Naka, K., Hosokawa, K., Ikeda, Y., and Suda, T. (2006). Reactive oxygen species act through p38 MAPK to limit the lifespan of hematopoietic stem cells. Nat Med *12*, 446-451.

Ji, J., Liu, R., Tong, T., Song, Y., Jin, S., Wu, M., and Zhan, Q. (2007). Gadd45a regulates beta-catenin distribution and maintains cell-cell adhesion/contact. Oncogene *26*, 6396-6405.

Joazeiro, C. A., Wing, S. S., Huang, H., Leverson, J. D., Hunter, T., and Liu, Y. C. (1999). The tyrosine kinase negative regulator c-Cbl as a RING-type, E2-dependent ubiquitin-protein ligase. Science *286*, 309-312.

Johnstone, R. W., Ruefli, A. A., and Lowe, S. W. (2002). Apoptosis: a link between cancer genetics and chemotherapy. Cell *108*, 153-164.

Jozic, D., Cardenes, N., Deribe, Y. L., Moncalian, G., Hoeller, D., Groemping, Y., Dikic, I., Rittinger, K., and Bravo, J. (2005). Cbl promotes clustering of endocytic adaptor proteins. Nat Struct Mol Biol *12*, 972-979.

Karin, M. (2006). Nuclear factor-kappaB in cancer development and progression. Nature *441*, 431-436.

Kato, J. Y., Matsuoka, M., Strom, D. K., and Sherr, C. J. (1994). Regulation of cyclin D-dependent kinase 4 (cdk4) by cdk4-activating kinase. Molecular and cellular biology *14*, 2713-2721.

Kato, Y., Hirano, T., Yoshida, K., Yashima, K., Akimoto, S., Tsuji, K., Ohira, T., Tsuboi, M., Ikeda, N., Ebihara, Y., and Kato, H. (2005). Frequent loss of E-cadherin and/or catenins in intrabronchial lesions during carcinogenesis of the bronchial epithelium. Lung Cancer *48*, 323-330.

Katzmann, D. J., Odorizzi, G., and Emr, S. D. (2002). Receptor downregulation and multivesicular-body sorting. Nat Rev Mol Cell Biol *3*, 893-905.

Kawabe, T. (2004). G2 checkpoint abrogators as anticancer drugs. Mol Cancer Ther *3*, 513-519.

Kemler, R. (1993). From cadherins to catenins: cytoplasmic protein interactions and regulation of cell adhesion. Trends Genet *9*, 317-321.

Khurana, A., Nakayama, K., Williams, S., Davis, R. J., Mustelin, T., and Ronai, Z. (2006). Regulation of the ring finger E3 ligase Siah2 by p38 MAPK. J Biol Chem *281*, 35316-35326.

Kim, B. J., Ryu, S. W., and Song, B. J. (2006). JNK- and p38 kinase-mediated phosphorylation of Bax leads to its activation and mitochondrial translocation and to apoptosis of human hepatoma HepG2 cells. J Biol Chem *281*, 21256-21265.

Kim, G. Y., Mercer, S. E., Ewton, D. Z., Yan, Z., Jin, K., and Friedman, E. (2002). The stress-activated protein kinases p38 alpha and JNK1 stabilize p21(Cip1) by phosphorylation. J Biol Chem *277*, 29792-29802.

Kim, J., Jonasch, E., Alexander, A., Short, J. D., Cai, S., Wen, S., Tsavachidou, D., Tamboli, P., Czerniak, B. A., Do, K. A*., et al.* (2009). Cytoplasmic sequestration of p27 via AKT phosphorylation in renal cell carcinoma. Clin Cancer Res *15*, 81-90.

Kinders, R. J., Milenkovic, A. G., Nordin, P., and Johnson, T. C. (1980). Characterization of cell-surface glycopeptides from mouse cerebral cortex that inhibit cell growth and protein synthesis. Biochem J *190*, 605-614.

Kishi, H., Nakagawa, K., Matsumoto, M., Suga, M., Ando, M., Taya, Y., and Yamaizumi, M. (2001). Osmotic shock induces G1 arrest through p53 phosphorylation at Ser33 by activated p38MAPK without phosphorylation at Ser15 and Ser20. J Biol Chem *276*, 39115-39122.

Kiyokawa, H., Kineman, R. D., Manova-Todorova, K. O., Soares, V. C., Hoffman, E. S., Ono, M., Khanam, D., Hayday, A. C., Frohman, L. A., and Koff, A. (1996). Enhanced growth of mice lacking the cyclin-dependent kinase inhibitor function of p27(Kip1). Cell *85*, 721-732.

Klein, F., Feldhahn, N., Herzog, S., Sprangers, M., Mooster, J. L., Jumaa, H., and Muschen, M. (2006). BCR-ABL1 induces aberrant splicing of IKAROS and lineage infidelity in pre-B lymphoblastic leukemia cells. Oncogene *25*, 1118-1124.

Koff, A., Ohtsuki, M., Polyak, K., Roberts, J. M., and Massague, J. (1993). Negative regulation of G1 in mammalian cells: inhibition of cyclin E-dependent kinase by TGF-beta. Science *260*, 536-539.

Koga, T., Nakano, S., Nakayama, M., Kounoue, E., Nagafuchi, S., Niho, Y., and Yamada, H. (1986). Identification and partial purification of a low-molecular-weight growth inhibitor formed by density-inhibited, tumorigenic V79 Chinese hamster cells. Cancer Res *46*, 4431-4437.

Kossatz, U., Vervoorts, J., Nickeleit, I., Sundberg, H. A., Arthur, J. S., Manns, M. P., and Malek, N. P. (2006). C-terminal phosphorylation controls the stability and function of p27kip1. Embo J *25*, 5159-5170.

Kotlyarov, A., and Gaestel, M. (2007). Protein kinases as substrates for SAPKs. Top Curr Genet *19*, in press.

Kudo, Y., Kitajima, S., Ogawa, I., Hiraoka, M., Sargolzaei, S., Keikhaee, M. R., Sato, S., Miyauchi, M., and Takata, T. (2004). Invasion and metastasis of oral cancer cells require methylation of E-cadherin and/or degradation of membranous beta-catenin. Clin Cancer Res *10*, 5455-5463.

Kyriakis, J. M., and Avruch, J. (2001). Mammalian mitogen-activated protein kinase signal transduction pathways activated by stress and inflammation. Physiol Rev *81*, 807-869.

Lavoie, J. N., L'Allemain, G., Brunet, A., Muller, R., and Pouyssegur, J. (1996). Cyclin D1 expression is regulated positively by the p42/p44MAPK and negatively by the p38/HOGMAPK pathway. J Biol Chem *271*, 20608-20616.

Le Naour, F., Andre, M., Greco, C., Billard, M., Sordat, B., Emile, J. F., Lanza, F., Boucheix, C., and Rubinstein, E. (2006). Profiling of the tetraspanin web of human colon cancer cells. Mol Cell Proteomics *5*, 845-857.

Lee, S., Nakamura, E., Yang, H., Wei, W., Linggi, M. S., Sajan, M. P., Farese, R. V., Freeman, R. S., Carter, B. D., Kaelin, W. G., Jr., and Schlisio, S. (2005). Neuronal apoptosis linked to EglN3 prolyl hydroxylase and familial pheochromocytoma genes: developmental culling and cancer. Cancer Cell *8*, 155-167.

Lennon, S. V., Martin, S. J., and Cotter, T. G. (1991). Dose-dependent induction of apoptosis in human tumour cell lines by widely diverging stimuli. Cell Prolif *24*, 203-214.

Leone, G., DeGregori, J., Sears, R., Jakoi, L., and Nevins, J. R. (1997). Myc and Ras collaborate in inducing accumulation of active cyclin E/Cdk2 and E2F. Nature *387*, 422-426.

Levenberg, S., Yarden, A., Kam, Z., and Geiger, B. (1999). p27 is involved in N-cadherin-mediated contact inhibition of cell growth and S-phase entry. Oncogene *18*, 869-876.

Levine, E. M., Becker, Y., Boone, C. W., and Eagle, H. (1965). Contact Inhibition, Macromolecular Synthesis, and Polyribosomes in Cultured Human Diploid Fibroblasts. Proc Natl Acad Sci U S A *53*, 350-356.

Levine, M., and Tjian, R. (2003). Transcription regulation and animal diversity. Nature *424*, 147-151.

Levkowitz, G., Waterman, H., Ettenberg, S. A., Katz, M., Tsygankov, A. Y., Alroy, I., Lavi, S., Iwai, K., Reiss, Y., Ciechanover, A.*, et al.* (1999). Ubiquitin ligase activity and tyrosine phosphorylation underlie suppression of growth factor signaling by c-Cbl/Sli-1. Mol Cell *4*, 1029-1040.

Levkowitz, G., Waterman, H., Zamir, E., Kam, Z., Oved, S., Langdon, W. Y., Beguinot, L., Geiger, B., and Yarden, Y. (1998). c-Cbl/Sli-1 regulates endocytic sorting and ubiquitination of the epidermal growth factor receptor. Genes Dev *12*, 3663-3674.

Li, W., Hu, P., Skolnik, E. Y., Ullrich, A., and Schlessinger, J. (1992). The SH2 and SH3 domain-containing Nck protein is oncogenic and a common target for phosphorylation by different surface receptors. Molecular and cellular biology *12*, 5824-5833.

Li, Y., Jiang, B., Ensign, W. Y., Vogt, P. K., and Han, J. (2000). Myogenic differentiation requires signalling through both phosphatidylinositol 3-kinase and p38 MAP kinase. Cell Signal *12*, 751-757.

Lichtner, R. B., and Schirrmacher, V. (1990). Cellular distribution and biological activity of epidermal growth factor receptors in A431 cells are influenced by cell-cell contact. J Cell Physiol *144*, 303-312.

Lindqvist, A., Kallstrom, H., and Karlsson Rosenthal, C. (2004). Characterisation of Cdc25B localisation and nuclear export during the cell cycle and in response to stress. J Cell Sci *117*, 4979-4990.

Lipkin, G., Knecht, M. E., and Rosenberg, M. (1978). A potent inhibitor of normal and transformed cell growth derived from contact-inhibited cells. Cancer Res *38*, 635-643.

Lipkowitz, S. (2003). The role of the ubiquitination-proteasome pathway in breast cancer: ubiquitin mediated degradation of growth factor receptors in the pathogenesis and treatment of cancer. Breast Cancer Res *5*, 8-15.

Lito, P., Mets, B. D., Kleff, S., O'Reilly, S., Maher, V. M., and McCormick, J. J. (2008). Evidence that sprouty 2 is necessary for sarcoma formation by H-Ras oncogene-transformed human fibroblasts. J Biol Chem *283*, 2002-2009.

Lluis, F., Ballestar, E., Suelves, M., Esteller, M., and Munoz-Canoves, P. (2005). E47 phosphorylation by p38 MAPK promotes MyoD/E47 association and muscle-specific gene transcription. Embo J *24*, 974-984.

Lluis, F., Perdiguero, E., Nebreda, A. R., and Munoz-Canoves, P. (2006). Regulation of skeletal muscle gene expression by p38 MAP kinases. Trends Cell Biol *16*, 36-44.

Longva, K. E., Blystad, F. D., Stang, E., Larsen, A. M., Johannessen, L. E., and Madshus, I. H. (2002). Ubiquitination and proteasomal activity is required for transport of the EGF receptor to inner membranes of multivesicular bodies. The Journal of cell biology *156*, 843-854.

Mace, G., Miaczynska, M., Zerial, M., and Nebreda, A. R. (2005). Phosphorylation of EEA1 by p38 MAP kinase regulates mu opioid receptor endocytosis. Embo J *24*, 3235-3246.

Malumbres, M., and Barbacid, M. (2001). To cycle or not to cycle: a critical decision in cancer. Nat Rev Cancer *1*, 222-231.

Malumbres, M., and Barbacid, M. (2009). Cell cycle, CDKs and cancer: a changing paradigm. Nat Rev Cancer *9*, 153-166.

Manke, I. A., Nguyen, A., Lim, D., Stewart, M. Q., Elia, A. E., and Yaffe, M. B. (2005). MAPKAP kinase-2 is a cell cycle checkpoint kinase that regulates the G2/M transition and S phase progression in response to UV irradiation. Mol Cell *17*, 37-48.

Martin, A., Odajima, J., Hunt, S. L., Dubus, P., Ortega, S., Malumbres, M., and Barbacid, M. (2005). Cdk2 is dispensable for cell cycle inhibition and tumor suppression mediated by p27(Kip1) and p21(Cip1). Cancer Cell *7*, 591-598.

Martinez, N., Garcia-Dominguez, C. A., Domingo, B., Oliva, J. L., Zarich, N., Sanchez, A., Gutierrez-Eisman, S., Llopis, J., and Rojas, J. M. (2007). Sprouty2 binds Grb2 at two different proline-rich regions, and the mechanism of ERK inhibition is independent of this interaction. Cell Signal *19*, 2277-2285.

Mason, J. M., Morrison, D. J., Bassit, B., Dimri, M., Band, H., Licht, J. D., and Gross, I. (2004). Tyrosine phosphorylation of Sprouty proteins regulates their ability to inhibit growth factor signaling: a dual feedback loop. Mol Biol Cell *15*, 2176-2188.

Mason, J. M., Morrison, D. J., Basson, M. A., and Licht, J. D. (2006). Sprouty proteins: multifaceted negative-feedback regulators of receptor tyrosine kinase signaling. Trends Cell Biol *16*, 45-54.

Matoskova, B., Wong, W. T., Salcini, A. E., Pelicci, P. G., and Di Fiore, P. P. (1995). Constitutive phosphorylation of eps8 in tumor cell lines: relevance to malignant transformation. Molecular and cellular biology *15*, 3805-3812.

Matsukawa, J., Matsuzawa, A., Takeda, K., and Ichijo, H. (2004). The ASK1-MAP Kinase Cascades in Mammalian Stress Response J Biochem *136*, 261-265.

Matsuoka, M., Kato, J. Y., Fisher, R. P., Morgan, D. O., and Sherr, C. J. (1994). Activation of cyclin-dependent kinase 4 (cdk4) by mouse MO15-associated kinase. Molecular and cellular biology *14*, 7265-7275.

Maxwell, P. H. (2005). A common pathway for genetic events leading to pheochromocytoma. Cancer Cell *8*, 91-93.

Meerson, A., Milyavsky, M., and Rotter, V. (2004). p53 mediates density-dependent growth arrest. FEBS Lett *559*, 152-158.

Metzen, E. (2007). Enzyme substrate recognition in oxygen sensing: how the HIF trap snaps. Biochem J *408*, e5-6.

Mhawech, P., Dulguerov, P., Tschanz, E., Verdan, C., Ares, C., and Allal, A. S. (2004). Motility-related protein-1 (MRP-1/CD9) expression can predict disease-free survival in patients with squamous cell carcinoma of the head and neck. Br J Cancer *90*, 471-475.

Mikhailov, A., Shinohara, M., and Rieder, C. L. (2005). The p38-mediated stress-activated checkpoint. A rapid response system for delaying progression through antephase and entry into mitosis. Cell Cycle *4*, 57-62.

Miller, W. E., Cheshire, J. L., and Raab-Traub, N. (1998). Interaction of tumor necrosis factor receptor-associated factor signaling proteins with the latent membrane protein 1 PXQXT motif is essential for induction of epidermal growth factor receptor expression. Molecular and cellular biology *18*, 2835-2844.

Mitsushita, J., Lambeth, J. D., and Kamata, T. (2004). The superoxide-generating oxidase Nox1 is functionally required for Ras oncogene transformation. Cancer Res *64*, 3580-3585.

Mobley, C. K., Myers, J. K., Hadziselimovic, A., Ellis, C. D., and Sanders, C. R. (2007). Purification and initiation of structural characterization of human peripheral myelin protein 22, an integral membrane protein linked to peripheral neuropathies. Biochemistry *46*, 11185-11195.

Molnar, A., Theodoras, A. M., Zon, L. I., and Kyriakis, J. M. (1997). Cdc42Hs, but not Rac1, inhibits serum-stimulated cell cycle progression at G1/S through a mechanism requiring p38/RK. J Biol Chem *272*, 13229-13235.

Moreno, E. (2008). Is cell competition relevant to cancer? Nat Rev Cancer *8*, 141-147.

Mosesson, Y., Shtiegman, K., Katz, M., Zwang, Y., Vereb, G., Szollosi, J., and Yarden, Y. (2003). Endocytosis of receptor tyrosine kinases is driven by monoubiquitylation, not polyubiquitylation. J Biol Chem *278*, 21323-21326.

Mudgett, J. S., Ding, J., Guh-Siesel, L., Chartrain, N. A., Yang, L., Gopal, S., and Shen, M. M. (2000). Essential role for p38alpha mitogen-activated protein kinase in placental angiogenesis. Proc Natl Acad Sci U S A *97*, 10454-10459.

Murayama, Y., Miyagawa, J., Shinomura, Y., Kanayama, S., Isozaki, K., Yamamori, K., Mizuno, H., Ishiguro, S., Kiyohara, T., Miyazaki, Y.*, et al.* (2002). Significance of the association between heparin-binding epidermal growth factor-like growth factor and CD9 in human gastric cancer. Int J Cancer *98*, 505-513.

Nadeau, R. J., Toher, J. L., Yang, X., Kovalenko, D., and Friesel, R. (2007). Regulation of Sprouty2 stability by mammalian Seven-in-Absentia homolog 2. J Cell Biochem *100*, 151-160.

Nakayama, K., Ishida, N., Shirane, M., Inomata, A., Inoue, T., Shishido, N., Horii, I., Loh, D. Y., and Nakayama, K. (1996). Mice lacking p27(Kip1) display increased body size, multiple organ hyperplasia, retinal dysplasia, and pituitary tumors. Cell *85*, 707-720.

Nebert, D. W., and Vasiliou, V. (2004). Analysis of the glutathione S-transferase (GST) gene family. Hum Genomics *1*, 460-464.

Nebreda, A. R., and Porras, A. (2000). p38 MAP kinases: beyond the stress response. Trends Biochem Sci *25*, 257-260.

Nicke, B., Bastien, J., Khanna, S. J., Warne, P. H., Cowling, V., Cook, S. J., Peters, G., Delpuech, O., Schulze, A., Berns, K.*, et al.* (2005). Involvement of MINK, a Ste20 family kinase, in Ras oncogene-induced growth arrest in human ovarian surface epithelial cells. Mol Cell *20*, 673-685.

Nie, Z., Hirsch, D. S., Luo, R., Jian, X., Stauffer, S., Cremesti, A., Andrade, J., Lebowitz, J., Marino, M., Ahvazi, B.*, et al.* (2006). A BAR domain in the N terminus of the Arf GAP ASAP1 affects membrane structure and trafficking of epidermal growth factor receptor. Curr Biol *16*, 130-139.

Oertle, T., Merkler, D., and Schwab, M. E. (2003). Do cancer cells die because of Nogo-B? Oncogene *22*, 1390-1399.

Ogiso, H., Ishitani, R., Nureki, O., Fukai, S., Yamanaka, M., Kim, J. H., Saito, K., Sakamoto, A., Inoue, M., Shirouzu, M., and Yokoyama, S. (2002). Crystal structure of the complex of human epidermal growth factor and receptor extracellular domains. Cell *110*, 775-787.

Okada, T., You, L., and Giancotti, F. G. (2007). Shedding light on Merlin's wizardry. Trends Cell Biol *17*, 222-229.

Olson, J. M., and Hallahan, A. R. (2004). p38 MAP kinase: a convergence point in cancer therapy. Trends Mol Med *10*, 125-129.

Ono, K., and Han, J. (2000). The p38 signal transduction pathway: activation and function. Cell Signal *12*, 1-13.

Orphanides, G., and Reinberg, D. (2002). A unified theory of gene expression. Cell *108*, 439-451.

Overall, C. M., and Dean, R. A. (2006). Degradomics: systems biology of the protease web. Pleiotropic roles of MMPs in cancer. Cancer Metastasis Rev *25*, 69-75.

Pages, G., Lenormand, P., L'Allemain, G., Chambard, J. C., Meloche, S., and Pouyssegur, J. (1993). Mitogen-activated protein kinases p42mapk and p44mapk are required for fibroblast proliferation. Proc Natl Acad Sci U S A *90*, 8319-8323.

Palermo, C., and Joyce, J. A. (2008). Cysteine cathepsin proteases as pharmacological targets in cancer. Trends Pharmacol Sci *29*, 22-28.

Pang, S. T., Fang, X., Valdman, A., Norstedt, G., Pousette, A., Egevad, L., and Ekman, P. (2004). Expression of ezrin in prostatic intraepithelial neoplasia. Urology *63*, 609-612.

Pascual-Ahuir, A., Struhl, K., and Proft, M. (2006). Genome-wide location analysis of the stress-activated MAP kinase Hog1 in yeast. Methods *40*, 272-278.

Pedersen, K., Angelini, P. D., Laos, S., Bach-Faig, A., Cunningham, M. P., Ferrer-Ramon, C., Luque-Garcia, A., Garcia-Castillo, J., Parra-Palau, J. L., Scaltriti, M.*, et al.* (2009). A naturally occurring HER2 carboxy-terminal fragment promotes mammary tumor growth and metastasis. Molecular and cellular biology *29*, 3319-3331.

Pedraza-Alva, G., Koulnis, M., Charland, C., Thornton, T., Clements, J. L., Schlissel, M. S., and Rincon, M. (2006). Activation of p38 MAP kinase by DNA double-strand breaks in V(D)J recombination induces a G2/M cell cycle checkpoint. Embo J *25*, 763-773.

Pennock, S., and Wang, Z. (2003). Stimulation of cell proliferation by endosomal epidermal growth factor receptor as revealed through two distinct phases of signaling. Molecular and cellular biology *23*, 5803-5815.

Perdiguero, E., and Munoz-Canoves, P. (2008). Transcriptional regulation by the p38 MAPK signaling pathway in mammalian cells. Top Curr Genet *20*, 51-79.

Perdiguero, E., Ruiz-Bonilla, V., Gresh, L., Hui, L., Ballestar, E., Sousa-Victor, P., Baeza-Raja, B., Jardi, M., Bosch-Comas, A., Esteller, M.*, et al.* (2007). Genetic analysis of p38 MAP kinases in myogenesis: fundamental role of p38alpha in abrogating myoblast proliferation. Embo J *26*, 1245-1256.

Perucca, P., Cazzalini, O., Madine, M., Savio, M., Laskey, R. A., Vannini, V., Prosperi, E., and Stivala, L. A. (2009). Loss of p21 CDKN1A impairs entry to quiescence and activates a DNA damage response in normal fibroblasts induced to quiescence. Cell Cycle *8*, 105-114.

Pickering, M., Cumiskey, D., and O'Connor, J. J. (2005). Actions of TNF-alpha on glutamatergic synaptic transmission in the central nervous system. Exp Physiol *90*, 663-670.

Pokholok, D. K., Zeitlinger, J., Hannett, N. M., Reynolds, D. B., and Young, R. A. (2006). Activated signal transduction kinases frequently occupy target genes. Science *313*, 533-536.

Pollack, R. E., Green, H., and Todaro, G. J. (1968). Growth control in cultured cells: selection of sublines with increased sensitivity to contact inhibition and decreased tumor-producing ability. Proc Natl Acad Sci U S A *60*, 126-133.

Polo, S., Pece, S., and Di Fiore, P. P. (2004). Endocytosis and cancer. Curr Opin Cell Biol *16*, 156-161.

Polyak, K., Kato, J. Y., Solomon, M. J., Sherr, C. J., Massague, J., Roberts, J. M., and Koff, A. (1994). p27Kip1, a cyclin-Cdk inhibitor, links transforming growth factor-beta and contact inhibition to cell cycle arrest. Genes Dev *8*, 9-22.

Porras, A., Zuluaga, S., Black, E., Valladares, A., Alvarez, A. M., Ambrosino, C., Benito, M., and Nebreda, A. R. (2004). P38 alpha mitogen-activated protein kinase sensitizes cells to apoptosis induced by different stimuli. Mol Biol Cell *15*, 922-933.

Potter, V. R. (1978). Phenotypic diversity in experimental hepatomas: the concept of partially blocked ontogeny. The 10th Walter Hubert Lecture. Br J Cancer *38*, 1-23.

Proft, M., Mas, G., de Nadal, E., Vendrell, A., Noriega, N., Struhl, K., and Posas, F. (2006). The stress-activated Hog1 kinase is a selective transcriptional elongation factor for genes responding to osmotic stress. Mol Cell *23*, 241-250.

Puri, P. L., Wu, Z., Zhang, P., Wood, L. D., Bhakta, K. S., Han, J., Feramisco, J. R., Karin, M., and Wang, J. Y. (2000). Induction of terminal differentiation by constitutive activation of p38 MAP kinase in human rhabdomyosarcoma cells. Genes Dev *14*, 574-584.

Radisky, D. C., Levy, D. D., Littlepage, L. E., Liu, H., Nelson, C. M., Fata, J. E., Leake, D., Godden, E. L., Albertson, D. G., Nieto, M. A.*, et al.* (2005). Rac1b and reactive oxygen species mediate MMP-3-induced EMT and genomic instability. Nature *436*, 123-127.

Radke, S., Austermann, J., Russo-Marie, F., Gerke, V., and Rescher, U. (2004). Specific association of annexin 1 with plasma membrane-resident and internalized EGF receptors mediated through the protein core domain. FEBS Lett *578*, 95-98.

Ravid, T., Heidinger, J. M., Gee, P., Khan, E. M., and Goldkorn, T. (2004). c-Cbl-mediated ubiquitinylation is required for epidermal growth factor receptor exit from the early endosomes. J Biol Chem *279*, 37153-37162.

Reinheckel, T., Hagemann, S., Dollwet-Mack, S., Martinez, E., Lohmuller, T., Zlatkovic, G., Tobin, D. J., Maas-Szabowski, N., and Peters, C. (2005). The lysosomal cysteine protease cathepsin L regulates keratinocyte proliferation by control of growth factor recycling. J Cell Sci *118*, 3387-3395.

Rio, C., Buxbaum, J. D., Peschon, J. J., and Corfas, G. (2000). Tumor necrosis factor-alpha-converting enzyme is required for cleavage of erbB4/HER4. J Biol Chem *275*, 10379-10387.

Rousseau, S., Peggie, M., Campbell, D. G., Nebreda, A. R., and Cohen, P. (2005). Nogo-B is a new physiological substrate for MAPKAP-K2. Biochem J *391*, 433-440.

Rubin, C., Zwang, Y., Vaisman, N., Ron, D., and Yarden, Y. (2005). Phosphorylation of carboxyl-terminal tyrosines modulates the specificity of Sprouty-2 inhibition of different signaling pathways. J Biol Chem *280*, 9735-9744.

Rubin, H. (2008). Cell-cell contact interactions conditionally determine suppression and selection of the neoplastic phenotype. Proc Natl Acad Sci U S A *105*, 6215-6221.

Ruusala, A., Pawson, T., Heldin, C. H., and Aspenstrom, P. (2008). Nck adapters are involved in the formation of dorsal ruffles, cell migration, and Rho signaling downstream of the platelet-derived growth factor beta receptor. J Biol Chem *283*, 30034-30044.

Sabio, G., Arthur, J. S., Kuma, Y., Peggie, M., Carr, J., Murray-Tait, V., Centeno, F., Goedert, M., Morrice, N. A., and Cuenda, A. (2005). p38gamma regulates the localisation of SAP97 in the cytoskeleton by modulating its interaction with GKAP. Embo J *24*, 1134-1145.

Saklatvala, J. (2004). The p38 MAP kinase pathway as a therapeutic target in inflammatory disease. Curr Opin Pharmacol *4*, 372-377.

Salon, C., Moro, D., Lantuejoul, S., Brichon Py, P., Drabkin, H., Brambilla, C., and Brambilla, E. (2004). E-cadherin-beta-catenin adhesion complex in neuroendocrine tumors of the lung: a suggested role upon local invasion and metastasis. Hum Pathol *35*, 1148-1155.

Sanchez-Prieto, R., Rojas, J. M., Taya, Y., and Gutkind, J. S. (2000). A role for the p38 mitogen-acitvated protein kinase pathway in the transcriptional activation of p53 on genotoxic stress by chemotherapeutic agents. Cancer Res *60*, 2464-2472.

Santamaria, P. G., and Pagano, M. (2007). The pRb-Cdh1-p27 autoamplifying network. Nat Cell Biol *9*, 137-138.

Schlessinger, J. (2000). New roles for Src kinases in control of cell survival and angiogenesis. Cell *100*, 293-296.

Schmelter, M., Ateghang, B., Helmig, S., Wartenberg, M., and Sauer, H. (2006). Embryonic stem cells utilize reactive oxygen species as transducers of mechanical strain-induced cardiovascular differentiation. Faseb J *20*, 1182-1184.

Schutz, L., and Mora, P. T. (1968). The need for direct cell contact in "contact" inhibition of cell division in culture. J Cell Physiol *71*, 1-6.

Schweiger, A., Christensen, I. J., Nielsen, H. J., Sorensen, S., Brunner, N., and Kos, J. (2004). Serum cathepsin H as a potential prognostic marker in patients with colorectal cancer. Int J Biol Markers *19*, 289-294.

Seo, J., Kim, J., and Kim, M. (2001). Cloning of androgen-inducible gene 1 (AIG1) from human dermal papilla cells. Mol Cells *11*, 35-40.

Serrano, M., Lin, A. W., McCurrach, M. E., Beach, D., and Lowe, S. W. (1997). Oncogenic ras provokes premature cell senescence associated with accumulation of p53 and p16INK4a. Cell *88*, 593-602.

Sharpless, N. E., Bardeesy, N., Lee, K. H., Carrasco, D., Castrillon, D. H., Aguirre, A. J., Wu, E. A., Horner, J. W., and DePinho, R. A. (2001). Loss of p16Ink4a with retention of p19Arf predisposes mice to tumorigenesis. Nature *413*, 86-91.

Sherr, C. J., and Roberts, J. M. (1995). Inhibitors of mammalian G1 cyclin-dependent kinases. Genes Dev *9*, 1149-1163.

Shi, W., Fan, H., Shum, L., and Derynck, R. (2000). The tetraspanin CD9 associates with transmembrane TGF-alpha and regulates TGF-alpha-induced EGF receptor activation and cell proliferation. The Journal of cell biology *148*, 591-602.

Shin, I., Yakes, F. M., Rojo, F., Shin, N. Y., Bakin, A. V., Baselga, J., and Arteaga, C. L. (2002). PKB/Akt mediates cell-cycle progression by phosphorylation of p27(Kip1) at threonine 157 and modulation of its cellular localization. Nat Med *8*, 1145-1152.

Shin, S. I., Freedman, V. H., Risser, R., and Pollack, R. (1975). Tumorigenicity of virus-transformed cells in nude mice is correlated specifically with anchorage independent growth in vitro. Proc Natl Acad Sci U S A *72*, 4435-4439.

Shtiegman, K., Kochupurakkal, B. S., Zwang, Y., Pines, G., Starr, A., Vexler, A., Citri, A., Katz, M., Lavi, S., Ben-Basat, Y.*, et al.* (2007). Defective ubiquitinylation of EGFR mutants of lung cancer confers prolonged signaling. Oncogene *26*, 6968-6978.

Shtiegman, K., and Yarden, Y. (2003). The role of ubiquitylation in signaling by growth factors: implications to cancer. Semin Cancer Biol *13*, 29-40.

Si-Tayeb, K., Monvoisin, A., Mazzocco, C., Lepreux, S., Decossas, M., Cubel, G., Taras, D., Blanc, J. F., Robinson, D. R., and Rosenbaum, J. (2006). Matrix metalloproteinase 3 is present in the cell nucleus and is involved in apoptosis. Am J Pathol *169*, 1390-1401.

Sibilia, M., Fleischmann, A., Behrens, A., Stingl, L., Carroll, J., Watt, F. M., Schlessinger, J., and Wagner, E. F. (2000). The EGF receptor provides an essential survival signal for SOS-dependent skin tumor development. Cell *102*, 211-220.

Sjolund, J., Manetopoulos, C., Stockhausen, M. T., and Axelson, H. (2005). The Notch pathway in cancer: differentiation gone awry. Eur J Cancer *41*, 2620-2629.

Slamon, D. J., Clark, G. M., Wong, S. G., Levin, W. J., Ullrich, A., and McGuire, W. L. (1987). Human breast cancer: correlation of relapse and survival with amplification of the HER-2/neu oncogene. Science *235*, 177-182.

Slingerland, J. M., Hengst, L., Pan, C. H., Alexander, D., Stampfer, M. R., and Reed, S. I. (1994). A novel inhibitor of cyclin-Cdk activity detected in transforming growth factor beta-arrested epithelial cells. Molecular and cellular biology *14*, 3683-3694.

Stalheim, L., and Johnson, G. L. (2007). MAPK kinase kinase regulation of SAPK/JNK pathways. Top Curr Genet *19*, in press.

Stepniak, E., Ricci, R., Eferl, R., Sumara, G., Sumara, I., Rath, M., Hui, L., and Wagner, E. F. (2006). c-Jun/AP-1 controls liver regeneration by repressing p53/p21 and p38 MAPK activity. Genes Dev *20*, 2306-2314.

Sternlicht, M. D., Lochter, A., Sympson, C. J., Huey, B., Rougier, J. P., Gray, J. W., Pinkel, D., Bissell, M. J., and Werb, Z. (1999). The stromal proteinase MMP3/stromelysin-1 promotes mammary carcinogenesis. Cell *98*, 137-146.

Sternlicht, M. D., and Werb, Z. (2001). How matrix metalloproteinases regulate cell behavior. Annu Rev Cell Dev Biol *17*, 463-516.

Stewart, J. R., and O'Brian, C. A. (2005). Protein kinase C-{alpha} mediates epidermal growth factor receptor transactivation in human prostate cancer cells. Mol Cancer Ther *4*, 726-732.

Striedinger, K., VandenBerg, S. R., Baia, G. S., McDermott, M. W., Gutmann, D. H., and Lal, A. (2008). The neurofibromatosis 2 tumor suppressor gene product, merlin, regulates human meningioma cell growth by signaling through YAP. Neoplasia (New York, NY *10*, 1204-1212.

Sun, P., Yoshizuka, N., New, L., Moser, B. A., Li, Y., Liao, R., Xie, C., Chen, J., Deng, Q., Yamout, M.*, et al.* (2007). PRAK is essential for ras-induced senescence and tumor suppression. Cell *128*, 295-308.

Swaminathan, G., and Tsygankov, A. Y. (2006). The Cbl family proteins: ring leaders in regulation of cell signaling. J Cell Physiol *209*, 21-43.

Tachibana, I., and Hemler, M. E. (1999). Role of transmembrane 4 superfamily (TM4SF) proteins CD9 and CD81 in muscle cell fusion and myotube maintenance. The Journal of cell biology *146*, 893-904.

Takahashi, K., and Suzuki, K. (1996). Density-dependent inhibition of growth involves prevention of EGF receptor activation by E-cadherin-mediated cell-cell adhesion. Exp Cell Res *226*, 214-222.

Takekawa, M., and Saito, H. (1998). A family of stress-inducible GADD45-like proteins mediate activation of the stress-responsive MTK1/MEKK4 MAPKKK. Cell *95*, 521-530.

Takuwa, N., and Takuwa, Y. (1997). Ras activity late in G1 phase required for p27kip1 downregulation, passage through the restriction point, and entry into S phase in growth factor-stimulated NIH 3T3 fibroblasts. Molecular and cellular biology *17*, 5348-5358.

Tamura, K., Sudo, T., Senftleben, U., Dadak, A. M., Johnson, R., and Karin, M. (2000). Requirement for p38alpha in erythropoietin expression: a role for stress kinases in erythropoiesis. Cell *102*, 221-231.

Tanoue, T., and Takeichi, M. (2004). Mammalian Fat1 cadherin regulates actin dynamics and cell-cell contact. The Journal of cell biology *165*, 517-528.

Thien, C. B., and Langdon, W. Y. (2001). Cbl: many adaptations to regulate protein tyrosine kinases. Nat Rev Mol Cell Biol *2*, 294-307.

Thornton, T. M., and Rincon, M. (2009). Non-classical p38 map kinase functions: cell cycle checkpoints and survival. Int J Biol Sci *5*, 44-51.

Tlsty, T. D., and Hein, P. W. (2001). Know thy neighbor: stromal cells can contribute oncogenic signals. Curr Opin Genet Dev *11*, 54-59.

Todaro, G. J., and Green, H. (1963). Quantitative studies of the growth of mouse embryo cells in culture and their development into established lines. The Journal of cell biology *17*, 299-313.

Tran Quang, C., Gautreau, A., Arpin, M., and Treisman, R. (2000). Ezrin function is required for ROCK-mediated fibroblast transformation by the Net and Dbl oncogenes. Embo J *19*, 4565-4576.

Trost, T. M., Lausch, E. U., Fees, S. A., Schmitt, S., Enklaar, T., Reutzel, D., Brixel, L. R., Schmidtke, P., Maringer, M., Schiffer, I. B.*, et al.* (2005). Premature senescence is a primary fail-safe mechanism of ERBB2-driven tumorigenesis in breast carcinoma cells. Cancer Res *65*, 840-849.

Tsvetkov, L. M., Yeh, K. H., Lee, S. J., Sun, H., and Zhang, H. (1999). p27(Kip1) ubiquitination and degradation is regulated by the SCF(Skp2) complex through phosphorylated Thr187 in p27. Curr Biol *9*, 661-664.

Ueda, S., Basaki, Y., Yoshie, M., Ogawa, K., Sakisaka, S., Kuwano, M., and Ono, M. (2006). PTEN/Akt signaling through epidermal growth factor receptor is prerequisite for angiogenesis by hepatocellular carcinoma cells that is susceptible to inhibition by gefitinib. Cancer Res *66*, 5346-5353.

Uttamsingh, S., Bao, X., Nguyen, K. T., Bhanot, M., Gong, J., Chan, J. L., Liu, F., Chu, T. T., and Wang, L. H. (2008). Synergistic effect between EGF and TGF-beta1 in inducing oncogenic properties of intestinal epithelial cells. Oncogene *27*, 2626-2634.

Valladares, A., Alvarez, A. M., Ventura, J. J., Roncero, C., Benito, M., and Porras, A. (2000). p38 mitogen-activated protein kinase mediates tumor necrosis factor-alpha-induced apoptosis in rat fetal brown adipocytes. Endocrinology *141*, 4383-4395.

Ventura, J. J., Tenbaum, S., Perdiguero, E., Huth, M., Guerra, C., Barbacid, M., Pasparakis, M., and Nebreda, A. R. (2007). p38alpha MAP kinase is essential in lung stem and progenitor cell proliferation and differentiation. Nat Genet *39*, 750-758.

Vergarajauregui, S., San Miguel, A., and Puertollano, R. (2006). Activation of p38 mitogen-activated protein kinase promotes epidermal growth factor receptor internalization. Traffic *7*, 686-698.

Vieira, A. V., Lamaze, C., and Schmid, S. L. (1996). Control of EGF receptor signaling by clathrin-mediated endocytosis. Science *274*, 2086-2089.

Vizirianakis, I. S., Chen, Y. Q., Kantak, S. S., Tsiftsoglou, A. S., and Kramer, R. H. (2002). Dominant-negative E-cadherin alters adhesion and reverses contact inhibition of growth in breast carcinoma cells. Int J Oncol *21*, 135-144.

Wang, W., Chen, J. X., Liao, R., Deng, Q., Zhou, J. J., Huang, S., and Sun, P. (2002). Sequential activation of the MEK-extracellular signal-regulated kinase and MKK3/6-p38 mitogen-activated protein kinase pathways mediates oncogenic ras-induced premature senescence. Molecular and cellular biology *22*, 3389-3403.

Wang, Y., Du, D., Fang, L., Yang, G., Zhang, C., Zeng, R., Ullrich, A., Lottspeich, F., and Chen, Z. (2006). Tyrosine phosphorylated Par3 regulates epithelial tight junction assembly promoted by EGFR signaling. Embo J *25*, 5058-5070.

Wang, Y., Huang, S., Sah, V. P., Ross, J., Jr., Brown, J. H., Han, J., and Chien, K. R. (1998). Cardiac muscle cell hypertrophy and apoptosis induced by distinct members of the p38 mitogen-activated protein kinase family. J Biol Chem *273*, 2161-2168.

Warren, R. A., Green, F. A., Stenberg, P. E., and Enns, C. A. (1998). Distinct saturable pathways for the endocytosis of different tyrosine motifs. J Biol Chem *273*, 17056-17063.

Waskiewicz, A. J., Johnson, J. C., Penn, B., Mahalingam, M., Kimball, S. R., and Cooper, J. A. (1999). Phosphorylation of the cap-binding protein eukaryotic translation initiation factor 4E by protein kinase Mnk1 in vivo. Molecular and cellular biology *19*, 1871-1880.

Weber, J. D., Raben, D. M., Phillips, P. J., and Baldassare, J. J. (1997). Sustained activation of extracellular-signal-regulated kinase 1 (ERK1) is required for the continued expression of cyclin D1 in G1 phase. Biochem J *326 (Pt 1)*, 61-68.

Weinberg, R. A. (1995). The retinoblastoma protein and cell cycle control. Cell *81*, 323-330.

Wells, A., Welsh, J. B., Lazar, C. S., Wiley, H. S., Gill, G. N., and Rosenfeld, M. G. (1990). Ligand-induced transformation by a noninternalizing epidermal growth factor receptor. Science *247*, 962-964.

Werb, Z., and Chin, J. R. (1998). Extracellular matrix remodeling during morphogenesis. Ann N Y Acad Sci *857*, 110-118.

Wieser, R. J., Faust, D., Dietrich, C., and Oesch, F. (1999). p16INK4 mediates contact-inhibition of growth. Oncogene *18*, 277-281.

Winograd-Katz, S. E., and Levitzki, A. (2006). Cisplatin induces PKB/Akt activation and p38(MAPK) phosphorylation of the EGF receptor. Oncogene *25*, 7381-7390.

Wolthuis, R. M., Zwartkruis, F., Moen, T. C., and Bos, J. L. (1998). Ras-dependent activation of the small GTPase Ral. Curr Biol *8*, 471-474.

Wong, E. S., Fong, C. W., Lim, J., Yusoff, P., Low, B. C., Langdon, W. Y., and Guy, G. R. (2002). Sprouty2 attenuates epidermal growth factor receptor ubiquitylation and endocytosis, and consequently enhances Ras/ERK signalling. Embo J *21*, 4796-4808.

Wong, E. S., Lim, J., Low, B. C., Chen, Q., and Guy, G. R. (2001). Evidence for direct interaction between Sprouty and Cbl. J Biol Chem *276*, 5866-5875.

Woo, R. A., and Poon, R. Y. (2004). Activated oncogenes promote and cooperate with chromosomal instability for neoplastic transformation. Genes Dev *18*, 1317-1330.

Wu, Z., Woodring, P. J., Bhakta, K. S., Tamura, K., Wen, F., Feramisco, J. R., Karin, M., Wang, J. Y., and Puri, P. L. (2000). p38 and extracellular signal-regulated kinases regulate the myogenic program at multiple steps. Molecular and cellular biology *20*, 3951-3964.

Yanagisawa, K., Kosaka, A., Iwahana, H., Nakanishi, M., and Tominaga, S. (1999). Opposite regulation of the expression of cyclin-dependent kinase inhibitors during contact inhibition. J Biochem *125*, 36-40.

Yang, X. H., Kovalenko, O. V., Kolesnikova, T. V., Andzelm, M. M., Rubinstein, E., Strominger, J. L., and Hemler, M. E. (2006). Contrasting effects of EWI proteins, integrins, and protein palmitoylation on cell surface CD9 organization. J Biol Chem *281*, 12976-12985.

Yang, Y., Goldstein, B. G., Nakagawa, H., and Katz, J. P. (2007). Kruppel-like factor 5 activates MEK/ERK signaling via EGFR in primary squamous epithelial cells. Faseb J *21*, 543-550.

Yarden, Y., and Ullrich, A. (1988). Growth factor receptor tyrosine kinases. Annu Rev Biochem *57*, 443-478.

Yee, A. S., Paulson, E. K., McDevitt, M. A., Rieger-Christ, K., Summerhayes, I., Berasi, S. P., Kim, J., Huang, C. Y., and Zhang, X. (2004). The HBP1 transcriptional repressor and the p38 MAP kinase: unlikely partners in G1 regulation and tumor suppression. Gene *336*, 1-13.

Yu, W., Imoto, I., Inoue, J., Onda, M., Emi, M., and Inazawa, J. (2007). A novel amplification target, DUSP26, promotes anaplastic thyroid cancer cell growth by inhibiting p38 MAPK activity. Oncogene *26*, 1178-1187.

Zandi, R., Larsen, A. B., Andersen, P., Stockhausen, M. T., and Poulsen, H. S. (2007). Mechanisms for oncogenic activation of the epidermal growth factor receptor. Cell Signal *19*, 2013-2023.

Zeng, Q., and Hong, W. (2008). The emerging role of the hippo pathway in cell contact inhibition, organ size control, and cancer development in mammals. Cancer Cell *13*, 188-192.

Zetser, A., Gredinger, E., and Bengal, E. (1999). p38 mitogen-activated protein kinase pathway promotes skeletal muscle differentiation. Participation of the Mef2c transcription factor. J Biol Chem *274*, 5193-5200.

Zhang, J., Kalyankrishna, S., Wislez, M., Thilaganathan, N., Saigal, B., Wei, W., Ma, L., Wistuba, II, Johnson, F. M., and Kurie, J. M. (2007). SRC-family kinases are activated in non-small cell lung cancer and promote the survival of epidermal growth factor receptor-dependent cell lines. Am J Pathol *170*, 366-376.

Zhang, X., Ma, L., Enkemann, S. A., and Pledger, W. J. (2003). Role of Gadd45alpha in the density-dependent G1 arrest induced by p27(Kip1). Oncogene *22*, 4166-4174.

Zhao, B., Wei, X., Li, W., Udan, R. S., Yang, Q., Kim, J., Xie, J., Ikenoue, T., Yu, J., Li, L.*, et al.* (2007). Inactivation of YAP oncoprotein by the Hippo pathway is involved in cell contact inhibition and tissue growth control. Genes Dev *21*, 2747-2761.

Zhao, M., New, L., Kravchenko, V. V., Kato, Y., Gram, H., di Padova, F., Olson, E. N., Ulevitch, R. J., and Han, J. (1999). Regulation of the MEF2 family of transcription factors by p38. Molecular and cellular biology *19*, 21-30.

Zheng, N., Wang, P., Jeffrey, P. D., and Pavletich, N. P. (2000). Structure of a c-Cbl-UbcH7 complex: RING domain function in ubiquitin-protein ligases. Cell *102*, 533-539.

Zhou, B. B., and Elledge, S. J. (2000). The DNA damage response: putting checkpoints in perspective. Nature *408*, 433-439.

Zhou, S. G., Wang, P., Pi, R. B., Gao, J., Fu, J. J., Fang, J., Qin, J., Zhang, H. J., Li, R. F., Chen, S. R.*, et al.* (2008). Reduced expression of GSTM2 and increased oxidative stress in spontaneously hypertensive rat. Mol Cell Biochem *309*, 99-107.

Zoidl, G., Blass-Kampmann, S., D'Urso, D., Schmalenbach, C., and Muller, H. W. (1995). Retroviral-mediated gene transfer of the peripheral myelin protein PMP22 in Schwann cells: modulation of cell growth. Embo J *14*, 1122-1128.

Zwang, Y., and Yarden, Y. (2006). p38 MAP kinase mediates stress-induced internalization of EGFR: implications for cancer chemotherapy. Embo J *25*, 4195-4206.

Appendix 1: Tables and Figures

Appendix Table 1. Semiquantitative RT-PCR primers used for microarray gene expression validation

Gene symbol	Genbank Acc. No.	Forward (5'-3')	Reverse (5'-3')
Aig1	NM_025446	GCTCCATCCTGTGCAACTAC	TTTAGTACTTCTCCAAGCAGG
Loxl1	NM_010729	GCCTTGACCGTCGTTACTCG	GCTTCGCACGGGCAAGTAAG
Mmp3	NM_010809	TACTGAAGGTGGTACAGAGC	GCATAGGCATGAGCCAAGAC
Nr4a1	NM_010444	ATCCTCCAGCGGCTCTGAG	TTTAGATCGGTATGCCAGGC
Ctsh	NM_007801	AGATTCAAGCCCACAACCAG	ATGATGTCACGTGGGTGGG
Egln3	NM_028133	TCAGACACTCTCTTTGCCAG	CGAGGGTGGCTAACTTTCG
Plcg2	NM_172285	CCACTACTGTGCCATTGCTG	TCCATAGTAGACCGGATCCG
Ramp3	NM_019511	CTGCAACGAGACAGGGATGC	GAACCGCGATCAGTGGGATG
Pde8a	NM_008803	CAAATTCATGACTTGTGTGTGC	GAGGCAGGCTTTTAGAAATTC
Sardh	NM_138665	GCTCCTCTGGCATGTATGC	TGATATGGATCCAATCGGGG
Rab3b	NM_023537	TGGGTTTGACTTCTTTGAAGC	AATGGAGAGAAGCGGAGGAG
Ralgds	NM_009058	AATGCCATCTCCTCCATCCTG	ATGTCACCACTTGGCTGGGC
Cd9	NM_007657	CTGCTCTTCGGATTTAACTTC	TCTTCAATATAACTTACAACCTG
Pmp22	NM_008885	TTTAGCAGAAGTATCCACTGC	CATCTTAGTCCACACAGTTGG
Dpep	NM_007876	AGACATCCTACAGGCTTTCC	AGACATCCTACAGGCTTTCC
Ctsl	NM_009984	AACGCCTTCGGTGACATGAC	TCCAGACTCAGAATTAAGCAC
Nck2	NM_010879	GGCACTGCACTGAGCAATG	GGACACAGCTCTCGGAGTG
Gstm2	NM_008183	CACCAGCACTATGCTTATGAC	ACTTTATTGAGAACCAAATGGG
Brca2	NM_009765	ACTCCTGGGCTTCTGCCAC	GCCCTTGTGTGTGGCTGAG
Rtn4	NM_024226	TATTGCCAGAGGACACCTGC	GCCCCAACTGATCAAACAAAC
Krt1-19	NM_008471	CAGATTGACAATGCTCGCCTG	TCGACACCGGGAGTGGAATC
Tnfrsf23	NM_024290	TTCAGCCACGTCTCCAGTC	TGAAAGAGTTGCCTCCATGG
Cxcl1	NM_008176	GGATTCACCTCAAGAACATCC	AAATAAAAACCACACACTTTGTG
Foxd1	NM_008242	GAAGTTCCCCGCCTTGGCAG	CTCTCGATGGAGAAGGGCG
Arhgdib	NM_007486	CCAACAGTTCCCAACGTGAC	ACTCTGAGATGGGGTAAG
Dock8	NM_028785	GAGACGGTTAATGAAGTCTAC	CTCTTCTGACTGTCAACTCTG
Snf1lk	NM_010831	GCTAGCAGATTTTGGATTTGG	GCAGAGGAGGAGACAATTATG

Appendix Table 2. 202 differentially regulated genes between H-Ras^{V12}-expressing p38α-/- and WT MEFs

NCBI RefSeq	Gene symbol	p38α-/- [1]	WT [1]	Fold Change*	Description
NM_025446	*Aig1*	5.5090	0.0118	+466.9	androgen-induced 1
NM_008218	*Hba-a1*	293.300	0.983	+298.4	hemoglobin alpha, adult chain 1
AK013904	*Slc14a1*	253.4000	0.9690	+261.5	solute carrier family 14, member 1
NM_013473	*Anxa8*	5.543	0.027	+202.3	annexin A8
NM_008471	*Krt1-19*	1.174	0.011	+106.7	keratin complex 1, acidic, gene 19
NM_146178	*Ccdc106*	1.0400	0.0101	+103.0	coiled-coil domain containing 106
NM_023537	*Rab3b*	0.9630	0.0101	+95.3	RAB3B, member RAS oncogene family
M55181	*Penk1*	1.0960	0.0124	+88.4	preproenkephalin 1
U79144	*Loxl1*	0.951	0.012	+78.0	lysyl oxidase-like 1
NM_019511	*Ramp3*	4.659	0.067	+69.3	receptor (calcitonin) activity modifying protein 3
NM_146028	*Stac2*	7.5930	0.1110	+68.4	SH3 and cysteine-rich domain-containing 2
BM506663	*Lrrc32*	0.9620	0.0160	+60.1	Leucine-rich repeat-containing 32
NM_009846	*Cd24a*	0.9340	0.0169	+55.3	CD24a antigen
AK008273	*Arhgdib*	1.3760	0.0272	+50.6	Rho, GDP dissociation inhibitor (GDI) beta
NM_021273	*Ckb*	1.4600	0.0462	+31.6	creatine kinase, brain
NM_010809	*Mmp3*	12.490	0.532	+23.5	matrix metalloproteinase 3
NM_009922	*Cnn1*	0.9840	0.0422	+23.3	calponin 1
NM_029466	*Arl5b*	20.2000	0.8850	+22.8	ADP-ribosylation factor-like 5B
NM_009430	*Prss2*	22.7600	1.0080	+22.6	protease, serine, 2 (trypsin 2)
NM_009285	*Stc1*	8.3730	0.4130	+20.3	stanniocalcin 1
NM_009964	*Cryab*	4.3470	0.2150	+20.2	crystallin, alpha B
NM_025359	*Tspan13*	10.4900	0.5320	+19.7	tetraspanin 13
BC011290	*Tceal1*	0.965	0.049	+19.6	transcription elongation factor A (SII)-like 1
NM_025779	*Ccdc109b*	3.355	0.192	+17.5	coiled-coil domain containing 109B
NM_025543	*Mcts2*	1.6440	0.1000	+16.4	malignant T cell amplified sequence 2
NM_010738	*Sca1*	11.230	0.709	+15.8	lymphocyte antigen 6 complex, locus A
NM_172296	*Dmrta2*	1.1300	0.0739	+15.3	doublesex and mab-3 related transcription factor like family A2
AK002518	*Olfml3*	2.2380	0.1530	+14.6	olfactomedin-like 3
NM_024228	*Gdpd3*	5.0110	0.3590	+14.0	glycerophosphodiester phosphodiesterase domain-containing 3
AK018071	*Lrrc17*	0.9580	0.0687	+13.9	leucine rich repeat containing 17
NM_019978	*Dclk1*	0.9770	0.0706	+13.8	double cortin-like kinase 1
NM_013515	*Stom*	1.3320	0.1020	+13.1	stomatin
AF065162	*Kcnk3*	12.8800	1.0040	+12.8	potassium channel, subfamily K, member 3
NM_024406	*Fabp4*	0.999	0.079	+12.7	fatty acid binding protein 4, adipocyte
NM_173379	*Leprel1*	3.8310	0.3060	+12.5	leprecan-like 1
NM_013496	*Crabp1*	12.3500	1.0150	+12.2	cellular retinoic acid binding protein I
NM_010407	*Hck*	3.225	0.309	+10.4	hemopoietic cell kinase
NM_019949	*Ube2l6*	3.0700	0.3290	+9.3	ubiquitin-conjugating enzyme E2L 6
NM_133733	*9030425E11Rik*	3.771	0.430	+8.8	RIKEN cDNA 9030425E11 gene
NM_025564	*Magohb*	0.9710	0.1110	+8.7	mago-nashi homolog B
NM_008803	*Pde8a*	1.0140	0.1220	+8.3	phosphodiesterase 8A
NM_153782	*BC029169*	7.7410	0.9420	+8.2	cDNA sequence BC029169
NM_010444	*Nr4a1*	4.4920	0.5540	+8.1	nuclear receptor subfamily 4, group A, member 1
AK005141	*Pik3ip1*	1.0200	0.1270	+8.0	phosphoinositide-3-kinase interacting protein 1
NM_009058	*Ralgds*	2.2390	0.2930	+7.6	ral guanine nucleotide dissociation stimulator
AK004963	*Tax1bp3*	1.0640	0.1420	+7.5	human T-cell leukemia virus type I-interacting protein 3
NM_025768	*Grtp1*	7.3800	1.0010	+7.4	GH regulated TBC protein 1
NM_008047	*Fstl1*	0.9800	0.1340	+7.3	follistatin-like 1

NM_054049	*Osr2*	1.3210	0.1850	+7.1	odd-skipped related 2
NM_009704	*Areg*	7.0840	1.0010	+7.1	amphiregulin
BY754798	*Pax7*	3.1150	0.4430	+7.0	paired box gene 7
NM_008597	*Mgp*	1.0980	0.1580	+6.9	matrix gamma-carboxyglutamate (gla) protein
NM_016909	*Tsnax*	0.989	0.147	+6.7	translin-associated factor X
NM_009073	*Rom1*	4.9530	0.7450	+6.6	rod outer segment membrane protein 1
NM_024495	*Car13*	1.5560	0.2600	+6.0	carbonic anhydrase 13
NM_133217	*Bco2*	3.6240	0.6230	+5.8	beta-carotene 9', 10'-dioxygenase 2
AK020110	*Lbh*	1.6010	0.2820	+5.7	limb-bud and heart
NM_018764	*Pcdh7*	3.8970	0.6920	+5.6	protocadherin 7
NM_013560	*Hspb1*	3.1190	0.5680	+5.5	heat shock protein 1
NM_153565	*Pcsk9*	5.2640	0.9640	+5.5	proprotein convertase subtilisin/kexin type 9
NM_007657	*Cd9*	2.0450	0.3920	+5.2	CD9 antigen
NM_133943	*Hsd3b7*	5.0110	0.9760	+5.1	hydroxy-delta-5-steroid dehydrogenase, 3 beta- and steroid delta-isomerase 7
NM_010930	*Nov*	2.5370	0.4980	+5.1	nephroblastoma overexpressed gene
NM_019738	*Nupr1*	3.8660	0.7690	+5.0	nuclear protein 1
NM_011891	*Sgcd*	2.2840	0.4630	+4.9	sarcoglycan, delta (dystrophin-associated glycoprotein)
NM_022993	*Lrp10*	1.3410	0.2830	+4.7	low-density lipoprotein receptor-related protein 10
S67386	*Sdpr*	1.1240	0.2410	+4.7	serum deprivation response
AK007494	*1810014F10Rik*	1.2370	0.2630	+4.7	RIKEN cDNA 1810014F10 gene
NM_024290	*Tnfrsf23*	2.1750	0.4690	+4.6	tumor necrosis factor receptor superfamily, member 23
NM_008885	*Pmp22*	0.9650	0.2090	+4.6	peripheral myelin protein
NM_007876	*Dpep1*	2.6330	0.5880	+4.5	dipeptidase 1 (renal)
NM_009413	*Tpd52l1*	0.9700	0.2180	+4.4	tumor protein D52-like 1
NM_009853	*Cd68*	4.3580	0.9970	+4.4	CD68 antigen
NM_021454	*Cdc42ep5*	1.4750	0.3450	+4.3	CDC42 effector protein (Rho GTPase binding) 5
NM_007609	*Casp4*	3.5900	0.8670	+4.1	caspase 4, apoptosis-related cysteine protease
NM_020520	*Slc25a20*	1.4590	0.3530	+4.1	solute carrier family 25, member 20
NM_011127	*Prrx1*	1.5330	0.3720	+4.1	paired related homeobox 1
NM_013654	*Ccl7*	1.1420	0.2780	+4.1	chemokine (C-C motif) ligand 7
AK017185	*Rab30*	0.9750	0.2430	+4.0	RAB30, member RAS oncogene family
NM_007970	*Ezh1*	4.0250	1.0370	+3.9	enhancer of zeste homolog 1
NM_013935	*Ptpla*	2.4370	0.6330	+3.8	protein tyrosine phosphatase-like (proline instead of catalytic arginine), member a
NM_009769	*Klf5*	3.5500	0.9230	+3.8	Kruppel-like factor 5
AK016764	*4933411B09Rik*	3.5390	0.9750	+3.6	RIKEN cDNA 4933411B09 gene
AK003046	*Nrn1*	2.0320	0.5800	+3.5	neuritin 1
NM_138315	*Mical1*	0.9800	0.2870	+3.4	microtubule associated monoxygenase, calponin and LIM domain containing 1
NM_030260	*Zxdc*	2.9360	0.9500	+3.1	ZXD family zinc finger C
NM_025445	*Arfgap3*	1.6510	0.5300	+3.1	ADP-ribosylation factor GTPase activating protein 3
NM_011315	*Saa3*	1.0040	0.3250	+3.1	serum amyloid A 3
NM_028943	*Sgms2*	3.2030	1.0440	+3.1	Sphingomyelin synthase 2
NM_007933	*Eno3*	3.1740	1.0420	+3.0	enolase 3, beta muscle
NM_153136	*Nudt18*	1.0680	0.3620	+3.0	nudix-type motif 18
NM_010216	*Figf*	1.0410	0.3570	+2.9	c-fos induced growth factor
NM_010847	*Mxi1*	1.3390	0.4570	+2.9	Max interacting protein 1
AK014166	*Tm7sf2*	1.5980	0.5520	+2.9	transmembrane 7 superfamily member 2
NM_009674	*Anxa7*	2.5310	0.8810	+2.9	annexin A7
NM_009907	*Cln3*	1.7540	0.6310	+2.8	ceroid lipofuscinosis, neuronal 3, juvenile (Batten, Spielmeyer-Vogt disease)
NM_029510	*Bcor*	1.0550	0.3830	+2.8	BCL6 interacting corepressor
NM_025408	*Phca*	1.0280	0.3780	+2.7	phytoceramidase, alkaline
NM_133684	*Mosc2*	1.0360	0.3810	+2.7	MOCO sulphurase C-terminal domain

					containing 2
NM_010212	*Fhl2*	1.0450	0.3830	+2.7	four and a half LIM domains 2
NM_010145	*Ephx1*	1.0610	0.4100	+2.6	epoxide hydrolase 1, microsomal
NM_013471	*Anxa4*	1.6690	0.6740	+2.5	annexin A4
NM_009984	*Ctsl*	2.4780	1.0010	+2.5	cathepsin L
BC017532	*Abhd4*	1.9850	0.7990	+2.5	abhydrolase domain containing 4
NM_021550	*C1galt1c1*	2.2530	0.9310	+2.4	C1GALT1-specific chaperone 1
NM_010879	*Nck2*	2.0980	0.8870	+2.4	non-catalytic region of tyrosine kinase adaptor protein 2
BC010331	*Rnh1*	2.1260	0.8860	+2.4	ribonuclease/angiogenin inhibitor 1
NM_023626	*Ing3*	1.9990	0.8690	+2.3	inhibitor of growth family, member 3
AK018321	*Fbxo28*	2.1840	0.9670	+2.3	F-box protein 28
NM_024226	*Rtn4*	1.3640	0.6130	+2.2	reticulon 4
AK003390	*Ppap2b*	1.0460	0.4830	+2.2	phosphatidic acid phosphatase type 2B
NM_009730	*Atrn*	1.6510	0.7640	+2.2	attractin
NM_010959	*Oit3*	2.2170	0.9880	+2.2	oncoprotein induced transcript 3
NM_028344	*Mpp10*	1.2500	0.5770	+2.2	M-phase phosphoprotein 10
NM_008133	*Glud1*	1.1970	0.5700	+2.1	glutamate dehydrogenase
AK010201	*Ypel5*	1.8100	0.8760	+2.1	yippee-like 5
X55499	*Cebpg*	1.4380	0.6830	+2.1	CCAAT/enhancer binding protein (C/EBP), gamma
AK004097	*Fam115a*	1.0670	0.5190	+2.1	family with sequence similarity 115, member A
NM_007945	*Eps8*	2.0850	1.0250	+2.0	epidermal growth factor receptor pathway substrate 8
NM_031256	*Plekha3*	1.4230	0.7000	+2.0	pleckstrin homology domain-containing, family A (phosphoinositide binding specific) member 3
BC005558	*Ppap2b*	1.0590	0.5290	+2.0	phosphatidic acid phosphatase type 2B
NM_016883	*Psmd10*	1.8110	0.9190	+2.0	proteasome (prosome, macropain) 26S subunit, non-ATPase, 10
AK005167	*Clip3*	1.0100	0.4930	+2.0	CAP-GLY domain containing linker protein 3
NM_010685	*Lamp2*	1.0150	0.4960	+2.0	lysosomal membrane glycoprotein 2
NM_027719		1.0800	0.5270	+2.0	RIKEN cDNA 4933436E20 gene
NM_018793	*Tyk2*	1.8040	0.9080	+2.0	tyrosine kinase 2
NM_030250	*Nus1*	1.3590	0.7210	+1.9	nuclear undecaprenyl pyrophosphate synthase 1 homolog
NM_026787	*1110012L19Rik*	1.0260	0.5280	+1.9	RIKEN cDNA 1110012L19 gene
NM_023063	*Lima1*	1.0080	0.5310	+1.9	LIM domain and actin binding 1
AI047357	*Dleu2*	0.9980	0.5300	+1.9	deleted in lymphocytic leukemia 2
NM_011824	*Grem1*	1.8770	1.0080	+1.9	gremlin 1
NM_026169	*Frmd8*	1.7490	0.9590	+1.8	FERM domain containing 8
NM_029101	*Rrp7a*	1.6610	1.0040	+1.7	ribosomal RNA processing 7 homolog A
NM_053181	*Pdxdc1*	0.9960	0.5870	+1.7	pyridoxal-dependent decarboxylase domain containing 1
NM_011101	*Prkca*	1.0160	0.6510	+1.6	protein kinase C, alpha
NM_009510	*Ezr*	1.5320	0.9980	+1.5	ezrin
NM_018768	*Stx8*	1.0300	0.6650	+1.5	syntaxin 8
AK005174	*Arfrp1*	0.8340	1.2230	-1.5	ADP-ribosylation factor related protein 1
NM_025464	*Tmem218*	0.844	1.291	-1.5	transmembrane protein 218
U70139	*Ccrn4l*	0.8510	1.3890	-1.6	CCR4 carbon catabolite repression 4-like
BC031201	*Rtel1*	0.7340	1.2460	-1.7	regulator of telomere elongation helicase 1
AK018051	*Dock8*	1.0080	1.7210	-1.7	dedicator of cytokinesis 8
AK011476	*Mrps30*	1.0180	1.7810	-1.7	mitochondrial ribosomal protein S30
NM_030704	*Hspb8*	0.9160	1.6220	-1.8	heat shock 27kDa protein 8
AK017491	*Mipep*	1.0090	1.7890	-1.8	mitochondrial intermediate peptidase
NM_145398	*Casd1*	0.9070	1.6690	-1.8	CAS1 domain containing 1
NM_172683	*Pogz*	0.7810	1.4120	-1.8	pogo transposable element with ZNF domain
NM_139309	*Fktn*	0.9830	1.8660	-1.9	fukutin
AK010337	*Cxxc1*	1.0160	2.0910	-2.1	CXXC finger 1 (PHD domain)

NM_015768	*Prok2*	0.8010	1.6510	-2.1	prokineticin 2
BE947970		0.8500	1.9010	-2.2	mouse EST
NM_033175	*Lce3c*	0.9200	2.2360	-2.4	late cornified envelope 3
NM_010492	*Ica1*	0.9950	2.6220	-2.6	islet cell autoantigen 1
NM_012059	*Sh3d19*	0.4080	1.0740	-2.6	SH3 domain protein D19
NM_025471	*1810030N24Rik*	0.5900	1.6290	-2.8	RIKEN cDNA 1810030N24 gene
AK013543	*Ppm1a*	0.6960	1.9590	-2.8	protein phosphatase 1A, magnesium dependent, alpha isoform
NM_025620	*2210417D09Rik*	0.6500	1.9390	-3.0	RIKEN cDNA 2210417D09 gene
NM_008572	*Mcpt8*	0.9790	2.9310	-3.0	mast cell protease 8
NM_008183	*Gstm2*	1.0120	3.0410	-3.0	glutathione S-transferase, mu 2
AK004078	*Hddc3*	0.4060	1.2260	-3.0	HD domain containing 3
NM_025748	*Adat2*	0.8680	2.6880	-3.1	adenosin deaminase, tRNA-specific 2
BC009089	*Arl16*	0.9930	3.1320	-3.2	ADP-rybosilation factor-like 16
BG066910	*Klf7*	0.3360	1.0860	-3.2	Kruppel-like factor 7
NM_021540	*Rnf130*	0.3110	1.0080	-3.2	ring finger protein 130
NM_009701	*Aqp5*	1.0580	3.4750	-3.3	aquaporin 5
NM_145981	*Phyhip*	0.8880	3.0190	-3.4	phytanoyl-CoA hydroxylase interacting protein
NM_009765	*Brca2*	0.6450	2.2590	-3.5	breast cancer 2
AK011560	*Hist1h4i*	0.9390	3.4960	-3.7	histone cluster 1, H4i
NM_024223	*Crip2*	0.9650	3.6050	-3.7	cysteine rich protein 2
NM_023056	*Tmem176b*	0.7420	2.9480	-4.0	transmembrane protein 176B
BB425178	*Large*	0.9930	4.0850	-4.1	like-glycosyltransferase
BE630089	*Rab11b*	1.0040	4.2480	-4.2	RAB11B, member RAS oncogene family
BE981880	*Tmed8*	0.9190	4.1530	-4.5	transmembrane emp24 domain containing 8
NM_009421	*Traf1*	1.0240	4.7250	-4.6	Tnf receptor-associated factor 1
BB313974	*Pcdh10*	0.6640	3.1030	-4.7	protocadherin 10
NM_008452	*Klf2*	0.2020	0.9640	-4.8	Kruppel-like factor 2 (lung)
NM_138665	*Sardh*	0.3610	1.7760	-4.9	sarcosine dehydrogenase
AK017566	*Zdhhc2*	0.209	1.046	-5.0	zinc finger, DHHC domain containing 2
NM_028785	*Dock8*	1.0520	5.4420	-5.2	dedicator of cytokinesis 8
BQ551484	*Atad2*	0.9890	5.1150	-5.2	ATPase family, AAA domain containing 2
BC023877	*Plcg2*	0.389	2.079	-5.3	phospholipase C, gamma 2
NM_023476	*Tinagl*	0.9630	5.1100	-5.3	tubulointerstitial nephritis antigen-like 1
NM_028133	*Egln3*	0.8850	5.5590	-6.3	EGL nine homolog 3
BB559411	*Cyfip1*	0.9370	5.9300	-6.3	cytoplasmic FMR1 interacting protein 1
NM_025331	*Gng11*	0.1480	0.9740	-6.6	guanine nucleotide binding protein (G protein), gamma 11
NM_013886	*Hdgfrp3*	0.1940	1.3570	-7.0	hepatoma-derived growth factor, related protein 3
NM_146015	*Efemp1*	0.9820	6.8940	-7.0	epidermal growth factor-containing fibulin-like extracellular matrix protein 1
BC018517	*Prss23*	0.140	1.004	-7.2	protease, serine 23
NM_010453	*Hoxa5*	1.0120	7.9940	-7.9	homeo box A5
AK010356	*Def6*	0.6430	5.4800	-8.5	differentially expressed in FDCP 6
NM_010831	*Snf1lk*	0.8140	8.4270	-10.4	SNF1-like kinase
BC010495	*Tmlhe*	0.081	1.102	-13.6	trimethyllysine hydroxylase, epsilon
BC014695	*Lzts2*	0.965	18.470	-19.1	leucine zipper, putative tumor suppressor 2
NM_007801	*Ctsh*	0.221	5.099	-23.1	cathepsin H
NM_008176	*Cxcl1*	0.0462	1.0810	-23.4	chemokine (C-X-C motif) ligand 1
NM_008242	*Foxd1*	0.0299	1.1490	-38.4	forkhead box D1

1, normalized expression in exponentially proliferating cells constitutively expressing H-Ras^{V12}; *, fold change (log_2 ratio) in H-Ras^{V12}-p38α-/- *versus* H-Ras^{V12}-WT MEFs.

Appendix Table 3. Functional clustering of the 202 differentially expressed genes between H-Ras^{V12}-p38α-/- and H-Ras^{V12}-WT MEFs

Functional categories[1] (%)[**]	Subcategory / Gene symbol
signal transduction (20%)	**Small GTPase/tyrosine kinase signaling:** *Areg, Hck, Tyk2, Cd9, Klf5, Eps8, Prkca, Arfgap3, Nck2, Ctsl, Cdc42ep5, Anxa8, Lamp2, Mmp3, Hoxa5, Traf1, Aqp5, Plcg2, Cxcl1, Ralgds, Pik3ip1, Arhgdib, Cdc42ep5, Rab3b, Rab30, Rab11b* **Apoptosis**: *Traf1, Tnfrsf23* **DNA damage:** *Brca2* **Other:** *Ramp3, Sca1, Stc1, Dclk1, Stom, Kcnk3, Fabp4, Pde8a, Tax1bp3, Nupr1, Nov, Ptpla, Nrn1, Sgms2, Grem1, Stx8, Ica1, Dock8, Ppm1a, Zdhhc2, Gng11, Def6, Arl5B, Arl16, Arfrp1*
extracellular matrix remodeling / secreted proteins (14%)	**Proteases:** *Mmp3, Mcpt8, Stc1, Dpep1, Ctsl, Ctsh, Prss23, Prss2* **Chemokines/cytokines:** *Cxcl1, Ccl7* **Mitogenic factors:** *Areg, Figf, Fstl1* **Other:** *Aig1, Penk1, Tspan13, Ramp3, Olfml3, Grtp1, Pcsk9, Mgp, Saa3, Mosc2, Rtn4, Ppap2b, Ephx1, Grem1, Nov, Prok2, Rnf130, Tinagl1, Efemp1, Anxa7, Anxa8, Tmem218*
cell viability (11%)	**Apoptosis/survival:** *Brca2, Traf1, Tnfrsf23, Casp4, Egln3, Bcor, Nr4a1, Phca, Rtn4, Ralgds* **Proliferation:** *Pmp22, Lzts2, Nck2, Cd24a, Sca1, Nov, Hdgfrp3, Cxcl1* **Differentiation:** *Snf1lk, Anxa7, Egln3* **Other:** *Lrrc32, Tspan13, Tmem176b, Nupr1, Osr2, Mgp, Rtel1, Prkca, Crip2, Cyfip1*
transcription (11%)	**Transcription factors:** *Klf2, Klf5, Klf7, Hoxa5, Foxd1* **Chromatin topology:** *Prrx1, Ezh1, Snf1lk, Hist1h4i* **Receptors:** *Nr4a1, Atad2* **Other:** *Tceal1, Mcts2, Fabp4, Dmrta2, Tsnax, Tax1bp3, Pax7, Lbh, Zxdc, Mxi1, Bcor, Cebpg, Fhl2, Ing3, Pogz, Cxxc1*
metabolism / redox balance (10%)	**Inorganic metabolism:** *Bco2, Car13, Hsd3b7* **Protein metabolism:** *Eno3, Tmlhe , Glud1, Sardh* **Oxygen sensors:** *Gstm2, Egln3* **Other:** *Hba-a1, Ckb, 1810014F10Rik, Pcsk9, Tm7sf2, Leprel1, Gdpd3, Mosc2, Cln3, Nus1, Pdxdc1, Ccrn4l, Fktn, Adat2, Casd1, Large*
cytoskeleton / adhesion / migration (8%)	**Tetraspanins:** *Tspan13, Cd9* **Proto-/cadherins:** *Pcdh7, Pcdh10* **Actin-binding:** *Lima1, Ezr, Anxa8* **Other:** *Krt1-19, Cd24a, 9030425E11Rik, Ica1, Rom1, Sgcd, Nck2, Atrn, Rtn4, Frmd8, Cyfip1, Mical1, Eps8*
protein or RNA turn-over	**Ubiquitin/proteasome system:** *Fbxo28, Psmd10, Ube2l6* **Proteases:** *Prss2, Prss23, Dpep1, Mipep, Ctsl, Ctsh*

(7%)	**Chaperones:** *Hspb1, Hspb8* **Other:** *Abhd4, Rrp7a, Mrps30, Cryab , Eps8, Rnf130, Zdhhc2, Tinagl1*
transport of proteins or solutes (5%)	**Endosmal/exosomal transport:** *Rab3b, Rab30, Rab11b, Lamp2* **Inorganic solute transport:** *Slc14a1, Slc25a20, Anxa4* **Other:** *Stc1, Kcnk3, Cln3, Aqp5, Tmed8*
lipid homeostasis (4%)	*Fabp4, Abhd4, Crabp1, Sgms2, Ppap2b, Lrp10, Tpd52l1, Plekha3, Stx8*
unknown (10%)	*Ccdc106, Stac2, Ccdc109b, Lrrc17, Magohb, BC029169, Sdpr, Cd68, 4933411B09Rik, Mical1, Nudt18, C1galt1c1, Rnh1, Oit3, Mpp10, Ypel5, Fam115a, Clip3, Casd1, Lce3c, 1110012L19Rik, Dleu2, Sh3d19, 1810030N24Rik, 2210417D09Rik, Hddc3, Phyhip*

1, according to annotations filed in Gene Ontology, FatiGO, Source Batch and PubMed; **, percentage relative to the total added number of genes within all categories (genes can appear in more than one category)

Appendix Table 4. Genes selected for semiquantitative RT-PCR validation

Fold change (p38α$^{-/-}$ /WT)*	Genebank Acc. No.	Gene symbol	Gene description / function
+466.86	NM_025446	*Aig1*	Androgen induced-1, membrane
+106.70	NM_008471	*Krt1-19*	Keratin complex 1, acidic, gene 19 / formation of cytokeratin filaments
+95.35	NM_023537	*Rab3b*	RAB3B, member RAS oncogene family / exocytosis
+78.00	NM_010729	*Loxl1*	Lysyl oxidase-like 1 / elastic fiber homeostasis, metastasis
+69.30	NM_019511	*Ramp3*	Receptor (calcitonin) activity modifying protein 3 / trafficking of GPRC
+68.40	NM_146028	*Stac2*	SH3 and cysteine rich domain 2
+50.60	NM_007486	*Arhgdib*	Rho, GDP dissociation inhibitor (GDI) beta / regulation of Rho GTPase function
+23.50	NM_010809	*Mmp3*	Matrix metallopeptidase 3 / extracellular proteolysis, invasion, proliferation, metastasis
+8.30	NM_008803	*Pde8a*	Phosphodiesterase 8A / regulation of cyclic nucleotides
+8.11	NM_010444	*Nr4a1*	Nuclear receptor subfamily 4, group A, member 1 / survival, apoptosis
+7.60	NM_009058	*Ralgds*	Ral guanine nucleotide dissociation stimulator / Ras signaling
+6.60	NM_009073	*Rom1*	Rod outer segment membrane protein 1
+5.20	NM_007657	*Cd9*	CD9 antigen / adhesion, proliferation, motility
+4.64	NM_024290	*Tnfrsf23*	Tumor necrosis factor receptor superfamily, member 23 / putative decoy receptor in TNFR family
+4.60	NM_008885	*Pmp22*	Peripheral myelin protein 22 / proliferation, apoptosis
+4.50	NM_007876	*Dpep1*	Dipeptidase 1 (renal) / extracellular proteolysis
+2.50	NM_009984	*Ctsl*	Cathepsin L / extracellular proteolysis, metastasis
+2.40	NM_010879	*Nck2*	Non-catalytic region of tyrosine kinase adaptor protein 2 / actin cytoskeleton, migration
+2.20	NM_024226	*Rtn4*	Reticulon 4 / intracellular trafficking, apoptosis, migration
-3.00	NM_008183	*Gstm2*	Glutathione s-transferase, mu2 / oxidative stress, apoptosis
-3.50	NM_009765	*Brca2*	Breast cancer 2 / tumor suppressor, DNA damage
-4.60	NM_009421	*Traf1*	Tnf receptor-associated factor 1 / regulation of cell survival
-4.90	NM_138665	*Sardh*	Sarcosine dehydrogenase / metabolism
-5.20	NM_028785	*Dock8*	Dedicator of cytokinesis 8 / migration, growth, adhesion
-5.30	NM_172285	*Plcg2*	Phospholipase C, gamma 2 / calcium signaling
-6.28	NM_028133	*Egln3*	EGL nine homolog 3 (*C.elegans*) / negative regulator of HIF-1, apoptosis, angiogenesis
-10.40	NM_010831	*Snf1lk*	SNF-like kinase / metabolism
-19.10	**NM_001130525**	*Lzts2*	Leucine zipper / putative tumor suppressor, proliferation
-23.10	NM_007801	*Ctsh*	Cathepsin H / proteolysis, extracellular matrix degradation
-23.40	NM_008176	*Cxcl1*	Chemokine ligand 1 / inflammatory response, tumor progression, metastasis
-38.43	NM_008242	*Foxd1*	Forkhead box D1 / inflmatory responses, inhibition of NF-kB pathway

*, Selected differentially expressed genes ($p<0.01$) between H-Ras^{V12}-p38α-/- *versus* H-Ras^{V12}-WT MEFs listed according to decreasing fold change (log_2 ratio). Only genes with log_2 ratio >±1.5 are included.

Appendix Table 5. Quantitative RT-PCR analysis in samples from different biological systems

Gene symbol	Fold change*			Fold change**
	Microarray	**MEFs** (qRT-PCR)	**Nude mice** (qRT-PCR)	**Lung tissue** (qRT-PCR)
Aig1	+466.86	+490 ± 45	+53.0 ± 4.1	+5.82 ± 0.44
Rab3b	+95.35	+200 ± 10	+1.30 ± 0.12	+13.0 ± 1.2
Loxl1	+78.00	+320 ± 20	+23.6 ± 2.1	+50.0 ± 4.1
Mmp3	+23.50	+139 ± 11	+483 ± 40	+6.62 ± 0.52
Ralgds	+7.60	+14.9 ± 0.6	+4.72 ± 0.51	+2.91 ± 0.22
Cd9	+5.20	+7.32 ± 0.13	+2.80 ± 0.25	+3.21 ± 0.33
Tnfrsf23	+4.64	+1.70 ± 0.22	+1.80 ± 0.16	+1.73 ± 0.12
Nck2	+2.40	+2.00 ± 0.02	+1.22 ± 0.11	+2.54 ± 0.19
Rtn4	+2.20	+1.90 ± 0.01	+2.80 ± 0.19	+1.44 ± 0.11
Gstm2	-3.00	-15.0 ± 1.3	-2.82 ± 0.15	-5.05 ± 0.41
Egln3	-6.28	-31.6 ± 2.2	-17.90 ± 1.72	-5.60 ± 0.51

*, fold change in H-Ras^{V12}-p38α-/- MEFs or MEF-derived subcutaneous tumors *versus* H-Ras^{V12}-WT MEFs or MEF-derived subcutaneous tumors, respectively; **, fold change in lung tumors from K-Ras^{V12}/p38α$^{-/-}$ mice *versus* lung tumors from K-Ras^{V12}/WT littermates.

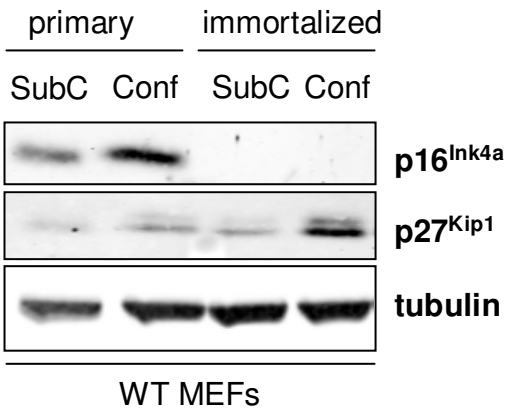

Appendix Figure 1. Interplay between $p16^{Ink4a}$ and $p27^{Kip1}$ in contact inhibition. Subconfluent (SubC) or confluent (Conf) MEFs, either primary (left) or immortalized by genetic ablation of the *Ink4a/Arf* locus (right), were immunoblotted with the indicated antibodies.

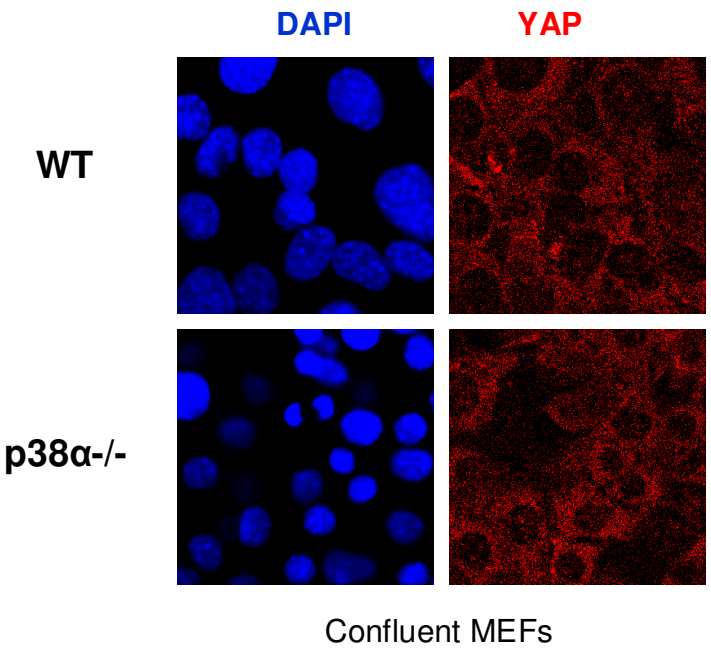

Appendix Figure 2. YAP is similarly localized in the cytoplasm of confluent WT and p38α-/- MEFs. Confluent WT and p38α-/- MEFs were grown on coverslips, fixed with 4% paraformaldehyde and stained with anti-YAP antibody (red) and 4',6-diamidino-2-phenylindole dihydrochloride (DAPI) to visualize cell nuclei (blue). Samples wer examined by confocal microscopy.

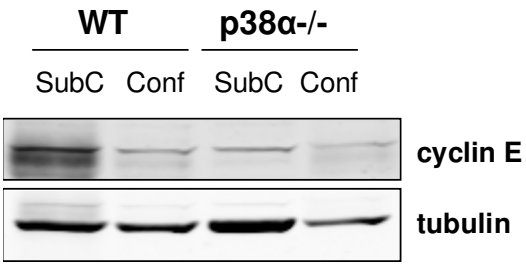

Appendix Figure 3. Cyclin E expression is similar in confluent WT and p38α-/- MEFs. Subconfluent (SubC) or confluent (Conf) WT and p38α-/- MEFs were immunoblotted with the indicated antibodies.

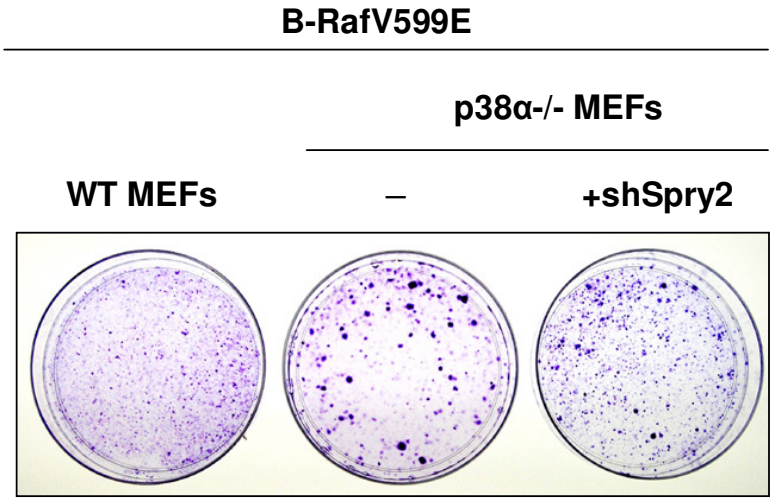

Appendix Figure 4. Spry2 downregulation inhibits the enhanced transformed phenotype of p38α-/- MEFs induced by oncogenic Raf (B-RafV599E). 90% confluent WT and p38α-/- MEFs, as well as p38α-/- MEFs stably expressing a shRNA against Spry2 (shSpry2), were transiently infected with oncogenic Raf and monitored for formation of transformed foci (blue dots) for 2 weeks. Note the bigger foci in p38α-/- cells that are absent in the other two samples.

Appendix 2: Articles